FACULTY OF PHARMACY AND
PHARMACEUTICAL SCIENCES
THE UNIVERSITY OF ALBERTA
EDMONTON 7, ALBERTA, CANADA.

Digitized by the Internet Archive
in 2017 with funding from
University of Alberta Libraries

https://archive.org/details/matte1983

THE UNIVERSITY OF ALBERTA

RELEASE FORM

NAME OF AUTHOR Gilbert Georges Matte

TITLE OF THESIS Biological Behavior of ^{67}Gallium pyrophosphate and ^{67}Ga methylenediphosphonate

DEGREE FOR WHICH THESIS WAS PRESENTED .....M.Sc.....

YEAR THIS DEGREE GRANTED.....1983.....

Permission is hereby granted to THE UNIVERSITY OF ALBERTA LIBRARY to reproduce single copies of this thesis and to lend or sell copies for private, scholarly or scientific research purposes only.

The author reserves other publication rights, and neither the thesis nor extensive extracts from it may be printed or otherwise reproduced without the author's written permission.

(signed).....

PERMANENT ADDRESS:

107 Versaille

Victoriaville, P.Q.

G6P 8C4

Dated...13 December...1983

THE UNIVERSITY OF ALBERTA

Biological Behavior of ^{67}Ga Pyrophosphate and ^{67}Ga Methylenediphosphonate

by

Gilbert Georges Matte

A THESIS

SUBMITTED TO THE FACULTY OF GRADUATE STUDIES AND RESEARCH

IN PARTIAL FULFILLMENT OF THE REQUIREMENTS FOR THE DEGREE

OF MASTER OF SCIENCE IN PHARMACEUTICAL SCIENCES (RADIOPHARMACY)

EDMONTON, ALBERTA

SPRING, 1983

THE UNIVERSITY OF ALBERTA

FACULTY OF GRADUATE STUDIES AND RESEARCH

The undersigned certify that they have read, and recommend to the Faculty of Graduate Studies and Research, for acceptance, a thesis entitled

Biological Behavior of ^{67}Ga Pyrophosphate and ^{67}Ga Methylenediphosphonate

submitted by Gilbert G. Matte in partial fulfillment of the requirements for the degree of MASTER of SCIENCE in PHARMACEUTICAL SCIENCES (Radiopharmacy).

.....

Supervisor

.....

Co-Supervisor

.....

.....

.....

Date...Dec. 13.....1982..

Au plaisir des gens d'ici

ABSTRACT

Various ^{67}Ga phosphate complexes were investigated for their biological distribution and their potential use as myocardial infarct seeking agents. Radiochromatographic methods were developed for the quantitative and qualitative characterization of ^{67}Ga pyrophosphate and ^{67}Ga methylene diphosphonate and ^{67}Ga hydroxide. Animal tissue distribution studies were performed which indicated that the two phosphate derivatives of gallium had almost identical biodistribution in mice. The blood level of the ^{67}Ga phosphates became similar to that of ^{67}Ga citrate after 2 hours post injection and a noticeable *in vitro* binding to transferrin was also observed. The ^{67}Ga pyrophosphate and ^{67}Ga methylene diphosphonate revealed a low liver accumulation when compared to ^{67}Ga hydroxide, suggesting that the phosphate complex, at the concentration, used was not in a colloidal form.

Using an isoproterenol-induced rat myocardial infarct model, the uptake of ^{67}Ga pyrophosphate (GaPPi) and ^{67}Ga methylene (GaMDP) diphosphonate into the affected heart was low with an infarct: normal ratio of 1.55:1 for $^{67}GaPPi$ and 1.78:1 for $^{67}GaMDP$ compared to 4:1 for $^{99}Tc^{m}PPi$ at 1 hour post injection.

ACKNOWLEDGEMENTS

I would like to express my sincere gratitude to Dr. A.A. Noujaim and Dr. A. Shysh for their support as well as their tremendous help throughout the whole project.

I would also extend a special thank you to Miss Kerry J. Logan and Mr. Steve McQuarrie for their willingness to help in the "translation" of this work.

The assistance of Mr. C. Ediss for his technical advice and of Mr. F. Jamali for his expertise in biokinetic were greatly appreciated.

Finally, I would also like to thank the Logan, Underwood Pumperloaf, Mercer, Flanagan, Abrams and Fourceault families as well Mr. D. Smith, Miss P. Zabel, Miss C. Turner and Miss L. McQueen for their constant support and encouragement.

Financial help in the form of an Alberta Heritage Foundation for Medical Research studentship is gratefully acknowledged.

TABLE OF CONTENTS

ABSTRACT V

ACKNOWLEDGEMENTS VI

TABLE OF CONTENTS VII

LIST OF TABLES XI

LIST OF FIGURES XIV

INTRODUCTION 1

SURVEY OF THE LITERATURE 3

I. GALLIUM

A. Chemical and physical properties of gallium 5

B. Gallium chloride 7

C. Gallium hydroxide 9

D. Gallium citrate 11

E. Gallium pyrophosphate 13

G. Biological behavior of gallium 15

1. Tissue distribution 15

2. Binding of gallium in the blood 17

3. Factors affecting the biodistribution of gallium 13

4. Cellular uptake of gallium 21

5. Subcellular localization of gallium 24

6. Excretion of gallium 26

7. Toxicity of gallium 28

8. Biological behavior of gallium phosphate 29

9. Gallium uptake in inflammatory lesion 32
a) Clinical observation 22
b) Mechanism of radiogallium uptake in inflammatory lesions 33
10. Gallium uptake in myocardial infarct 36

II. PHOSPHATE COMPLEXES 39
A. Chemistry of condensed phosphate complexes and phosphonates 39
B. Biological behavior of Technetium-99m phosphate complexes 44
1. Plasma disappearance 44
2. Binding to blood components 45
3. Tissue distribution 47
4. Excretion 49
5. Bone uptake 49
C. $^{99}Tc^{m}$ phosphate complexes in myocardial infarct 51
1. Clinical studies with $^{99}Tc^{m}$pyrosphosphate 51
2. Comparison of $^{99}Tc^{m}$Pyrophosphate and $^{99}Tc^{m}$methylenediphosphonate 56
3. Mechanism of $^{99}Tc^{m}$Pyrosphosphate uptake in myocardial infarction 58

EXPERIMENTAL 62
I. MATERIALS 63
A. Chemicals and materials 63
B. Radioiosotopes 64

II. METHODS

A. Preparation of ^{67}Gallium complexes 64

1. ^{67}Gallium pyrophosphate 64

2. ^{67}Gallium methylene diphosphonate 65

3. ^{67}Gallium hydroxide 65

4. ^{67}Gallium citrate 65

5. Human apotransferrin labelling 65

B. Sample analysis techniques 66

1. Paper chromatography 67

2. Gel chromatography 67

3. Ultracentrifugation 68

C. Animals studies 69

1. Tissue distribution in normal mice 69

2. Myocardial infarct model in rats 40

D. Kinetic analysis 71

RESULTS AND DISCUSSION 72

I. CHARACTERIZATION OF ^{67}GALLIUM PHOSPHATE COMPLEXES 73

A. Paper chromatography 73

B. Gel filtration 85

C. Ultracentrifugation 91

II. BIOLOGICAL BEHAVIOR OF ^{67}GALLIUM PHOSPHATE COMPLEXES 95

A. Blood clearance of ^{67}Ga complexes 96

B. Uptake of ^{67}Ga complexes by liver 115

C. Uptake of ^{67}Ga complexes by the kidneys 117

D. Uptake of ^{67}Ga complexes by the GIT 120

E. Uptake of ^{67}Ga complexes by the bone 121

F. Uptake of ^{67}Ga complexes by the myocardium 124

G. Uptake of ^{67}Ga phosphates derivatives in cardiac infarct tissue 127

SUMMARY AND CONCLUSIONS 136

REFERENCES 139

APPENDIX I 156

APPENDIX II 157

LIST OF TABLES

Table		
I	Physical constants of gallium	6
II	Decay characteristics of gallium radioisotopes	8
III	Influence of the nature of the gallium salts on their precipitation pattern as a hydroxide	10
IV	^{67}Gallium citrate distribution in mice after iv injection expressed in percent of the injected dose per gram of tissue	16
V	Summary of estimated absorbed dose per unit of administrated activity from a single intravenous administration of radioactive gallium citrate	30
VI	Concentration ratios between infarct and normal tissue of different infarct seeking agents	38
VII	Dissociation constant of PPi and MDP at an ionic strength of 1	42
VIII	Tissue distribution of $^{99}Tc^{m}$PPi and $^{99}Tc^{m}$MDP	48
IX	Quantitative radiochromatographic changes of ^{67}GaPPi as a function of the pH	81
X	Effect of time and pH of the developing solvent on the radiochromatographic separation of ^{67}GaPPi	82
XI	Quantitative radiochromatographic changes of ^{67}GaMDP as function of pH	83
XII	Effect of the time and pH of the solvent system on the radiochromatographic separation of ^{67}GaMDP	84

XIII	Solubilities of various gallium complexes	94
XIV	Blood level of various ^{67}Ga complexes following i.v. injection in mice	97
XV	Blood level following i.v. injection of $^{67}GaPPi$ in mice	103
XVI	Blood level following i.v. injection of $^{67}GaMDP$ in mice	104
XVII	Blood level following i.v. injection of $^{67}Ga(OH)_3$ in mice	105
XVIII	Blood level following i.v. injection of ^{67}Ga citrate in mice	106
XIX	Compartmental analysis of blood clearance of $^{67}GaPPi$, $^{67}GaMDP$ and $^{67}Ga(OH)_3$	107
XX	Compartmental analysis of blood clearance of ^{67}Ga citrate	109
XXI	Binding of ^{67}Ga phosphate complexes to different blood fractions	111
XXII	Liver uptake of various ^{67}Ga complexes following i.v. injection in mice	116
XXIII	Kidney uptake of various ^{67}Ga complexes following i.v. injection in mice	119
XXIV	GIT uptake of various ^{67}Ga complexes after i.v. injection in mice	122
XXV	Bone uptake of various ^{67}Ga complexes after i.v. injection in mice	123
XXVI	Heart uptake of various ^{67}Ga complexes after i.v. injection in mice	125

XXVII Heart to blood ratio of various ^{67}Ga phosphate complexes after i.v. administration in mice 126

XXVIII Accumulation of ^{67}Ga and $^{99}Tc^{m}$ radioactivities in normal and infarcted heart of rats after injection of $^{67}GaPPI$ and $^{99}Tc^{m}PPi$ 129

XXIX Accumulation of ^{67}Ga and $^{99}Tc^{m}$ radioactivities in normal and infarcted heart of rats after injection of $^{67}GaMDP$ and $^{99}Tc^{m}PPi$ 130

LIST OF FIGURES

Figure		
1	The effect of $[H]^+$ on the rate of hydrolysis of pyrophosphoric acid at 70^oC in water.	40
2	Structure of pyrophosphate and methylenediphosphonate	41
3	Paper radiochromatographic separation of $^{67}GaPPi$: effect of pH alteration	75
4	Radiochromatographic profiles of $^{67}GaPPi$ and $^{67}GaCl_3$: effect of pH alteration	76
5	Radiochromatographic profiles of $^{67}GaPPi$: effect of pH alteration	78
6	Gel radiochromatographic profiles of $^{67}GaPPi$ on Sephadex G-25	86
7	Gel radiochromatographic profiles of $^{67}GaPPi$ and $^{67}Ga(OH)_3$ on Sephadex G-25	87
8	Radiochromatographic profiles of $^{67}GaMDP$	88
9	Paper radiochromatographic profiles of $^{67}GaPPi$ prior to- and post- gel filtration	90
10	Blood radioactivity levels in mice after injection of $^{67}GaPPi$, $^{67}GaMDP$ and $^{67}Ga(OH)_3$	98
11	Blood radioactivity levels in mice after injection of $^{67}GaPPi$ and ^{67}Ga citrate	99
12	Computer-fitted curve of blood clearance of $^{67}GaPPi$, $^{67}GaMDP$, ^{67}Ga citrate and $^{67}Ga(OH)_3$	102
13	Gel radiochromatographic profiles of $^{67}GaPPi$ and ^{125}I-TF on Sephadex G-200	113

14 Gel chromatographic profiles of a mixture of ^{67}GaPPi and ^{125}I-TF on Sephadex G-200 114

INTRODUCTION

Myocardial infarcts may be detected by the electrocardiogram (ECG) and changes in serum enzyme levels. Over the past few years, scintigraphic imaging techniques with radionuclides have been developed and are now widely practised.

There are two different approaches to myocardial infarct scanning. In the first approach, there is uptake of the radiopharmaceutical in all the normal perfused area. When the cardiac cells are deprived of oxygen and an infarct is produced, the transport properties of the membrane are changed and the radionuclide cannot enter the cell resulting in a photon-deficient spot in the infarcted area. Such a mechanism of uptake is seen with ^{43}K and ^{201}Tl. Secondly, there are radiopharmaceuticals which have been shown to accumulate in the damaged cells of the infarcted region, resulting in an area of increased radioactivity. Examples of those agents include ^{99m}Technetium pyrophosphate, ^{99m}Technetium methylenediphosphonate and ^{67}Gallium citrate (1).

The purpose of this investigation was to prepare and evaluate a complex of two known cardiac seeking agents: gallium and phosphate. The phosphate derivatives used were pyrophosphate because of its present clinical use, and methylenediphosphonate because of its faster blood clearance resulting in a better contrast (2,3). The ultimate objective was to prepare a ^{68}Gallium labelled radiopharmaceutical

which would provide a positron-emission tomographic agent for visualizing myocardial damage.

Dewanjee et al. (4) reported that gallium pyrophosphate has very low solubility, and proposed that at physiologic pH levels it would dissociate, leading to the formation of gallium hydroxide. Thus, it was important to develop a chromatographic system to test the radiochemical purity of gallium phosphates.

To determine the influence of the phosphate moiety on gallium distribution in vivo, distribution studies were performed on mice. Finally, myocardial infarcts were produced in rats to evaluate the specific uptake of the radiogallium phosphates in damaged myocardium using $^{99}Tc^{m}$ pyrophosphate as a comparison standard.

SURVEY OF LITERATURE

I. Gallium

Gallium is an element of atomic weight 69.72 and atomic number of 31. Its presence was predicted by Mendeleev in 1870, who placed it in group III of the periodic table and named it eka-aluminum (5).

Five years later (1875), the French spectroscopist Lecoq de Boisbeaudran, analyzed a zinc blend from the Pyrenee and separated a substance which upon spectroscopic examination with an oxygen-hydrogen flame and an electric arc revealed two intense lines in the UV emission at 4172 A and 4033 A. He attributed those to a new element which he called gallium (6).

Gallium is a widely dispersed element and its average content in the earth's crust is 15 g/ton or 1.5×10^{-3}% of the earth's weight (5,6). It is usually found associated with the elements surrounding it in the periodic table. Independent minerals of gallium are not known, except for $CuGaS_2$ which contains 35% of gallium by weight (5).

Gallium is encountered in many ores, meteorites, sea water (0.02mg/ton), bituminous ores, coals and bauxites (6). The main procedure for the extraction of gallium from its natural source is based on the solubility characteristics of the hydroxide or of certain organic complexes. Aluminate ores are treated with strong alkali, and the aluminum and gallium hydroxides are separated via slow

acidification with carbonic acid. Their respective hydroxides precipitate at different pH with the gallium hydroxide appearing at a lower pH (5). Strong acids such as HCl, H_2SO_4 mixed with NH_4Cl and $(NH_4)_2SO_4$ may also used, followed by an extraction with methyl ethyl ketone which can separate gallium from the other elements of group III. Only traces of Al (0.004%), Ge(0.08%) and Fe(0.03%) are extracted, but there is a 98% extraction efficiency for gallium after 2 washings (7).

Pradhue (8) used the compound monothiodibenzoylmethane (mtdm) to form a Ga $(mtdm)_3$ complex which was extracted with benzene from an aqueous solution in the presence of other metals. It is interesting to note that the presence of certain sequestrating agents such as ethylenediaminetetraacetic acid (EDTA), citrate or oxalate completely prevented the formation of the $Ga(mtdm)_3$ complex, while others such as PO_4^{-3}, CN^- and SCN^- produced a similar effect but to a lesser extent (8).

A. Chemical and Physical Properties of Gallium

Pure gallium appears as a soft, silvery-white metal with a faintly bluish tinge. In the liquid state, it resembles mercury. Natural gallium is a mixture of two stable isotopes ^{69}Ga and ^{71}Ga (60.5% and 39.5% abundance, respectively)(5,6). The crystalline structure is a rhombic (pseudotetragonal) lattice and contrary to most other metals, it exists as a diatomic molecule with an interatomic distance of 2.44 A. Gallium and its closest neighbours in the periodic table (Al, Zn,

Ge, Li) are frequently associated in nature and have an analogous structure of the outermost shell of electrons, similar chemical properties, and only a small difference in their ionic radii (Al^{+} = 0.57 Å, Ga^{+3} = 0.62 Å). The similarity in ionic radii of gallium and iron permits an isomorphous substitution (Fe^{+3} = 0.67 Å)(6).

Gallium as a pure metal, shows a strong tendency for supercooling: molten gallium will remain liquid for several months at temperatures below the solidification point but if a crystal of gallium is added or if the liquid is stirred, solidification occurs immediately. However, in contrast to most metals, a fairly strong force of expansion will occur during the solidification process with an increase of volume of 3.2% (6). Table I summarizes the physical constants of

Table I

PHYSICAL CONSTANTS OF GALLIUM (a)

Atomic number	31
Atomic weight	69.72
Atomic radius	1.39 Å
Atomic volume	11.8 cm^3/g atom
Density^{20}	5.907
Density liq at 29.8°C	6.095
Melting point	29.78°C
Boiling point	2516°C

(a) from references 5 and 6

There are several isotopes of gallium. The principle radioactive isotopes of gallium, ^{66}Ga, ^{67}Ga, ^{68}Ga, and ^{72}Ga, are described in Table II.

B. Gallium Chloride

Gallium, as a chloride, can exist in three different valence states: gallium monochloride, gallium dichloride and gallium trichloride (6).

The monochloride is obtained by prolonged heating of the trichloride salt with gallium metal. The resulting product is sublimed in a stream of CO_2. GaCl is highly hygroscopic and dissolution leads to the production of gallium metal and gallium trichloride (6):

$$3\ GaCl \longrightarrow GaCl_3 + 2\ Ga$$

The dichloride salt is obtained by heating gallium metal in a slow current of chlorine and nitrogen gas or by dissolving gallium metal in a small amount of HCl (6). It can also be produced by heating $GaCl_3$ with an excess of gallium metal, then vaporizing the product in a stream of CO_2 and collecting the sublimate (6). The crystals obtained as $Ga(GaCl_4)$ have a melting point of 170.5°C (6). The dichloride at 200°C decomposes as follows (6):

$$3\ GaCl_2 \longrightarrow 2GaCl_3 + Ga$$

Table II

DECAY CHARACTERISTICS OF GALLIUM RADIOISOTOPES (a)

Radionuclide	^{66}Ga		^{67}Ga		^{68}Ga		^{72}Ga	
t 1/2 (hrs)	9.3		78.0		1.14		14.1	
Decay constant (Hr^{-1})	0.0737		0.00885		0.607		0.04915	
Mode of Decay	Electron capture		Electron capture		Electron capture Beta+		Beta$^-$	
Principal energy (MeV)	n		Principal energy (MeV)	n	Principal energy (MeV)	n	Principal energy (MeV)	n
0.511	1.167		0.0933	0.380	0.511	1.76	0.63	0.27
1.0392	0.373		0.1845	0.239			0.83	0.96
2.752	0.227		0.3002	0.161			0.89	0.10
			0.3939	0.43			2.2	0.260
							2.50	0.140

(a) from reference 9

n = mean number per disintegration

The crystals are also very hygroscopic and when dissolved in water, the solution turns brown and a white precipitate appears (6).

The trichloride form of gallium chloride is the easiest one to obtain. It can be synthesized by action of CCl_4 and chlorine vapour on gallium metal at high temperature or by dissolving a fresh precipitate of gallium hydroxide or gallium metal in HCl (6). The product is a white substance crystallizing into a colorless needle-like pattern with a melting of 201.3°C (5). The salt, freshly produced, is in a dimeric form Ga_2Cl_6, which readily dissociates to $GaCl_3$ with liberation of 21 Kcal/mol.

C. Gallium Hydroxide

$Ga(OH)_3$ is obtained by either the action of a base on gallium salts or an acid on gallate ions $[Ga(OH)_4]^-$. The different salts are soluble in acidic media. Upon neutralization, they form gallium hydroxide of varying solubilities depending of the amount of OH^- ions in the solution (10).

$$Ga^{3+} + H_2O \longrightarrow Ga(OH)^{2+} + H^+$$
$$Ga(OH)^{2+} + H_2O \longrightarrow Ga(OH)_2^{1+} + H^+$$
$$Ga(OH)_2^{1+} + H_2O \longrightarrow Ga(OH)_3 + H^+$$

At a molar ratio of hydroxide: Ga of 3:1 complete precipitation is achieved at room temperature (10). After 6 weeks at a ratio of 2:1

only a slight precipitation will occur (1% of the original gallium). At a ratio of 1:1 or lower ratio no precipitation appears (11). The nature of the anion of the gallium salt, the concentration and the temperature influence the pH of precipitation (Table III).

Table III

INFLUENCE OF THE NATURE OF THE GALLIUM SALTS

ON THEIR PRECIPITATION PATTERN AS A HYDROXIDE(a)

	incipient ppt		marked ppt		dissolution	
Ga Salt	pH	OH/Ga	pH	OH/Ga	pH	OH/Ga
$Ga_2(SO_4)_3$ (0.005M)	3.40	0.2	4.7	2.5	9.4	4.1
$GaCl_3$ (0.01M)	3.48	2.6	6.7	2.8	9.6	4.0

(a) from reference 5

The precipitate, when studied by X-ray diffraction, demonstrates an amorphous gel pattern containing mostly water and only 22% of $Ga(OH)_3$, with the appearance of some GaO(OH) over a long period of time (12).

Gallium hydroxide has been classified by Friecke (6) as an ideal amphoteric substance but it reveals a predominantly acidic character:

$$H_3GaO_3 \qquad H^+ + H_2GaO_3^- \qquad K_d = 1.4 \times 10^7$$

$$H_2GaO_3^- \qquad H^+ + HGaO_3^{2-} \qquad K_d = 4.8 \times 10^4$$

$$HGaO^2{}_3^- \qquad H^+ + GaO_3^{3-} \qquad K_d = 2 \times 10^2$$

K_d = dissociation constant

A simple method to characterize gallium hydroxide qualitatively by paper chromatography has been described by Hnatowich (13) using two different solvent systems: water: ethanol: ammonia (70:20:0.35) or isopropanol:water:trichloroacetic acid:ammonia (275:125:15:1). The $Ga(OH)_3$ stays at the origin while the more soluble form of hydroxide migrates.

D. Gallium Citrate

Due to its high electron affinity, the free gallium ion can readily form a complex with an organic compound containing electron dense atoms such as citrate (14).

Gallium citrate is a soluble complex at neutral pH and has a wide clinical application as ^{67}Ga citrate. There are many forms of gallium

citrate. A molar concentration ratio of citrate:gallium of 1:1 or less, will result in a complex composed of one gallium with one citrate (15). Titration of the complex with NaOH will result in a partial hydrolysis of the complex (5):

$$[C_3H_4OGa(COOH)_3]^{2+}$$
$$[C_3H_4OGa(OH)_2(COOH)_3]^{o} \quad (pH\ \ 3)$$
$$[C_3H_4OGa(OH)_2(COO)(COOH)_2]^{-} \quad (pH\ \ 4)$$
$$[C_3H_4OGa(OH)_2(COO)_3]^{3-} \quad (pH > 8)$$

Further addition of NaOH will result in the hydrolysis of the complex yielding $Ga(OH)_4^-$ ions at pH=9 (15). Hydrolysis is not the only event which occurs during neutralization; Glickson (15), and Kul'ba (16) reported that as the pH increased, the gallium citrate complex, also polymerized. The polymer is unstable and will dissociate into gallium dicitrate. As neutral pH is reached, an equilibrium is formed between ($Ga_1Citrate_1$), its polymer and the gallium dicitrate (17). The gallium dicitrate complex appears in acidic pH when the molar ratio of citrate to gallium is greater than one (16).

Although less stable, the gallium complex can be compared to the iron citrate polymer. Both have an isomorphous structure with an inner core of the metal linked by oxy and hydroxy bridges. The citrate surrounding the core acts as a counter ion which solubilizes the spherical polymer (17).

E. Gallium Pyrophosphate

There are few publications about the complexation of gallium to pyrophosphate. It is generally accepted that a mixture of gallium salts with either phosphoric acid or its salts will result in the precipitation of a phosphate complex (5,6).

Chudinova et al. (18,19), using thermography, titration and X-ray diffraction showed that the compound produced by mixing sodium pyrophosphate ($Na_4P_2O_7$) with gallium can have three different forms:

A- $Ga_4P_2O_7$

B- $NaGaP_2O_7$

C- $Na_2GaOHP_2O_7$

Product A is obtained by the addition of an amount of sodium pyrophosphate (Na_4PPi) to a gallium chloride solution with a molar concentration ratio Na_4PPi:Ga less than one, and results in the formation of an amorphous precipitate (18). Further addition of Na_4PPi will cause an increase in the solubility as product B is formed (19). If the nature of the PPi cation is K^+ the precipitate will not dissolve completely. If Na_4PPi is used instead this precipitate will dissolve completely but can be re-isolated by addition of NaCl (19). Finally, if the molar concentration ratio is increased to 1.25:1 or more the third compound appears and precipitates after 48 hours (18).

In a study on the effect of pH on a solution of gallium pyrophosphate (Ga:PPi=1:1), a precipitate of the GaPPi was observed at

pH 3.3 and the solid phase was found to consist of the mixed salt (form B). When the pH of the solution was increased to above 4.6, the precipitated compound was slowly changed to the basic salt (form C)(20). It should be noted that when the solution was neutralized, the precipitate dissolved initially, followed by the precipitation of the basic mixed salt a few minutes later. It took from several hours up to one month to obtain the complete transition depending on the pH of the solution, and the concentration as well as the nature of the anion of the PPi salt used (20). When the pH was raised to 8, the precipitate started to dissolve and at pH 9, the complex was broken down into $Ga(OH)^-$ and PPi (19,20). If a ratio of Ga:PPi of 10:1 was used, the solubility was improved, and was even greater if the Na salt was used (20).

Sheka et al. (21) studied the GaPPi complex using infrared (IR) spectrophotometry, at molar ratio concentrations of PPi:Ga of 1:1 and 1:1.5. They observed that the usual symmetrical feature of the PO_3^- portion was destroyed when the gallium was added to a solution of PPi salts, in a way similar to that seen after protonation. Their interpretation was that the gallium is more tightly bound to one of the oxygen atoms resulting in what they called an inner sphere complex. This is different from other cations such as calcium which form an outer sphere complex where the cation is equally distant from the two oxygen atoms. The same group of workers established that in acidic medium (pH 1 to 3.5) the gallium assumed a $GaHP_2O_7$ complex with a formation constant of 12.36 0.16 (22). This is in agreement with the finding of Chudinova (18), and both workers concluded that at a

molar concentration ratio of Ga:PPi greater than 1:1, the complex will contain one atom of Ga with one molecule of PPi.

F. Biological Behavior of Gallium

1. Tissue Distribution

The use of radiogallium was first introduced into the biological area by Dudley in the late 1940's when its osteophilic properties were recognized (23,24).

In the early 1970's, radiogallium became a very popular diagnostic agent as a ^{67}Ga citrate complex. When injected intravenously (i.v.) in normal mice, apart from a gradual and progressive clearance from the plasma, the tissue distribution was essentially established within an hour after injection. The main localization, at this time, occurred in the bone which contained about 7% of the injected dose (ID) per gram. The kidneys and intestine localized from 3.5 to 5% of the injected dose per gram of organ, and the muscle and lungs accumulated the tracer to a lesser extent (Table IV)(25). In rats, radioactivity was cleared very slowly from the blood, but except for the blood and lung, other tissues did not show any significant variation in uptake after 24 hours, and the gallium appeared to be firmly bound to the tissues (26).

Table IV

^{67}GALLIUM CITRATE DISTRIBUTION IN MICE

AFTER IV INJECTION EXPRESSED IN % INJECTED DOSE PER GRAM TISSUE (a)

Tissues	1h	3h	7h	24h	72h
Blood	10	6.7	3.7	0.8	0.15
Liver	3.5	4.2	4.1	4.5	3.5
Spleen	2.8	2.9	2.7	2.3	1.9
Kidney	4.3	4.3	4.3	3.6	2.1
S. Intestine	4.2	9.5	4.3	4.5	1.2
Bone + marrow	6.8	7.1	8.2	12.8	9.0

(a) from reference 25

5 mice per group

2. Binding of Gallium in Blood

When no-carrier-added radiogallium citrate is injected i.v., the radioactivity becomes bound to plasma proteins very rapidly. In humans, 85% of the radioactivity in the blood is bound in the plasma at 3 hours increasing to 97% of the radioactivity at 24 hours (27). The cellular fraction accumulates only a small amount of the radioactivity. In mice, the blood cells showed a maximum uptake of 1% of the injected dose per gram at 0.05 hours (25). In an *in vitro* study, when human blood cells were separated and cultured as a monolayer with ^{67}Ga citrate, red blood cells showed a negligible affinity (20 cpm/10 million cells after 30 minutes of incubation with 20 μCi). Lymphocytes and polymorphonuclear leucocytes showed an higher uptake (948 and 1041 cpm respectively)(28). In rabbits, administration of ^{67}Ga citrate revealed that twenty four hours after injection, less than 14% of the remaining activity in the blood was bound to the polymorphonuclear leucocytes (28).

Following i.v. injection of ^{67}Ga citrate, radiogallium is mostly bound to transferrin (TF), a high molecular weight iron transport protein, and to a small extent, to other globulins (29,31).

According to Clausen *et al.* (30), no-carrier-added ^{67}Ga citrate is bound to TF by Van der Waals forces and hydrophobic bonds. They calculated the presence of fourteen binding sites for gallium on the transferrin molecule, but Harris *et al.* (32) could only detect the presence of two sites by titration of TF with gallium. The serum binding protein sites occupied by gallium appear to be the same as the

one for iron, but the latter cation has a higher affinity. Plotting the ratio of bound to free radioisotope as a function of the molar concentration of the TF metal-binding site (assuming two binding sites per protein), a linear relationship was obtained and the association constant at equilibrium was determined by the slope. The values of this constant were estimated to be 2.85×10^5 L/mol for ^{67}Ga and 9.0×10^6 L/mol for ^{59}Fe (33). The association constant varies depending upon on the species. The complex of gallium with human apo-transferrin dissociates more easily than the comparable rat transferrin complex. This was shown by the higher dissociation of the human plasma ^{67}Ga complex encountered when filtered on a Sephadex G-200 column (26).

3. Factors Affecting the Distribution of Gallium

The binding of radiogallium to protein is a very important factor in the biodistribution of ^{67}Ga citrate. Sephton et al. (25) noticed that the ^{67}Ga adsorption to bone in vitro was reduced in the presence of serum in the incubation media. Other factors can influence the binding of gallium to protein, and thus its distribution. Such factors include, for example: the presence of carrier gallium, scandium, iron and radiation therapy.

The administration of carrier gallium, six hours after injection of ^{67}Ga citrate into mice bearing S180 tumors, resulted in an increase of the radiogallium uptake by the femur but tumor and soft tissue uptake were decreased (34). When ^{67}Ga citrate and carrier Ga were administered at the same time, a fall in the soft tissue uptake was

seen but in such a way that the ratio of tumor/nontumor uptake remained the same (34). Halpern et al. (35) reported that in rats bearing 7777 Morris hepatoma, the administration of carrier Ga two hours prior to or two hours after the administration of ^{67}Ga citrate caused a decrease in the concentration of ^{67}Ga in blood, liver, spleen, skeletal muscle, and viable and non viable tumors at all periods of time. The greatest decrease of utake occurred with simultaneous injection of the carrier and the least effect was seen when the carrier was given 2 hours prior to ^{67}Ga citrate. If the carrier was injected 24 hours after the radionuclide, the uptake was essentially complete and accumulation was not changed (34,35).

The administration of scandium, given simultaneously or after ^{67}Ga citrate, reduced the tumor (PC6 plasmacytoma) uptake of radiogallium in mice to a greater extent than it decreased uptake in normal tissue. If other tumors were used such as 15 august carcinoma in rat, blood and soft tissues decreased while tumor uptake was not affected (34). Administration of the scandium also caused a decreased abcess uptake in a similar extent to that seen in normal tissue (36).

Prior injection of Fe^{+++} ions generally had the greatest effect in reducing the level of radiogallium in soft tissues but it did not enhance the tumor/normal ratio very much (34). Iron given four hours after ^{67}Ga citrate resulted in a decreased uptake in all tissues but the tumor uptake was less affected, resulting in an improvement of the tumor to normal ratio. Addition of iron caused a rapid elimination of gallium during the first phase of blood clearance (34). The second

phase of blood clearance was not influenced probably due to the tissue binding during this period of time. The injection of Desferoxamine Mesylate (Desferal) which has a high iron affinity, 3 to 6 hours after administration of ^{67}Ga citrate produced a decrease in the blood activity and an increase in urine elimination of ^{67}Ga. If the Desferal was administered more than 16 hours after the radiotracer, the effect was less dramatic (37).

Iron deficiency caused an increase in the accumulation of radiogallium in the liver and spleen and in its fecal secretion (36,38). In addition, a decrease in urinary excretion, blood level and abcess uptake were also observed (36,38). No effect was seen on the bone uptake (38). Radiation therapy also produces a decrease in the gallium citrate retention and serum binding. This was associated with an increase in the iron blood level while the TF level was unchanged. The change in excretion was believed to be due to the saturation of TF by iron (39).

According to Anghileri (40,41), gallium shows a similarity to calcium. This is based on the demonstration of gallium accumulation in calcium-rich tissue such as liver, milk, calcified tissues (hydroxyapatite-rich) and also binding to macromolecular calcium compounds such as calcium heparinate, calcium caseinate and calcium ribonucleate (40,41,42). The presence of gallium was also noticed in experimental calcification (43). Simultaneous intraperitoneal (i.p.) injection of $GaCl_3$ and ^{45}Ca in tumor-bearing mice (lymphatic leukemia BW 5147) showed that at 24 hours after injection, the ratio of ^{45}Ca

specific activity (SA) in $GaCl_3$ treated animal: specific activity (activity per gram) in nontreated animal had a value of 2.09:1 for the tumor, 3.12:1 for the liver and 2.43:1 for the kidney. Intracellular localization was also affected by the concomitant administration, causing an increase in the mitochondrial fraction (43). In vitro studies of binding of the calcium to phospholipids showed that the presence of gallium decreased the calcium uptake by 8% to 66.7% (44).

4. Cellular Uptake of Radiogallium

Several mechanisms have been postulated for the entry of radiogallium into the cells. However, most researchers have agreed that transferrin influences the uptake of this cation (25,45).

Sephton and Harris (46), with different tumor lines, observed that in tissue culture media, the ^{67}Ga citrate uptake was very modest (2 to 5 times that of the culture media). Addition of certain sera (rabbit, horse and human) had a stimulatory effect on the uptake of radiogallium citrate. After separation of sera and the addition of different serum fractions to the culture media, the increased uptake of ^{67}Ga was found to be associated with the TF fraction (46). Noujaim and colleagues (47), incubated melanoma cells with different proteins, and found that only the TF caused a significant uptake of radiogallium citrate. Normal cells such as cultured Lavallee fibroblasts showed very little uptake of either ^{67}Ga citrate alone, or with increasing concentration of apotransferrin (47).

Larson and colleagues (33,45) in a tissue culture study with EMT6 sarcoma cells concluded that the addition of TF to the medium was

required before an appreciable uptake of ^{67}Ga citrate occurred.

Addition of iron to the culture media containing TF and radiogallium resulted in a decrease of ^{67}Ga uptake by tumor cells (48). However, the accumulation of gallium is not similar to the uptake of iron. Unlike ^{59}Fe uptake, the ^{67}Ga response seemed to be more affected by the degree of iron added to the culture media than the degree of iron saturation of the added TF (48). That led Harris and Sephton (48) to conclude that the cell uptake of Ga and Fe complex of TF was dissimilar.

Aulbert et al. (49) proposed endocytosis as a mechanism for the cellular uptake of the radiogallium-TF complex, based on the knowledge that rat liver and tumor cells can accumulate TF by endocytosis. Immunophoresis of liver cell contents revealed that ^{67}Ga radioactivity was associated with a protein acting similarly to TF. Thus, the author suggested that the ^{67}Ga TF complex was first incorporated into the cell by phagocytic vacuoles, then incorporated into the lysosomes where the complex was broken down, with subsequent binding of the radiogallium by a high molecular weight protein such as ferritin.

Wong et al. (50) incubated human melanoma cells with $^{125}Iodine$ labelled ^{67}Ga TF and noted that the ^{125}I associated with the cell fraction remained constant after 15 minutes while the ^{67}Ga uptake increased with time. Using an in vivo venereal transmissible tumor model in dogs and the same dual labelled protein, they noted that while the radiogallium uptake in the tumor increased with time, no

significant increase was seen with radioiodine (50). They postulated that the uptake was due to the binding of the ^{67}Ga TF on a membrane receptor with subsequent entry of the gallium into the cell and release of TF, or alternatively, entry of the whole complex with fast dissociation and release of the TF in the extracellular fluid (50).

Larson et al. (33) worked with an EMT6 sarcoma and showed that the ^{67}Ga citrate was bound to TF in the blood and carried to the tumor site where the complex was bound to a cell receptor. Using an incubation mixture of iodine labelled transferrin and gallium citrate, these authors found that the activity of ^{125}I and ^{67}Ga in the cells was greater than the radioactivity in the culture media after 24 hours of incubation. They concluded that the whole complex can be incorporated or tightly bound to the cell membrane. Ultracentrifugation of the cellular components showed that the gallium was in the lysosomal fraction bound to some unidentified macromolecule and followed a metabolic pathway similar to that of iron.

Anghileri et al. (40) used solubilization and dilution methods on cultured cells to extract the soluble fraction from Ehrlich ascites tumor cells. They found that 50% of the intracellular radiogallium was bound to the nonsoluble, non dializable fraction containing phospholipids, nucleic acids, and the cell membrane (40). Phospholipids appear to be very important in the cellular incorporation of gallium. Studying the binding of ^{67}Ga TF and ^{67}Ga citrate in artificial membranes, Rogers and Noujaim (51) noticed that the addition of diacetylphosphate to phosphatidyl choline yielded a

remarkable level of radiogallium incorporation (95% for Ga citrate and 99% for Ga TF). They suggested that in a cellular environment, the gallium would possibly have a high affinity for negatively charged membranes, such as the phosphate rich membranes.

5. Subcellular Localization of Radiogallium

Some of the early work in the intracellular localization of radiogallium was performed by Swartzendruber et al. (52). After the injection of no-carrier-added gallium-67 citrate intraperitoneally (i.p) in rats, and using electron microscopy autoradiographic techniques, he concluded that the intracellular localization of gallium after 24 and 72 hours was mainly in organelles such as lysosomes and phagolysosomes, which are abundant in gallium-avid cells. However, because of the similarity of lysosomes and peroxysomes, the possibility of accumulation in the latter as well was not ruled out.

Orii, in 1972 (53), studying solid subcutaneous Yoshida sarcoma in rats, investigated the subcellular localization of no-carrier-added ^{67}Ga citrate. Subcellular distribution in tumor cells was similar to that seen in liver and spleen cells. The gallium was associated with the 105,000 x g supernatant fraction and not with the lysosome fraction. The same authors (53) have stated that gel filtration of the supernatant showed that the gallium was bound nonionically to an undentified macromolecule which could be digested by Pronase but not by DNAase or RNAase.

In 1973, Brown et al. (54), using ^{67}Ga citrate i.v. in mice with different types of tumors (RFT sarcoma, Morris 7777, 5123C, 7794A hepatoma) corroborated the previous results of lysosomal localization by ultracentrifugation.

Aulbert et al. (55) studied the behavior of no-carrier-added ^{67}Ga citrate IV in the rat liver. Homogenization of the tissue 40 hours after injection, followed by differential centrifugation, showed that 91% of the radiogallium was in the centrifugation zone which contained 82% of the acid phosphatase activity (an intralysosomal enzyme), compared to all other fractionation zones (22.5%). Intralysosomal gallium was mainly associated with the soluble fraction and very little was associated with the membrane. Little gallium was also found to be bound to the plasma membrane and to the mitochondrial fraction.

Brown et al. (56) isolated two types of ^{67}Ga binding granules from rat liver and Morris 5123C hepatoma homogenates by zonal centrifugation of the tissue 24 hours after IV injection: lysosomes and the rough surface endoplasmic reticulum (RSER). A difference existed between the subcellular localization in the liver and the hepatoma. In both cases, 80% of the cellular radioactivity was in the centrifugation zone of the lysosomes and RSER. However, in hepatoma, 50% was associated with the RSER, compared to 30% in the normal rat liver.

Samezina and Orii (57) studied the subcellular localization of

^{67}Ga citrate in normal rat liver as a function of time, and reported that 30 minutes after an i.v. dose, fractional centrifugation showed that 76% of the cell radioactivity was found in the supernatant. Twenty-four hours after injection, the largest amount of radioactivity was in the zonal fraction containing the lysosomes and the heavy endoplasmic reticulum.

Pierrez et al. (58) employed zone fractionation techniques with rat liver homogenates. Forty-eight hours after i.v. ^{67}Ga citrate injection, the organelles accumulating the gallium were identified as the peroxysomes (43.3% of the radioactivity). The lysosomal and mitochondrial fractions together accumulated only 10.4% of the radioactivity. The same authors also considered that the techniques previously used were not sensitive enough to separate peroxysomes from lysosomes leading to misinterpretation of results.

6. Excretion of Gallium

Clausen et al. (30) reported that ^{67}Ga citrate, following i.v. injection in humans, is cleared rapidly from the plasma following a 3 component elimination curve. The half-life (T 1/2) of the first component was 5 to 10 minutes, the second 2 hours, and the third was 48 hours. Logan et al.(59), also revealed a three-compartment model (59). Forty hours after an i.v. dose of ^{67}Ga citrate in humans, only 5% of the dose remained in the blood and the blood level fell to 2% after 5 days (60). However, one week after i.v. injection, 65% of the dose still remained in the body (60).

The gastrointestinal tract (GIT) and the kidney are the two main organs of excretion. The secretion into the GIT is rapid and corresponds to 2.5-15% of the injected dose of ^{67}Gallium citrate in humans (61). Three, six, and nine percent of an i.v. dose of ^{67}Ga citrate in rats was found in the GIT at one, six, and twenty-four hours, respectively (62). The major secretion was found to occur in the small intestinal mucosa, where 60% of the GIT secretion occurred (62). Only 10% of the GIT excretion took place in the large intestine, with the same percentage occurring in the esophagus and stomach together. The biliary system also contributed to the GIT content in humans as well as in rats (61,62). Gallium is not significantly absorbed by the GIT (26).

During the first twenty-four hours, 10-15% of the injected i.v. dose in humans is excreted in the urine (60). It has been reported that the gallium injected as Ga citrate complex appeared in the urine in the form of a low molecular weight salt or complex and was suggested to be a citrate complex (63). This view is disputed by Sykes *et al.*(64) who advocates that the complex is that of a phosphocarbonate nature. Konikowski *et al.* (65) reported that the renal clearance of radiogallium varied with the nature of the injected complex. In mice, after an i.v. dose ^{67}Ga-iron-DPTA showed the highest whole blood renal clearance of 33.8mL/min; gallium chloride, 6.1mL/min; gallium lactate, 3.8mL/min; and citrate 0.7mL/min. All four complexes showed a lower clearance than inulin. It was proposed that these complexes were reabsorbed by the tubules (65). Performing three dimensional autoradiography on kidney samples from mice after

^{67}Ga sulfate injection, it was found that the kidney concentrated the gallium in the lysosomes of the proximal tubules, and precipitated it as a crystal of non-soluble phosphate salts which were then expelled in the tubular lumen and eliminated in the urinary flow (66). This corroborated the fact that when a toxic dose of gallium is injected, kidney dysfunction appears to be due to the presence of gallium-calcium phosphate precipitate (67).

7. Toxicity of Gallium

There appears to be species differences in the toxicity of gallium: whereas the lethal dose for 50% of the animals after i.v. gallium citrate was greater than 220 mg/kg in rats, it was only 28.2mg/kg in dogs (68). In mice, the LD_{50} was found to be 115 mg/kg for gallium citrate and 520 mg/kg for the lactate complex (65). The effect of chronic gallium citrate administration in dogs, 5 mg/kg i.v. twice a week, was to lower the lethal dose. The cause of death appeared to be related to uremia secondary to GIT and kidney debilitation (68). A histologic study of the rat kidney showed the presence of a precipitate of a gallium-calcium phosphate complex in the tubular lumen (67). The damage appeared to be similar to that seen in the case of mercury poisoning (68). Gastrointestinal symptoms of acute toxicity in dogs included vomiting and bloody diarrhea. As the uremia became more severe, debility and weakness appeared and was followed by coma and death (68).

In man, following a massive dose of ^{72}Ga citrate (10-100 mCi, 15-70 mg Ga/kg body weight) toxic reactions were observed (69).

Certain symptoms such as persistent drowsiness, anorexia, nausea, vomiting, lymphopenia and hypoplasia of the bone marrow were common to all patients. Recovery occurred soon after the cessation of the gallium administration. Less common dermatologic symptoms such as exfoliative dermatitis, maculo papular rash, folliculitis and severe itching, were seen in many patients and developed after the second, third and fourth week of treatment. These symptoms disappeared a few days after the cessation of the therapy. A few patients exhibited a minor degree of retinal hemorrhage (69).

The absorbed radiation dose to the whole body and various organs from an i.v. injection of radioactive gallium citrate is presented in Table 5.

8. Biological Behavior of Gallium Phosphate

Few reports exist which describe the biological behavior of the gallium phosphate chelate. In an early work, Hnatowich et al. (4) studied the effect of pH on the stability of ^{67}Ga pyrophosphate and concluded that because of the low solubility of the compound, 30-50% of the complex would most likely concentrate in the reticuloendothelial system (70).

Dewanjee et al. (70) prepared some phosphate derivatives of gallium; ^{68}Ga ethylenediaminetetramethylenephosphonate (GaEDTMP) and ^{68}Ga diethylenetriaminepentamethylenephosphonate (GaDTPMP), and examined the bone seeking properties of these agents. They found that 50-60% of the injected dose accumulated in the bone of rats and 35% in

TABLE V

SUMMARY OF ESTIMATED ABSORBED DOSE PER UNIT OF ADMINISTERED ACTIVITY FROM A SINGLE INTRAVENOUS ADMINISTRATION OF RADIOACTIVE GALLIUM CITRATE[a]

Tissue	Radioisotope of gallium (rads/mCi injected)			
	^{66}Ga	^{67}Ga	^{68}Ga	^{72}Ga
Gastrointestinal tract				
Stomach	0.52	0.22	0.042	0.65
Small intestine	1.4	0.36	0.21	1.4
Upper large intestine	3.5	0.56	0.23	3.0
Lower large intestine	3.6	0.90	0.094	3.7
Gonards				
Ovaries	0.46	0.28	0.048	0.84
Testes	0.54	0.24	0.039	0.74
Kidneys	1.1	0.41	0.089	1.2
Liver	1.2	0.46	0.096	1.3
Marrow	1.2	0.58	0.10	1.4
Skeleton	1.1	0.44	0.094	1.2
Spleen	1.5	0.53	0.13	1.5
Total body	0.66	0.26	0.052	0.76

(a) All dose calculations assume a uniform distribution of activity in an organ. This was verified by gross autoradiography of the liver and spleen, but similar studies in kidney and bone showed a very nonuniform distribution.

Skeleton = bone + marrow

Dose calculated assuming a uniform distribution of radioactivity in total body.

from ref. 9.

dogs. The elimination was mainly through urinary excretion (40-50% in the first 3 hours), and the liver uptake was very low (3.2% of the ID)(71). A fairly large amount of GaEDTMP was protein bound (70-80.9% as determined by gel filtration or ethyl alcohol precipitation). Electrophoresis of rabbit serum showed that 43.4% of the radioactivity was bound to albumin; 22.7%, 11% and 4.1% with alpha-1 and alpha-2 globulin, beta-1, beta-2 globulin and fibrinogen respectively; the rest was not bound (71).

Goulet et al. (72) investigated ^{68}Ga tripolyphosphate as a bone scanning agent. They found that in mice, 50% of the dose accumulated in the bone after 6 hours, and a relatively high uptake was seen in the GIT (8%). Other soft tissues, such as the heart, did not accumulate the product.

Tissue culture studies have indicated that the presence of phosphate ions in the incubating media inhibited the incorporation of radiogallium by either leukemic L1210 tumor cells (73) or by the melanoma AB cells (74). It appears that the phosphate ion will complex with the gallium or interact with the cellular membrane making it impermeable to gallium (73). An alternative theory is that the phosphate can block the receptor site resulting in an inhibitory effect. A concentration of 0.001M phosphate buffer reduced the uptake by more than 20% (75). It was also reported that the phosphate can remove the gallium from the binding site on the transferrin when ^{67}Ga labelled serum is dialyzed with a phosphate buffer solution (27).

9. Gallium Uptake in Inflammatory Lesions

a. Clinical Applications

^{67}Ga citrate accumulates at various localized or diffuse inflammatory sites. In clinical work on bone and joints, it has been possible to visualize inflamed areas and differentiate between them using both $^{99}Tc^{m}$ phosphate and ^{67}Ga citrate. Osteomyelitis will cause an increase in uptake of both radioisotopes but septic arthritis will show concentration of gallium in the synovia while the $^{99}Tc^{m}$ phosphate uptake may increase in the surrounding bone due to the periarticular lesion and the increase in blood flow (76). The $^{99}Tc^{m}$ phosphate scan will remain positive after osteomyelitis while the uptake observed from the gallium scan will disappear more rapidly (76).

The radiogallium scans can also correlate with the active sites of inflammation of the lung. ^{67}Ga citrate uptake has been reported in cases of pneumonia (77), tuberculosis (76), scarcoidosis (78), also in less localized diseases such as interstitial lung disease, pulmonary fibrosis (79) and pleural inflammation (80).

Myocardial uptake of ^{67}Gallium citrate has been reported when abcess and bacterial endocarditis were present (81,82). A patient with infective endocarditis due to Staphylococcus aureus showed a significant radiogallium uptake. After the abcess had been drained by surgery, a repeat of the gallium citrate scan was normal (82).

Gallium-67 has also been efficient in detecting cerebral and cranial inflammatory conditions, but it is non specific. Neoplasm and

infarction may also give a positive scan (76). Early imaging can point out nondiagnosed bowel disease (83) and gallbladder empyema (84). Correlation of data from blood culture and gallium scanning, has made it possible to differentiate abcess in patient with leukemia (85). Abdominal abcess can easily be localized (86).

Renal inflammation is indicated as areas of an increased radioactivity uptake following ^{67}Ga-citrate injection (87). In humans, renal radioactivity is normally low 48 hours following i.v. injection (76). The presence of unilateral or bilateral uptake increasing with time, has been associated with pyelonephritis, interstitial nephritis, abcess and acute tubular necrosis (76,88).

Radiogallium accumulation is well recognized in surgical wounds where the uptake and persistence is variable depending on the speed of healing. It usually resolves in about 2 weeks or less, but high uptake in a recent surgical wound can also be due to a wound abcess (88).

b. Mechanism of Radiogallium Uptake in Inflammatory Lesions

Different laboratory experiments have been performed to determine the mechanism of uptake of ^{67}Ga citrate in inflammatory lesions. In both sterile (turpentine induced) and nonsterile (S. aureus-induced) inflammation sites, a significant uptake was noted 45 minutes after the injection of ^{67}Ga citrate, and a maximum uptake was observed after 2 hours. These observations were recorded 24 hours after the inflammation had been initiated (85). Camargo (89) reported slower

accumulation in rabbits with S. aureus abcesses, where at 48 hours after injection, the radioactivity in the abcess was equal to the blood concentration. If leukopenia was induced, the intensity of the uptake was found to be either significantly decreased or delayed (85). The conclusion drawn was that the delivery of gallium from the blood by extravasation is not the central mechanism, and an important part of ^{67}Ga accumulation is related to the leucocyte migration into the inflammed area (76,85). This was also supported by the fact that the injection of ^{67}Ga labelled polymorphonuclear (PMN) leucocytes will localize in the abcess area (80).

Different hypotheses were presented to explain the PMN leucocyte uptake of radiogallium in vitro: carrier mediated transfer, binding to the cell membrane, or simple diffusion. Addition of a metabolic inhibitor or an increase in gallium concentration did not change the PMN uptake. The action of trypsin and neuramidase on the cell wall removed 50-80% of the activity respectively. Thus, the hypothesis of carrier or simple diffusion were ruled out in favor of the membrane binding (28).

Later studies showed that the amount of radiogallium incorporated by granulocytes was very small, but in the case of in vitro hypoxia of granulocytes, the gallium uptake was found to be more than 6 times its normal value after 45 minutes of incubation (90). Also centrifugation of the exudate of an abcess after ^{67}Ga scanning revealed that the proportion of ^{67}Ga found correlated with the number of nonviable granulocytes (89).

PMNs are rich in lactoferrin (LF), another storage protein for iron which appears to be the major intracellular binding protein for gallium in the neutrophil (91,92). The binding of gallium to lactoferrin is stronger than for transferrin (91). After 1/2 hour of incubation of gallium labelled TF with unlabelled LF, not only will LF bind any unbound gallium present, but it will also remove almost all the Ga from the TF (93). Intramuscular injection of LF was reported to cause accumulation of i.v. ^{67}Ga at the injection site (94). Thus, it has been suggested that the accumulation of gallium radioactivity at the inflammatory site may be caused by the passage of free or bound gallium from the blood pool with subsequent binding to lactoferrin of the damaged PMN, or to lactoferrin released into the inflammatory exudate by the damaged PMN (89,92,94).

Clinical and laboratory studies have demonstrated that the radiogallium accumulation in the inflamed area will take place even if leukopenia is present (95,96). Thus, a nonviable PMN accumulation appears not to be essential (95). Uptake by bacteria such as *S. aureus* has been demonstrated to be an alternative pathway of accumulation but it is not essential either (96).

Terner *et al.* (97), injected ^{125}I and ^{67}Ga dual-labelled TF, followed by injection of ^{68}Ga citrate, to dogs with inflammatory lesions. The ratio between ^{125}I and ^{67}Ga was found to be constant, and the similarity between the uptake of ^{68}Ga citrate and ^{67}Ga-^{125}I TF suggested a similar pattern of uptake. The dissociation of ^{67}Ga TF and the accumulation of the radioisotope due to subsequent binding to

lactoferrin cannot be accounted for in such a case. Injection of $^{99}Tc^{m}$ labelled leucocytes did not show as much accumulation as the ^{67}Ga . It then appeared to those workers that the uptake of gallium in abcess would have many mechanisms involved, such as binding of the ^{67}Ga to cellular components of fragmented or damaged cells as well as proteins accumulation due to increase in permeability.

10. Gallium Uptake in Myocardial Infarct

Myocardial infarction is accompanied by an inflammatory response, and the accumulation of ^{67}Ga citrate in inflammatory areas in the heart (such as infarction or abcess) has been described. Kramer et al. (98) postulated that gallium can show accumulation in an infarcted area of the heart. A myocardial infarct (MI) in a dog, induced by coronary artery ligation (correlated with CPK and histological studies) showed an accumulation of radiogallium 24 hours after the MI, and could be related to PMN infiltration. In a histological study, an accumulation of radiogallium was seen 24 hours after the MI, and could be related to PMN infiltration. Histological examination of all the tissues which were positive on the radiogallium scan revealed the presence of PMN. In all negative scan areas, few or no PMN were present. Also, the uptake decreased as the granulocyte invasion diminished.

Comparing ^{67}Ga citrate uptake with other infarct mapping agents ($^{99}Tc^{m}$ diphosphonate, $^{99}Tc^{m}$ glucoheptonate and $^{99}Tc^{m}$ tetracycline) Zweiman et al. (99), reported an accumulation of gallium citrate in the infarct area with a ratio of MI:normal of 1.9:1 after infarction.

This ratio was the lowest one of all the compounds studied (Table 6).

A problem that limits the usefulness of ^{67}Ga citrate as a differential diagnostic agent in MI is that the gallium will accumulate in any sterile or nonsterile inflammatory process (100).

Dewanjee et al. (71) injected ^{68}Ga phosphate chelates (GaEMDP and GaDTPMP) into a rabbit with a ligated coronary artery. The first product showed a significant accumulation, while other one did not. The only other difference observed between these two products was that the GaDTPMP was not protein bound in the plasma to the same extent as the GaEMDP.

TABLE VI

CONCENTRATION RATIOS BETWEEN INFARCT AND SURROUNDING TISSUES

(±s.e.m.)[a]

	Percent injected dose x 1000 / gm infarcted tissue	Infarct:normal
^{99m}Tc-diphosphonate	5.9 ± 1.9	27.9 ± 6.5
^{99m}Tc-glucoheptonate	3.6 ± 1.2	11.2 ± 2.7
^{99m}Tc-oxytetracycline	3.4 ± 0.2	9.2 ± 1.6
^{99m}Tc-tetracycline	4.3 ± 0.3	7.7 ± 1.5
^{99m}Tc-chlorotetracycline	3.2 ± 0.8	7.7 ± 0.7
^{99m}Tc-chlorodimethyl tetracycline	2.7 ± 0.5	6.9 ± 1.1
^{67}Ga-citrate	-	1.9 0.6

(a) from reference 99

II. Phosphate Complexes

A. Chemistry of Condensed Phosphate Complexes and Phosphonate

Pyrophosphate (PPi) is classified as a condensed phosphate and represents two units of orthophosphate which is the basic phosphate unit. It is generally obtained by heating orthophosphoric acid (H_3PO_4), which dimerizes *via* elimination of H_2O (101). The resulting molecule has a tetrahedric structure linked together by an oxygen atom. The molecule is not linear and the P-O-P bond is rarely at 180^o. The product is highly hygroscopic and is hydrolyzed in moist air or in solution at a rate dependent on pH (Fig. 1.).

Methylenediphosphonate (MDP) has a structure similar to that of pyrophosphate but instead of an oxygen atom linking the two units of phosphate, the MDP has a CH_2 bridging the two moieties (Fig. 2). The presence of a carbon atom increases the resistance to hydrolysis. Hydrolysis of MDP requires 62 Kcal of energy per mole while the PPi needs 29 Kcal per mole at a pH of 6.2 (102).

The MDP cannot be prepared as easily as the PPi. The production of MDP is done *via* preparation and hydrolysis of a tetra alkyl ether: (103). Table VII lists the dissociation constants of pyrophosphoric acid and methylenediphosphoric acid.

FIGURE 1

THE EFFECT OF H^+ ON THE RATE OF HYDROLYSIS OF PYROPHOSPHORIC ACID AT 70°C IN WATER (a)

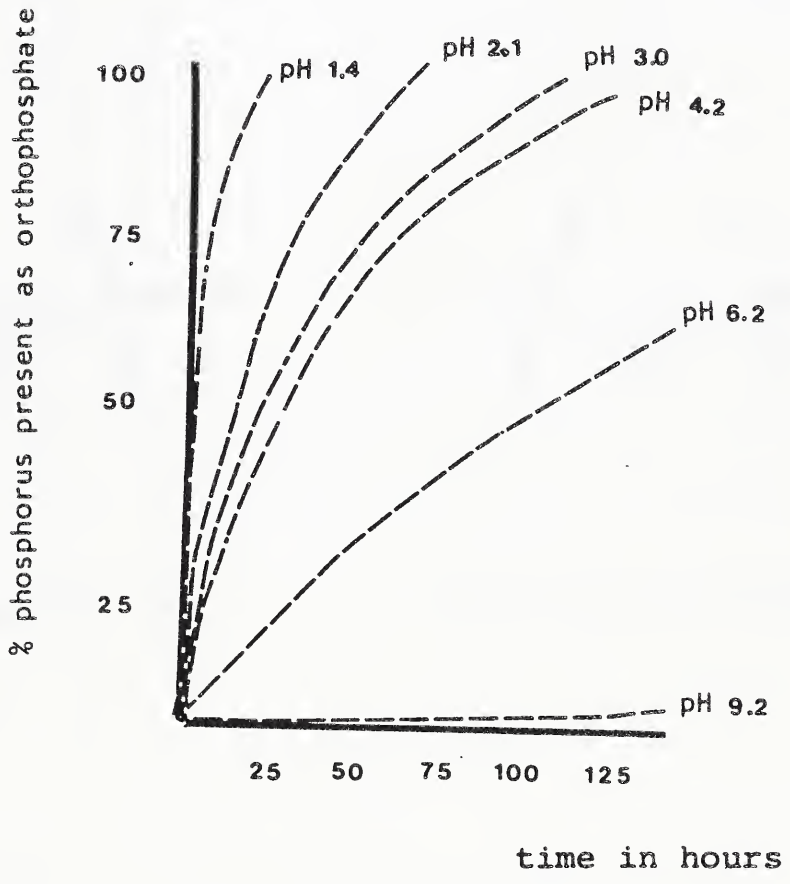

(a) from reference 101

FIGURE 2

STRUCTURE OF PYROPHOSPHATE AND METHYLENEDIPHOSPHONONATE (a)

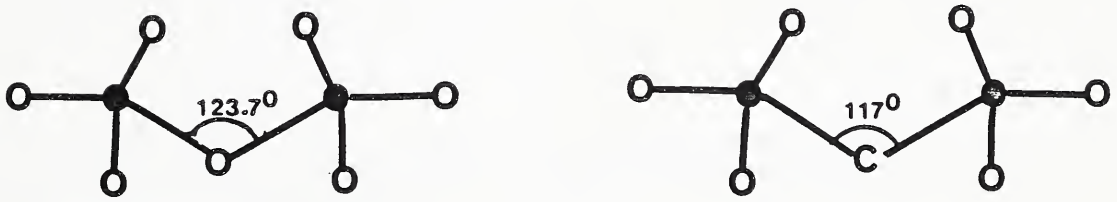

PYROPHOSPHATE

METHYLENEDIPHOSPHONONATE

● Phosphorus

O Oxygen

C Carbon

(a) from reference 115

Table VII

DISSOCIATION CONSTANTS OF PPi AND MDP AT AN IONIC STRENGTH OF 1[a]

PPi		MDP	
pK_1	0.46	pK_1	2.20
pK_2	1.18	pK_2	2.87
pK_3	5.34	pK_3	7.45
pK_4	7.70	pK_4	10.64

[a] From References 101,102

In the presence of multivalent ions, the phosphate derivative will chelate and form an amorphous precipitate which remains in this form until crystallization occurs (101). The calcium chelate of phosphate is a good example of this precipitate formation, and the resulting product is an important biological complex. When phosphoric acid is mixed with Ca^{2+}, an amorphous precipitate appears which is a mixture of $CaHPO_4$ (Ca:P=1), $Ca_4(HPO_4)_3$ octacalcium phosphate (Ca:P=1.33) and even $Ca_3(PO_4)_2$ tricalcium phosphate (Ca:P=1.5) (104). In vitro, a mixture of these amorphous forms is converted into hydroxyapatite $[Ca_0(PO_4)_6(OH)_2]$ which is the predominant form of calcium phosphate in the bone (105,106). This is a very complicated structure and the final model has not yet been determined.

The different factors which are known to affect the aggregation of the crystalline structure of hydroxyapatite are: the Ca:P ratio, the [Ca][P] product, the pH, and the presence of other phosphate compounds such as PPi and MDP. The mechanism of aggregation is probably due to electrostatic forces (107). In a supersaturated solution, the amorphous calcium phosphate will be in constant exchange with the active growing site of the crystal (108).

The presence of PPi, MDP or ethylenehydroxydiphosphonate (EHDP) affects the growth and the dissolution of the crystal both in vitro and in vivo (109). PPi, MDP and EHDP assume a "W" shape which results in three possible bidentates for MDP and PPi and a bidentate and a tridentate structure for EHDP (106). These products are chemisorbed at the active site strongly enough to inhibit any further exchange or

capture of phosphate by the crystal (108,110,111).

It is speculated that the calcium can assume two coordinate forms at the crystal surface. One has an irregular seven coordinate environment which can bind the polydentate residue (eg. MDP, EHDP, PPi) in a number of ways. Secondly, the calcium can have a symmetrical triangular face which can fit the EHDP tridentate in a manner such they bind tightly together and prevent any further exchange of phosphate with calcium at this site (108). The higher attraction of phosphonate compound for hydroxyapatite can be demonstrated in a simple experiment whereby the hydroxyapatite crystal is exposed to PPi, MDP, EHDP in a continual flow of solution. The dissolution of hydroxyapatite measured by the appearance of Ca^{2+} and PO_4^{3-} in the solution, is hindered by the presence of all products. However, less EHDP than PPi is required to block the active site of dissolution (112).

When chelated with technetium, each MDP molecule will be linked to two atoms of $^{99}Tc^m$ to form a polymer where the ratio of MDP:$^{99}Tc^m$ is 1:1. The W shape is preserved. If a suitable functional group is present on the central carbon atom, the complex is able to act as a bidentate-tridentate and its sorption to the hydroxyapatite crystal is enhanced (106).

B. Biological Behavior of Technetium Phosphate Complexes

1. Plasma Disappearance

Following intravenous injection in humans, technetium-99m

pyrophosphate ($^{99}Tc^{m}PPi$) blood levels follow a biexponential disappearance curve during the first four hours. The disappearance half-life (T 1/2) was found to be 13.6 min for the first component and 380 minutes for the second (113). Over a longer period of time, $^{99}Tc^{m}PPi$ and technetium-99m methylenediphosphonate ($^{99}Tc^{m}MDP$) demonstrate a triexponential blood disappearance pattern. For $^{99}Tc^{m}PPi$, the T 1/2 of the first, second and third component were reported to be 0.03 hr, 0.64 hr and 53.7 hr respectively, while for the $^{99}Tc^{m}MDP$ they were 0.04 hr, 0.85 hr and 14.5 hr respectively (114). In a more sophisticated experiment, Makler and Charkes (115) used a 5 compartment model to describe the biodistribution of $^{99}Tc^{m}MDP$ in humans. The blood clearance was rapid, the $^{99}Tc^{m}MDP$ being eliminated faster than $^{99}Tc^{m}PPi$ (116). After 10 minutes, only 10% of the injected dose of $^{99}Tc^{m}MDP$/liter was still in circulation and 1% remained after 4 hours (116). At similar times, the blood levels of $^{99}Tc^{m}PPi$ were 6.4%/liter and 1.9%/liter respectively (113).

2. Binding to Blood Components

It was found that a large proportion of the radioactivity was bound to blood proteins after intravenous administration of $^{99}Tc^{m}PPi$ (113,118). Because dilution of the radiopharmaceutical resulted in a decrease in bone uptake, an increased uptake by the kidney and an increased uptake by albumin, it was proposed that some of the complex dissociated, with subsequent binding of the reduced technetium to the proteins (119,120). It was concluded that the extent of protein binding of technetium in plasma could be an indirect measure of the *in vivo* stability of the phosphate complex (119). There is more $^{99}Tc^{m}PPi$

bound to the blood proteins than $^{99}Tc^{m}MDP$ (121). For both complexes, the fraction of blood radioactivity that is protein bound increases with time, while the percent of the injected dose bound to this fraction decreases (118). Due to fast urinary excretion and rapid bone uptake, the unbound phosphate complexes are removed from the blood before the protein bound fraction, thus producing a relatively higher amount of protein bound activity in the blood (117). One *in vitro* study showed that the bindingf $^{99}Tc^{m}$ phosphate complexes to albumin increased with time: 19.7% of ^{99}TcmMDP in solution was bound after 5 minutes and 33% after 30 minutes; $^{99}Tc^{m}PPi$ was 58% bound after 5 minutes and 79% after 30 minutes (119). In humans, 35 to 50% of the plasma $^{99}Tc^{m}PPi$ was bound to proteins after the first hours, and 55 to 66% after 3 to 4 hours (114,118). The $^{99}Tc^{m}MDP$ was bound to the extent of 22.4% to 30% after the first hour, and 39% to 45% after three hours (114,118). A somewhat lower value was observed by other investigators (117). The binding affinity of $^{99}Tc^{m}PPi$ to various proteins has been reported as follows: albumin 32.6%, alpha-globulin 29.4%, beta-globulin 23.3%, fibrinogen 5.7% and gamma-globulin 8.9% (113).

In contrast to the $^{99}Tc^{m}MDP$ behavior (120), a fraction of $^{99}Tc^{m}PPi$ has been found to be associated with the red blood cells: 1.2% of the injected dose per liter of RBC at 3 hours (114,116,122). Of the $^{99}Tc^{m}PPi$ remaining in the vascular compartment 10-30% is bound to the RBC after 1-3 hours, 40% after 4 hours and up to 60% after 24 hours (114,116). It has not been established whether the association of TcPPi with RBC is a result of binding of the whole complex to the

RBC membrane or due to the binding of a dissociated form of the complex (116).

3. Tissue Distribution of $^{99}Tc^{m}PPi$ and $^{99}Tc^{m}MDP$

With the exception of blood and bone tissue, the main organs of uptake are the liver and the kidney (123). The typical biodistribution of $^{99}Tc^{m}PPi$ and $^{99}Tc^{m}MDP$ in rabbit is shown in Table VIII. Significant accumulation in other organs such as the thyroid and stomach can be observed (123,124). This is usually due to the presence of free pertechnetate resulting from poor labelling or aging of the solution. As early as 5 hours after preparation, stomach uptake was noted (126). It was also shown that a dilution of the labelled MDP complex resulted in hydrolysis of the complex, leading to the formation of TcO_4^- ions (119). When a solution of potassium perchlorate was administered to reduce any artifacts due to pertechnetate accumulation in the thyroid, it was found that some activity was seen in the neck region, as a result of uptake of the MDP complex in the thyroid cartilage (127).

The phosphate complexes of technetium have been shown to accumulate in different pathologies such as a bone malignancy and metastasis, in lesions such as bursitis, in soft tissue tumors such as those of the breast and lung, in liver during hypercalcemia, and in the exudate of malignant ascites (123,128,129).

TABLE VIII

Organ Distribution of $^{99}Tc^{m}PPi$ and $^{99}Tc^{m}MDP$ at 2 hrs in rabbits (a,b,c,)

	PPi	MDP
Blood	3.76	0.96
Liver	1.30	0.34
Kidney	1.75	1.70
Femur	0.80	2.34
Marrow	0.37	0.30

(a) value expressed as percent dose in the entire organ

(b) expressed as mean of at least 6 animals

(c) from ref. 125

4. Excretion of $^{99}Tc^{m}$PPi and $^{99}Tc^{m}$MDP complexes

The $^{99}Tc^{m}$ phosphate complexes are readily eliminated in the urine, which is the major route of excretion. GIT excretion is negligible (114). The blood clearance of $^{99}Tc^{m}$MDP is faster than that of $^{99}Tc^{m}$PPi (114,130). Depending on the species studied, $^{99}Tc^{m}$MDP exhibits different excretion rates; its elimination is faster in dogs than in humans (114). The excretion of $^{99}Tc^{m}$PPi is mainly influenced by two factors: the degradability of the P-O-P bond and the protein binding. $^{99}Tc^{m}$MDP is not protein bound to the same extent, and will therefore show a higher renal clearance than $^{99}Tc^{m}$PPi. It has been proposed that their distribution would be similar if no protein were present (118). In general, the age of the subject also influences the excretion of $^{99}Tc^{m}$MDP and there is an inverse relationship between age and excretion rate (122).

5. Bone Uptake

It has been observed that the bone uptake of $^{99}Tc^{m}$phosphate complexes occurs mainly during the first distribution phase and maximum uptake can be seen after 30 to 56 minutes (113,115). The rate of blood clearance influences the degree of bone uptake; those complexes with the highest blood clearance have the greatest bone uptake (131). Additionally, an inverse relationship exists between bone uptake and the degree of protein binding (118). Because of the long delay in the clearance of $^{99}Tc^{m}$PPi from soft tissues, it is necessary to wait 4 hours to obtain a satisfactory scan (114) while $^{99}Tc^{m}$MDP will give the best image after 2 hours (115).

The mode of action of this kind of scanning agent is believed to be by sorption to the calcium of hydroxyapatite in bone (132). The accumulation of the complex was shown to occur in areas such as the growing centers of the bone and in inflammatory lesions where high blood flow is seen (132). Apparently, vascularity is not the only determinant factor for the $^{99}Tc^{m}$MDP bone deposition (133). A directly proportional increase in bone uptake was not seen when the rate of arterial blood flow in a dog tibia was altered: a four fold increase in blood flow resulted in an increased bone uptake of only 38%, and a saturation effect was suggested (133). However, a second injection of $^{99}Tc^{m}$MDP produced additional bone uptake, which discounted the saturation theory. The authors then suggested the existence of a rate limiting step in the transfer of the complex from blood to bone. Diffusion from the vascular compartment to the extravascular space is rapid when compared to the rate of diffusion from the extracellular fluid to bone, and increased vascularity would not be expected to greatly increase this rate (133).

The exact mechanism of deposition of the tracer in bone is not well understood. Autoradiography of bone tissue suggested that the $^{99}Tc^{m}$phosphate complex was deposited along the surface of the small vascular channels and the narrow space in the less mineralized surface (134). It was assumed that the complex travelled to the bone, remained there as a unit and was deposited by chemisorption to the hydroxyapatite crystal (132,135). Other histological studies by autoradiography suggested a different distribution of $^{99}Tc^{m}$PPi and ^{47}Ca in bone tissue; the labelled pyrophosphate stayed in the protein

vicinity while the calcium was mixed with the mineral pool (136). However, a comparison of $^{99}Tc^{m}PPi$, $^{99}Tc^{m}O_4^-$ ions, ^{32}P-PPi, and ^{47}Ca by incubation of the radiopharmaceuticals with normal, demineralized or inorganic (without matrix) bone, showed that the $^{99}Tc^{m}PPi$ had a high uptake in both demineralized bone and inorganic samples. Pertechnetate showed a lower uptake than in normal bone when the organic matrix was removed, and the ^{47}Ca uptake decreased after demineralization of the bone sample. ^{32}P-PPi still showed a high uptake in both demineralized and mineralized bone but not to the extent of the $^{99}Tc^{m}PPi$ uptake (137). Because $^{99}Tc^{m}PPi$ is bivalent, it has been suggested that the technetium moiety could bind to the organic matrix, while the phosphate would be incorporated in the mineral part. In immature collagen (which has less intermolecular linkage) an increase of uptake is seen (137). This explains why a scan is positive 24 to 48 hours after a bone trauma, since at this time the new tissue starts to develop (138). On the other hand, because of the instability of the $^{99}Tc^{m}PPi$ complex, Schumichen et al. (119,120,121) suggested that the complex would be hydrolyzed and the resulting $^{99}Tc^{m}(OH)_4$ would bind to the calcifying bone matrix.

C. Technetium Phosphate in Myocardial Infarction

1. Clinical Studies with $^{99}Tc^{m}$ Pyrophosphate

In 1974, Bonte et al (139) first described the localization of $^{99}Tc^{m}PPi$ in myocardial infarcts. In a study performed on dogs, a significant accumulation of the complex was noticed in the infarcted area, producing a ratio of radioactivity in myocardial infarcted tissue to normal tissue (MI/NO) of 10:1, twelve to twenty-four hours

after the infarction (139).

In an infarct model produced by ligation of the left anterior descending coronary artery in rabbits, significant uptake of $^{99}Tc^{m}PPi$ occurred twenty-four hours after surgery (140). The uptake became more pronounced after forty-eight hours and after seventy-two hours, it started to decrease, thus correlating with the removal of the dead cells (140,141). It was noticed that the inner endocardial layer of the heart contained ten times as much radioactivity as the outer layer because of the lesser degrees of infarction produced in the inner layers due to better blood flow (141).

The uptake of $^{99}Tc^{m}PPi$ was found to be a function of the time elapsed since the period of ligation (142). Buja et al. (142) submitted dogs to a ligation of the left anterior descending coronary artery, with reperfusion after eight minutes for some dogs, and permanent occlusion for others. The first group of dogs showed no myocardial accumulation, while the second group showed a diffuse uptake eight minutes after injection. When the blood pool effect had decreased, after twelve minutes, the infarct area could be delineated (142). One to two days after total ligation, the presence of a transmural myocardial infarct was seen as a doughnut shape (142) i.e. an area of increased uptake "hot" surrounding a "cold" central area (142,143). The hot area was due to the reperfusion of the peripheral areas of the infarct, allowing uptake of $^{99}Tc^{m}PPi$ (142), while the center still had reduced blood flow (142,143). The reperfused, but necrotic cells were responsible for the uptake (145). It was also pointed out that the uptake did not necessarily indicate only

irreversible injury, as a positive scan can occur in area with only moderate diminuation of blood flow (99,145). Partially necrotic regions containing $^{99}Tc^{m}PPi$ were found to be a small area and at the periphery of the infarcted area, and were typically located in the subepicardial region adjacent to the subendocardial area of the extrusive homogenous necrosis (145).

The time course of myocardial infarct uptake of $^{99}Tc^{m}PPi$ is very well defined and the majority of authors agree that the peak of uptake appears between forty-eight and seventy-two hours after the infarct, and ninety minutes or less after injection of the radiopharmaceutical (145,146). After seventy-two hours, the necrotic cells are replaced by fibroblasts, the image slowly fades and the ratio MI/NO slowly returns to a value of 1:1 (139,141). It was reported that in certain clinical cases where after the injection of $^{99}Tc^{m}PPi$, even six months after a documented infarct, a positive uptake was seen (147).

Clinically, the $^{99}Tc^{m}PPi$ uptake has been related to the usual manifestation of the myocardial infarct (148). High myocardial localization has been associated with a high blood level of creatine phosphokinase (CPK) and there is a highly significant inverse correlation ($r=0.85$, $p < 0.005$) between the radiopharmaceutical and the CPK content of the heart (149). There is also a correlation between the $^{99}Tc^{m}PPi$ uptake in the myocardial infarct and the specific ECG changes, the histological determinations, the infarct size determined by computer and the actual infarct weight (149,150).

In a study done on 1077 patients, Lyons et al. (146) established a good correlation between the myocardial infarct symptoms and the $^{99}Tc^{m}PPi$ scan. Myocardial scintigraphy using $^{99}Tc^{m}PPi$ was evaluated using a three-term grading system: 1+ where uptake was present; 2+ where uptake was equal or greater than the rib uptake; and 3+ where uptake was equal or greater than the sternum uptake (146). Ninety-two percent of 331 patients with an established MI showed a 2+ positive scan. The transmural infarct was the easiest to detect (96% yield); the lowest detection rate was in patients with a lateral transmural infarct (75%) and a left bundle branch block (73%). Lessem (151) mentioned that the subendocardial lesion was somewhat more difficult to diagnose than transmural.

In the case of patients without a definitely proven acute myocardial infarct (AMI), 26% showed a positive scintigram, and 5% showed localized activity. These positive patients were mainly patients with acute pericarditis with potentially lethal arrhythmia or who had received cardioversion and on which it was difficult to evaluate a new AMI (146). This led others to use $^{99}Tc^{m}PPi$ to localize the presence of perioperative infarcts when other methods were considered to be useless (146).

The determination of the size of the infarct is limited by the topography of the heart. It was possible to accurately localize an anterior and anterolateral transmural MI with a 2 dimensional technique, but anterior nontransmural infarcts (subendocardial) were easily missed and required a 3 dimensional reconstruction (152).

Infarcts larger than three grams were easily detected (145).

Two different patterns of $^{99}Tc^{m}PPi$ uptake were seen: a localized pattern with AMI and a diffuse pattern of uptake with non acute AMI. Sixty-five percent of the patients with definite AMI showed a localized activity, but if the infarct had a subendocardial localization, this value fell to 44% (146). Only 5% of patients with heart disease and no myocardial infarction have shown a localized pattern (146). The localized pattern has also been reported in other pathologies such as chest pain syndrome, unstable angina, resuscitated patients, after defibrillation procedures, acute pericarditis, heart failure and aneurysm calcification (146,147,153,154).

Other pathological states also show some uptake and lead to false positive results. Examples are patients with carcinoma of the left lung, radical mastectomy, a secondary effect of hypoparathyroidism with complicating pericarditis or any evidence of intercostal calcification (146,155). It has been suggested that a sequential scintigram should be performed to dissipate any doubt in the diagnostic procedure (147).

The shape of the infarct scan can help to determine the prognosis. Rude et al. (143,156) showed that the patients with a doughnut pattern had an increased evidence of left ventricular failure, recurrent chest pain after 24 hours, and a higher rate of complication (such as cardiac death, nonfatal myocardial infarct, unstable angina pectoris, or decompensated congestive failure) when

discharged from the hospital. Persistent abnormal uptake occurred in 41% to 57% of the patients with positive scans and these correlated with recurrent hospital admission due to heart failure (41%), angina pectoris (77%) or other causes (157). Cowley et al. (158) reported that a patient with a persistent positive scintigram for ten to twelve weeks after AMI had anterior or anterolateral infarcts and also had angiographic akinetic segments corresponding to the scintigram localization.

Dazt et al. (159) studied the histological changes in patients with a persistent scintigram with histological studies at necropsy. All showed focal coagulation necrosis, myocytolysis, and no evidence of dystrophic calcification or of mural thrombus as it was proposed by earlier workers (158).

2. Comparison of $^{99}Tc^{m}$ Pyrophosphate and $^{99}Tc^{m}$ MDP in Myocardial Infarct Imaging.

Several studies have been done to evaluate the different $^{99}Tc^{m}$ labelled phosphates in terms of myocardial uptake using different infarct models. Davis et al. (160) produced an infarct in rats with the application of a hot iron to the heart. One hour after radiopharmaceutical administration and four hours after infarction, $^{99}Tc^{m}MDP$ showed a higher uptake than $^{99}Tc^{m}PPi$ with a ratio of MI/NO of 30.3:1 for $^{99}Tc^{m}MDP$ compared to 25.2:1 for $^{99}Tc^{m}PPi$. However, the percent injected dose per gram of infarcted tissue was 2.3% for $^{99}Tc^{m}PPi$ and 0.9% for $^{99}Tc^{m}MDP$, while the MI/Blood ratio was similar for both radiopharmaceuticals.

In rabbits, where an infarct was produced by intramural injection of vasopressin into the heart muscle, the $^{99}Tc^{m}PPi$ showed a higher ratio of MI:NO (6:1) than the $^{99}Tc^{m}MDP$ (4.8:1) one hour after injection (3). However, at later times, the ratio was higher for the $^{99}Tc^{m}MDP$ which showed a MI:NO ratio of 29.7:1 and 39.4:1 at six and twenty-four hours respectively, while the $^{99}Tc^{m}PPi$ showed a ratio of 20:1 at both times. The $^{99}Tc^{m}MDP$ was judged superior to the $^{99}Tc^{m}PPi$ preparation.

In a rat study with MI induced by catecholamines and stress, the MI to Normal ratio at 100 minutes and 300 minutes after injection was higher for the $^{99}Tc^{m}MDP$ (161). Because of its lower blood levels, $^{99}Tc^{m}MDP$ was considered as good as $^{99}Tc^{m}PPi$ even though the $^{99}Tc^{m}PPi$ showed a higher % uptake per gram of infarcted tissue (162).

However, clinical experience does not always correlate well with animal findings. In a comparison of the two products in patients showing a definite MI, as reflected by the blood enzyme level changes and ECG changes, it was found that the two products were equally satisfactory (163). Even if the $^{99}Tc^{m}MDP$ did not have as great an uptake as $^{99}Tc^{m}PPi$, the lower background permitted a good resolution of the infarct image.

Lyons et al. (164) described a study whereby forty-eight hours after the patients were scanned with $^{99}Tc^{m}PPi$, a scan with $^{99}Tc^{m}MDP$ was performed which was followed by another $^{99}Tc^{m}PPi$ scan. The results showed that the $^{99}Tc^{m}MDP$ scan was sometimes negative. These

authors, as well as Makhler (165) concluded that the $^{99}Tc^{m}MDP$ scan was less reliable than the $^{99}Tc^{m}PPi$ scan. Finally, Kelly et al. (166) injected the two products at random in twenty-five patients with clinical evidence of AMI, followed two days later by the injection of the alternate product. Ninety-six percent had a positive scan with $^{99}Tc^{m}PPi$ compared to only 71% with $^{99}Tc^{m}MDP$. They concluded that $^{99}Tc^{m}PPi$ was superior over $^{99}Tc^{m}MDP$ in the clinical detection of MI.

3. Mechanism of $^{99}Tc^{m}$ Phosphate Uptake in Myocardial Infarction

D'Agostino (167,168) reported that after ischemic infarction, there was a rapid influx of calcium ions into the injured cells. Electron dense crystals were seen in the mitochondria, and were identified as hydroxyapatite. Based on these results, and the attraction of different phosphates for the hydroxyapatite crystal, Bonte et al. (139) investigated the possibility of uptake of $^{99}Tc^{m}PPi$ by the infarct area of the heart.

Shen et al. (169) injected $^{45}CaCl_2$ before and after occlusion of a major branch of a coronary artery in dogs, and noted that if the occlusion was permanent, there was little uptake of the tracer by infarcted cells. If ischemia was induced for 45 minutes and followed by reperfusion, significant uptake occurred. A shorter period of ischemia failed to produce a radionuclide accumulating lesion. The authors proposed that the calcium uptake occurred in irreversibly damaged cells, but required a certain blood flow to permit accumulation of the calcium. To corroborate this hypothesis, Tofe et al. (170) induced MI in dogs by permanent occlusion of the left

anterior coronary artery, followed three days later by injection of $^{99}Tc^{m}PPi$ and $^{45}CaCl_2$. At necropsy, the ratio of radioactivity present in infarcted and normal tissue was calculated. In the center of the infarct, the ratio of MI:NO was 6.5:1 for $^{99}Tc^{m}PPi$ and 6.2:1 for $^{45}CaCl_2$. At the periphery of the infarct, the ratios were 17:1 for $^{99}Tc^{m}PPi$ and 16:1 for $^{45}CaCl_2$. The conclusion drawn correlated with the previous hypothesis, that less accumulation occurs in non-reperfused areas. Also, there is a similarity in the accumulation of radiocalcium and $^{99}Tc^{m}PPi$. However, even though the ratio of uptake was similar for the two products, the total radioactivity in the tissue did not show a linear correlation.

Mukherjee et al. (171) reported that, after 60 minutes of left anterior descending coronary artery occlusion followed by reperfusion, there was a good correlation between $^{99}Tc^{m}PPi$ accumulation and mitochondrial dysfunction (measured by oxygen consumption, QO_2). A 15 fold increase in $^{99}Tc^{m}PPi$ accumulation was accompanied by a 4 to 5 fold decrease in QO_2, and a 3 fold decrease in citrate synthetase activity. The uptake of $^{99}Tc^{m}PPi$ was also correlated with membrane phospholipid depletion and in vitro sarcolemmal calcium ion permeability (171).

Dewanjee et al. (172) proposed that $^{99}Tc^{m}PPi$ uptake in MI is associated with protein binding. Infarcts of varying size were induced in rabbits by ligation of the left anterior descending coronary artery proximally and distally. After the injection of $^{45}CaCl_2$, $^{99}Tc^{m}PPi$, and ^{32}P-PPi, they found a strong correlation

between the size of the infarct and the uptake of all radiotracers. However, there were differences in the ratio of uptake in the infarcted versus normal tissue. The ratio was 3 to 4 times greater for $^{99}Tc^{m}PPi$ than $^{45}CaCl_2$, and 2 to 3 times greater for $^{45}CaCl_2$ than ^{32}P-PPi. These results differ from those reported by Tofe (170) where the ratio of uptake of $^{99}Tc^{m}PPi$ and ^{45}Ca were similar. Intracellularly, only a small fraction of the radioactivity was found associated with the mitochondria, and a large portion was found in the supernatant after centrifugation. Gel filtration and dialysis showed that the $^{99}Tc^{m}PPi$ in serum was associated with protein, while ^{32}P-PPi was not. They found a good correlation between MI uptake and protein binding with the different tracers. Even if bound to protein, $^{99}Tc^{m}PPi$ can still bind to hydroxyapatite (173). When a plasma sample taken 5 minutes after injection of $^{99}Tc^{m}PPi$ was incubated with hydroxyapatite crystal, it was found that 85% of the radioactivity was bound to hydroxyapatite crystal. At one hour after injection, 50% of $^{99}Tc^{m}PPi$ was bound to hydroxyapatite.

It was proposed that polymorphonuclear leucocytes are involved in the uptake mechanism $^{99}Tc^{m}PPi$ in MI, as they have been shown to accumulate in the heart following infarction (174). However, if leukopenia is induced, the uptake is not affected which discounts this hypothesis (174).

Shelberg et al. (175) isolated fetal mice hearts and insulted them reversibly or irreversibly by deprivation of oxygen and glucose at $37^{o}C$ or $42^{o}C$, respectively. Electron microscopy of the heart

tissue showed that with a reversible insult, there was glycogen granule depletion and appearance of dense mitochondrial material, which disappeared 24 hours after the oxygen and glucose were returned to normal. With the irreversibly damaged hearts, the granules did not disappear after normal conditions were restored. When $^{99}Tc^{m}PPi$ was added to the culture media, no significant uptake was seen in the reversibly damaged tissue, but in the irreversibly damaged hearts, uptake was 3 times that of normal tissue. A poor correlation was found between the calcium content and $^{99}Tc^{m}$phosphate accumulation, and if all calcium was removed from the medium, no differences in uptake were observed.

EXPERIMENTAL

MATERIALS AND METHODS

I. Materials

A. Chemicals and Materials.

All chemicals used were of analytical grade. The following chemicals and materials were used:

1. Sodium acid pyrophosphate, Ventura Co., Beverly, MA (Lot 111472).
2. Methylene diphosphonic acid, Sigma Chemical Co., St. Louis, MO (lot 86c-5055).
3. Hydrochloric acid, 0.1N, Fisher Scientific Co., New Jersey.
4. Sodium hydroxide, 0.1N, Fisher Scientific Co., New Jersey.
5. Normal saline (N.S.), Fisher Scientific Co., New Jersey, (lot 12958-12).
6. Pyridine, Fisher Scientific Co., New Jersey (lot 790844).
7. Whatman No. 1 chromatography paper, Terochem, Edmonton, Alta.
8. PEI cellulose, Baker-Flex, Phillisburg, PA.
9. PD-10 gel chromatography columns, Pharmacia Fine Chemicals, Uppsala, Sweden.
10. Human Apotransferrin, Cal-Biochem-Behring, La Jolla, CA, (lot 002176).
11. Millipore Filter Type VS (0.02 um), Millipore Corp., Bedford, MA.
12. Sephadex G-200, Fine size 40-120 u, Pharmacia Fine Chemicals, Uppsala, Sweden.
13. HEPES Buffer, 0.1 M. pH 7.45, Sigma Chemical Co., St. Louis, lot 19c5048.
14. Isoproterenol Sulfate, Fluka AG, Buchas, Switzerland.

15. Boric acid, J.T. Baker Chemical, Phillisburg, PA.
16. Iodine monochloride, Terochem Labs., Edmonton, Alta.
17. Potassium iodide, McArthur Chemical Co. Ltd., Montreal.
18. Sodium thiosulfate, J.T. Baker Chemical Co., Phillisburg, PA.

B. Radioisotopes

The following radioisotopes were used:

1. $^{67}GaCl_3$, Merck-Frosst Radiopharmaceuticals, Montreal, 148-222 MBq/100 L in 0.1 N HCl. (N.C.A.)
2. ^{67}Ga citrate, Merck-Frosst Radiopharmaceuticals, Montreal, 74.6 MBq/mL no-carrier-added. (N.C.A.).
3. $^{99}Tc^{m}PPi$, Edmonton Radiopharmaceutical Center, 0.18 MBq/mL; 1.25 mg PPi/mL.
4. ^{125}I Sodium iodide. Atomic Energy of Canada Ltd., 400 MBq/mL N.C.A.

II. Methods

A. Preparation of Gallium-67 Complexes

1. ^{67}Gallium Pyrophosphate

^{67}Gallium pyrophosphate was prepared by adding 2 mL of a 1 mg/mL solution of sodium acid pyrophosphate in 0.1 N hydrochloric acid to 10 µL of a solution containing 148-222 MBq/100 mL of $^{67}GaCl_3$ (N.C.A.) in 0.1 N HCl. The mixture was agitated for 5 minutes with a magnetic stirrer and the pH recorded on a Beckman digital pH meter Model 3500. The pH was lower than 1. The pH was raised to neutrality by the slow addition of 0.1 N NaOH in 10 µL aliquots.

2. ^{67}Gallium Methylenediphosphonate

^{67}Ga methylenediphosphonate (^{67}GaMDP) was prepared using a procedure similar to the one described above, with methylenediphosphonic acid being used instead of sodium pyrophosphate.

3. ^{67}Gallium Hydroxide

Gallium-67 hydroxide was prepared by the slow addition of 0.1N NaOH solution to a 2.0 mL volume of $^{67}GaCl_3$ (N.C.A.) in normal saline. The final pH of the mixture was adjusted to the desired value as required by the experiment with 0.1 N NaOH.

4. ^{67}Gallium Citrate

^{67}Ga citrate was purchased from Merck-Frosst Radiopharmaceuticals (Montreal). It was assayed at 74.6 MBq/mL and contained benzyl alcohol as preservative. The stock solution of ^{67}Ga citrate was diluted in normal saline to obtain a concentration of 17.26-24.66/MBq/mL.

5. Human Apotransferrin Labelling

Human apotransferrin (20 mg) was dissolved in 1.5 mL of a borate buffer (24.74 g H_3BO_3 dissolved in 300 ml of 1.37 M NaCl with pH adjustment to 7.85 and final dilution to one liter with distilled water). To the transferrin solution was added 2-4 µL of NaI^{125}(AECL) plus 100 µL of a dilution of stock iodine monochloride solution (made by diluting 0.2 ml of a 3.4×10^{-3} N ICl solution to 5.0 mL with 2.0 N saline). The reaction was

allowed to proceed for 30-40 seconds with gentle vortexing and terminated by addition of 100 µL of "fixing solution" (0.25 g $Na_2S_2O_3$ plus 0.2 g KI dissolved in 100 µL of distilled water). Unreacted iodide was removed by separation of the reaction mixture on a Sephadex PD-10 column that was equilibrated and eluted with 0.1 M HEPES. Usual labelling efficiency obtained was between 50% and 65%.

One ml of the resulting solution was incubated with 0.1 ml of the ^{67}GaPPi solution (1 KBq/ml ^{67}Ga, 0.5 mg/ml PPi) for 1 and 6 hours at room temperature. The resulting solution was analyzed by gel filtration on Sephadex G-200 and analyzed for ^{67}Ga and ^{125}I in a Beckman 8000 gamma spectrometer. Necessary adjustment for the spillover of the ^{67}Ga counts into the ^{125}I channel were made (see appendix I).

B. Sample Analysis Techniques

1. Paper Chromatography

Different chromatographic systems were used to determine the radiochemical purity of the prepared ^{67}Ga complexes. The first one consisted of a solvent phase containing ethanol (95%) and doubled distilled water in a 1:1 proportion. Whatman No. 1 filter paper was used as the stationary phase. Ten microliters of the solution to be analyzed was applied at the origin, and the strip was developed over 10 centimeters.

The second system consisted of 1 N NaCl solvent, migrating on a polyethylenimine cellulose (PEI cellulose) thin layer plate. PEI cellulose is an ion exchanger and is used to separate

different nucleotide phosphate sugars based on the size of the phosphate moiety (176).

The third system was described by Hnatowich (4) and consisted of Whatman No.1 chromatography paper as the stationary phase and a mixture of pyridine, ethanol 95%, and doubled distilled water in a 1:2:4 proportion, with the pH of the solvent adjusted to 3,4,6,7 or 11 with 1.0 N NaOH or 1.0 N HCl. The solution to be analyzed was applied at the origin and immediately developed over a distance of ten centimeters. The migration required 1 to 1.5 hours.

When the amount of radioactivity on the chromatogram was sufficient, it was measured using a chromatography strip scanner, consisting of a tray moving under a collimated NaI (Tl) crystal with analyzer levels set to detect ^{67}Ga. If the amount of radioactivity was too low for detection by this procedure, the ten centimeter strip was cut into segments of one centimeter each, which were counted separately in a Searle 1185 multisample well type NaI (Tl) gamma spectrometer calibrated to measure ^{67}Ga. The radioactivity on each one centimeter section was calculated as a percentage of the total radioactivity on the strip.

2. Gel Chromatography

Gel chromatography techniques were used for the analytic separation of various phosphate complexes, and their degradation products. For this purpose, a prepacked PD-10 column having a bed volume of 9.1 mL was used. The column was prepacked with Sephadex G-25 swollen in normal saline to a bed height of 5 cm. Normal saline (N.S.) was also used as an eluant and each column was

stabilized by elution with normal saline for 15 minutes prior to sample application. The void volume was determined with blue Dextran, and was found to be 4.5 ml. Between each repetitive run, each column was washed with a solution containing 1 mg sodium pyrophosphate in 1 mL of 0.1 N HCl to remove any residual radioactivity on the column.

In the later experiments, gel chromatography was used to separate the ^{67}Ga phosphate complexes from transferrin in order to study the binding of ^{67}GaPPi to this protein. In this case, Sephadex G-200 fine was packed in a column (1 cm diameter, 20 centimeter height) and elution was effected by means of HEPES (0.1 M, pH 7.45) buffer.

The eluates from the various columns were continuously monitored by means of a NaI(Tl) detector connected to a NIM type amplifier, SCA, rate meter and counter. The eluate was also monitored on line with a UV detector. All signal outputs were directed to a 2 channel X-Y recorder. Serial samples were collected in a fraction collector and counted later in an automatic gamma spectrometer.

3. Ultracentrifugation

A sample of 175 µL from each complexation product was centrifuged for one hour at 100,000 rpm at an average force of 132,000 g on a Beckman Airfuge. Ten microliter triplicates were withdrawn from the sample before centrifugation and similar aliquots were taken from near the top of the solution after centrifugation. Each aliquot was then counted in a gamma

spectrometer and the results were expressed as:

$$\frac{\text{radioactivity in 10 } \mu L \text{ after centrifugation}}{\text{radioactivity in 10 } \mu L \text{ before centrifugation}} \times 100$$

C. Animal Studies

1. Tissue Distribution in Normal Mice

Male ICR mice, weighing between to 20 to 30 g, and maintained on a Lab-blox® diet and water ad libitum were used. The animals received via tail-vein injection, a volume of 0.1 ml of the product being investigated: ^{67}GaPPi , ^{67}GaMDP, ^{67}Ga citrate, or $^{67}Ga(OH)_3$, all at pH 7. Before injection, the ^{67}Ga phosphate complex was purified via gel filtration and immediately after injection, each mouse was placed in a whole body counter, set to measure ^{67}Ga radioactivity, and the radioactivity in each mouse was counted for 1 minute. A similar dose was counted in a Searle 1185 gamma counter at the same time. By measuring a ^{67}Ga standard in both counters, a correction factor was calculated which was used to determine the exact injected dose in each mouse. Using this method, the dose was individualized for each mouse.

The mice were then sacrificed by exsanguination via cardiac puncture under ether anesthesia at 5, 10, 15, 30, 60, 120, 240, 360 and 720 minutes post injection and the blood removed by cardiac puncture. The liver, spleen, kidneys, GIT, tail and a sample of the bone (tibia shaft) was removed, washed in normal saline, dried on a paper towel, weighed and counted in the Searle 1185 gamma ray spectrometer. A sample of blood was also taken,

weighed and counted. The blood weight was assumed to constitute 6.5% of body weight (177).

A 0.5 ml sample of blood was drawn in a heparinized syringe and centrifuged for 10 minutes and the plasma separated from the cell fraction. The cell fraction was washed three times with normal saline and the wash solution added to the plasma. The red cell and plasma fractions were counted separately in a Searle 1185 gamma ray spectrometer. Fifty microliters of the plasma fraction was deposited on a desalting millipore membrane filter (Type VS) floating on a N.S. solution. The membrane filter can remove all highly diffusible salts (178). After 15 minutes, the sample was removed from the filter with a micropippet and assayed for radioactivity. The same volume of untreated plasma was also counted. The results are expressed as percentage of radioactivity of desalted to non-desalted plasma.

2. Myocardial Infarct Model in Rats

A cardiac infarct model was developed following a method similar to the one described by Kung et al (179,180). A 0.5 ml solution of isoproterenol sulfate (100 mg/mL) was injected subcutaneously in male Sprague Dawley rats weighing approximately 200 g each. The animals were allowed Lab-blox® and water ad libitum. Six hours after the isoproterenol injection, the femoral vein was exposed under sodium pentobarbital anesthesia, and 0.1 mL of the purified ^{67}GaPPi was injected. This was followed by a wash of normal saline and, through the same needle, 0.1 mL of a solution of $^{99}Tc^{m}$PPi was also injected. The rats were sacrified

at one and six hours after injection by exsanguination *via* the abdominal artery under ether anesthesia. The heart and liver were removed, washed in normal saline and weighed. A 0.1 mL sample of each injected solution was used as a standard to determine the injected dose. All selected organs and standard samples were counted in a Beckman 8000 gamma spectrometer. A correction for ^{67}Ga spillover activity into the $^{99}Tc^{m}$ channel was made (see appendix II).

D. Kinetic Analysis

A statistical program was used to determine the best fitting concentration-time curves in the whole blood and in each gram of blood. The programs used were AUTOAN and NONLIN which were made available and analyzed by a pharmacokinetic expert. AUTOAN is a curve stripping program that plots the observed data into the best fitting curve, determines the number of exponential components, and calculates the different kinetic parameters. The NONLIN program makes use of these parameters as well as the original data to obtain a better estimate of the parameters of the concentration-time curve.

RESULTS AND DISCUSSIONS

RESULTS AND DISCUSSION

I. Characterization of Gallium Phosphate Complexes

In the presence of an equimolar quantity of pyrophosphate and gallium, a complex or series of complexes are formed in which a 1:1 ratio of gallium to phosphate are present. This is also observed even in the presence of excess phosphate (19,20). The product so obtained generally has a very low solubility thus leading to the speculation that the gallium pyrophosphate complex decomposes with time and as a result of pH changes, to the formation of an insoluble gallium hydroxide species (4).

The major problem in the characterization of various gallium phosphate complexes is to differentiate between the particular phosphate derivative and the hydroxide form of gallium at neutral pH. Paper chromatography, gel chromatography and ultracentrifugation techniques were employed in this investigation to assay for various radiochemical species present initially in the preparation as well as for any decomposition products of the gallium complexes which result at later time intervals.

A. Paper Chromatography

Several solvent systems were used in an attempt to separate the various components of the ^{67}GaPPi complex. Using Whatman No 1 filter paper and an ethanol solvent system (ethanol 95%: water, 1:1) the migration of the radioactivity after the application of ^{67}Ga pyrophosphate at the origin was seen to change as a function of pH as

illustrated in Fig. 3. At a low pH value of 1.3, two radioactive peaks were obtained, one at the origin and one at a Rf value of 0.9. At pH 6 most of the radioactivity stayed at the origin as a broad peak. At pH 7 the peak was much sharper and also centered at the origin, while at pH 12, the product migrated with an Rf value of 4.5. The change observed in migration after varying the pH of the product indicated that the gallium pyrophosphate complex had undergone a transformation as a result of changes in hydrogen ion concentrations. Such behavior of gallium complexes had previously been observed by Kulprathipanja and Hnatowich (4).

Goulet et al. (72) used a similar chromatography system to differentiate ^{67}Ga tripolyphosphate from $Ga(OH)_3$ at neutral pH. But in their experiments, the ^{67}Ga tripolyphosphate at pH 7 was observed to migrate with a Rf value of 0.6 and the gallium hydroxide remained at the origin. Although under identical conditions in these experiments, ^{67}Ga pyrophosphate remained at the point of origin except in solutions with very low or high pH values.

According to Chudinova et al. (18,19,20), the gallium pyrophosphate can assume 3 different forms depending on the pH and the concentration ratio PPi/Ga. Initially, when the ratio of pyrophosphate to gallium is less than 0.75, the complex $Ga_4P_2O_7$ is present. When the ratio of PPi/Ga is increased and the pH is between 2.5 and 4.5, this results in the formation of the more soluble $NaGaP_2O_7$ complex (19,20). These two forms probably account for the presence of the two radioactive peaks at pH 1.3 (Fig. 3). As the pH

FIGURE 3

PAPER RADIOCHROMATOGRAPHIC SEPARATION

OF ^{67}GaPPi: EFFECT OF pH ALTERATION (a)

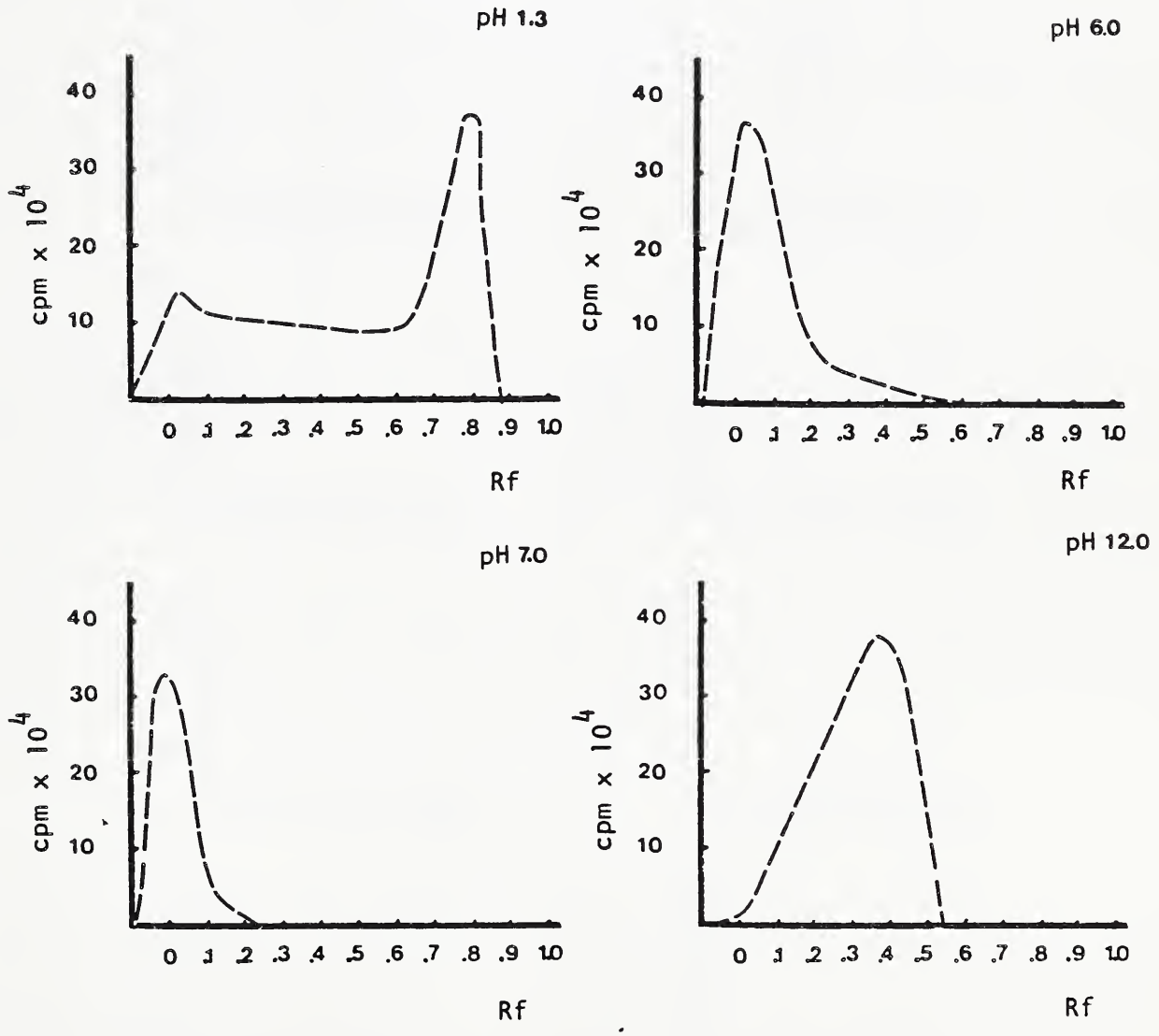

(a) Radiochromatographic system consisting of Whatman No. 1 paper with ethanol 95% water:(1:1) as solvent.

FIGURE 4

RADIOCHROMATOGRAPHIC PROFILES OF $^{67}GaPPi$ AND $^{67}GaCl_3$

EFFECT OF pH ALTERATION (a)

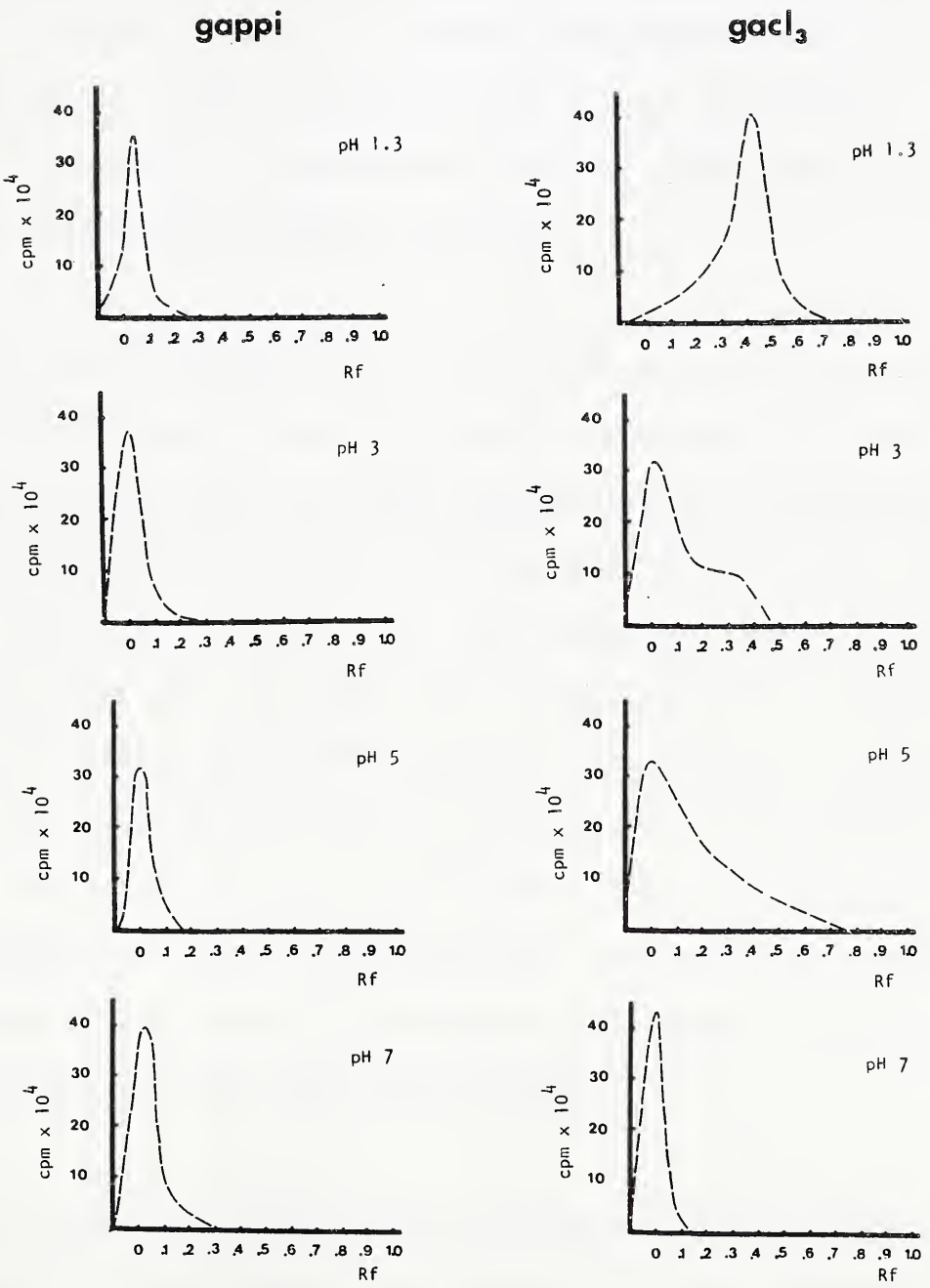

a) Radiochromatographic system consisting of PEI cellulose eluted with NaCl (1N) as solvent.

is raised even further (pH > 4.5), the $Na_2GaOHP_2O_7$ species is obtained and the latter exhibits a very low solubility. However, as the concentration ratio of PPi:Ga is increased further, as is the case in this experiment, one would expect $NaGaP_2O_7$ to appear at a low pH and would thus result in the presence of a soluble peak at lower pH. Finally, as the pH value is increased considerably to a value of 12, the migration of the radioactive spot is seen to increase. This is probably caused by the dissociation of the complex and the formation of the soluble gallate $Ga(OH)_4^-$ ion (21).

The second chromatographic system used consisted of PEI cellulose (polyethylenimine cellulose) and 1N NaCl as solvent. PEI cellulose is an ion exchanger and allows the differentiation of various phosphate nucleotides based on the size of the chain length (176). Figure 4 shows the results obtained when this system was used. It is quite apparent from this experiment that is not possible to differentiate between $^{67}Ga(OH)_3$ and $^{67}GaPPi$ complex. At a low pH, a difference in the Rf of these two products is perceived, due to the presence of the ionic form of gallium while the $^{67}GaPPi$ complex is not soluble enough to migrate. As the pH is increased, the transition between the different hydroxy species is noted due to the gradual formation of the less soluble and less ionic species $Ga(OH)_3$.

By using the solvent system (pyridine: ethanol: water, 1:2:4) described by Kulprathipanja and Hnatowich (4), the effect of the pH change of the solvent can also be seen to influence the migration of the radioactive peak (Fig. 5). A major peak having a Rf value of 0.8

FIGURE 5

RADIOCHROMATOGRAPHIC PROFILES OF ^{67}GaPPi

EFFECT OF pH ALTERATION (a)

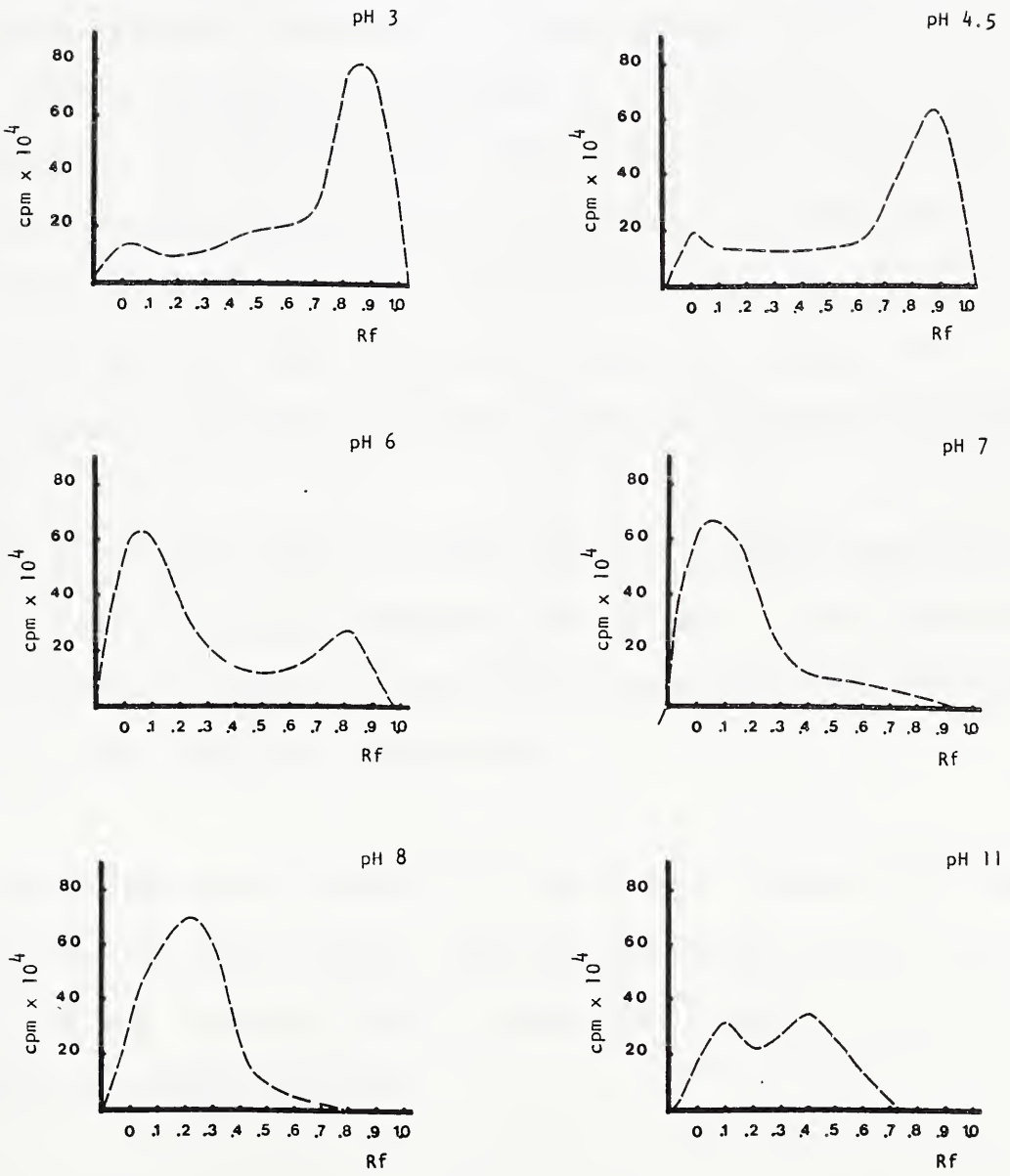

(a) Radiochromatographic system consisting of Whatman No. 1 paper developed with a mixture of pyridine:ethanol:water (1:2:4:) as solvent.

to 0.9 slowly disappears to give rise to a long tail and finally a second peak is observed at the origin (pH 6). As the pH is further increased beyond the neutralization point, the presence of the soluble $Ga(OH)_4^-$ ion is revealed by the appearance of a radioactive peak with an Rf value of 0.4-0.5 at pH 11.

The quantitative relationship of such changes is given in Table IX which reveals the drastic transformation of ^{67}GaPPi as a result of increased pH. Of interest is the finding that such a change was also influenced by time as seen in Table X whereby the concentration of the radioactive spot at the origin almost doubled after four hours. This indicated that both time and pH dependency play a major role in the chromatography separation of ^{67}GaPPi and its transformation products.

The pattern was almost identical when the ^{67}GaMDP preparation was subjected to this same chromatographic system. Such quantitative relationships are given in Tables XI and XII, which show the effects of pH and time dependence respectively.

Kulprathipanja and Hnatowich (4) explained the behavior of $^{67}GaCl_3$ in the same pyridine, ethanol, water solvent system by the fact that as the pH was increased, $Ga(OH)_3$ was gradually formed and the latter remained at the spot of origin.

Because the behaviour of $^{67}GaCl_3$ at neutral pH was not much different than that of ^{67}GaPPi and ^{67}GaMDP, the above methods were deemed not sufficient to isolate the phosphate complexes. Thus, other

radioanalytical methods were evaluated.

TABLE IX

QUANTITATIVE RADIOCHROMATOGRAPHIC CHANGES OF ^{67}GaPPi AS A FUNCTION OF pH [a,b]

pH	% at the origin	% from Rf .3 to .7	% at Rf 0.8
3	11.2	23.5	65.3
4	22.4	23.9	53.7
6	54.4	24.8	20.7
7	74.4	14.9	10.7
8	84	13.6	2.4
11	40	57.8	2.1

(a) chromatogram system consisting of Whatman chromatographic paper developed with a mixture of pyridine: ethanol: water, 1:2:4 as solvent.

(b) % activity calculated on the basis of the fractional activity of the whole chromatogram.

TABLE X

EFFECT OF TIME AND pH OF THE DEVELOPING SOLVENT ON THE RADIOCHROMATOGRAPHIC SEPARATION OF ^{67}GaPPi (a)

time	pH	% at the origin	% at Rf=0.8
0	6	42	16
	7	45	14
2 hrs	6	60	8
	7	62	10
4 hrs	6	84	5
	7	80	5

(a) Chromatographic system consisting of Whatman No. 2 paper developed with a mixture of pyridine: ethanol: water, 1:2:4 as solvent.

TABLE XI

QUANTITATIVE RADIOCHROMATOGRAPHIC CHANGE OF ^{67}Ga MDP AS A FUNCTION OF THE pH [a,b]

pH	% at the origin	% at Rf 0.3 to 0.7	% at Rf 0.8
3	2.5	10.6	86.9
4	10.1	11.3	78.6
6	25.2	23.0	51.8
7	35.1	21.5	44.4

(a) Chromatogram system consisting of Whatman chromatographic paper developed with a mixture of pyridine: ethanol: water, 1:2:4 as solvent.

(b) % of activity calculated on the basis of the fractional activity of the whole chromatogram.

TABLE XII

EFFECT OF THE TIME AND pH OF THE SOLVENT SYSTEM ON THE RADIOCHROMATOGRAPHIC SEPARATION OF $^{67}GaMDP$ (a)

Time	pH	% at the origin	% at Rf = 0.8
0	6	14	58
	7	24	51
2 hrs	6	33	36
	7	38	26
4 hrs	6	49	32
	7	51	13
6 hrs	6	61	23
	7	60	7
8 hrs	6	59	15
	7	73	4

(a) Chromatographic system consisting of Whatman chromatographic paper developed with a mixture of pyridine: ethanol: water, 1:2:4 as solvent.

B. Gel Filtration

Aliquots of the ^{67}Ga pyrophosphate complex were loaded onto a Sephadex G 25 column (PD-10) and eluted with normal saline. At neutral pH, $^{67}GaPPi$ appeared to have an elution volume peak at 5.5 mL. However, it was noted that an aqueous solution of this compound tended to give two peaks in the elution profile. Eventually, only the peak at the elution volume of 4.5 mL was observed (figure 6). The rate of change from one to the other was found to depend not only on the time but probably also on the room temperature with the result that a complete transition was noted to occur within 1 to 6 hours. Because we suspected the gradual formation of gallium hydroxide, an experiment was conducted in which $^{67}GaCl_3$ was diluted in normal saline and the pH adjusted to 7.2. The chromatographic profile of such a preparation is given in Figure 7. It was apparent that gallium hydroxide was eluted differently than either form of $^{67}GaPPi$. This is further confirmed by Aulbert (49) who also reported a late elution of $Ga(OH)_3$ on Sephadex G-25 superfine even though he used a different eluting solvent (veronal HCl pH 8.6) than the one used in this investigation. From the above experiments, we might conclude that the non-migrating spot in figure 5 (pH 7) was not the result of hydroxide formation, and it may be composed of different phosphate forms of radiogallium.

A similar set of experiments were conducted with ^{67}Ga MDP. Figure 8 illustrates the comparative paper chromatogram (Whatman No. 1, solvent system pyridine: ethanol: water, 1:2:4, pH 7) and gel chromatography (Sephadex G-25, PD 10 column) of the same aqueous

FIGURE 6

GEL RADIOCHROMATOGRAPHIC PROFILES OF ^{67}GaPPi ON SEPHADEX G-25 (a)

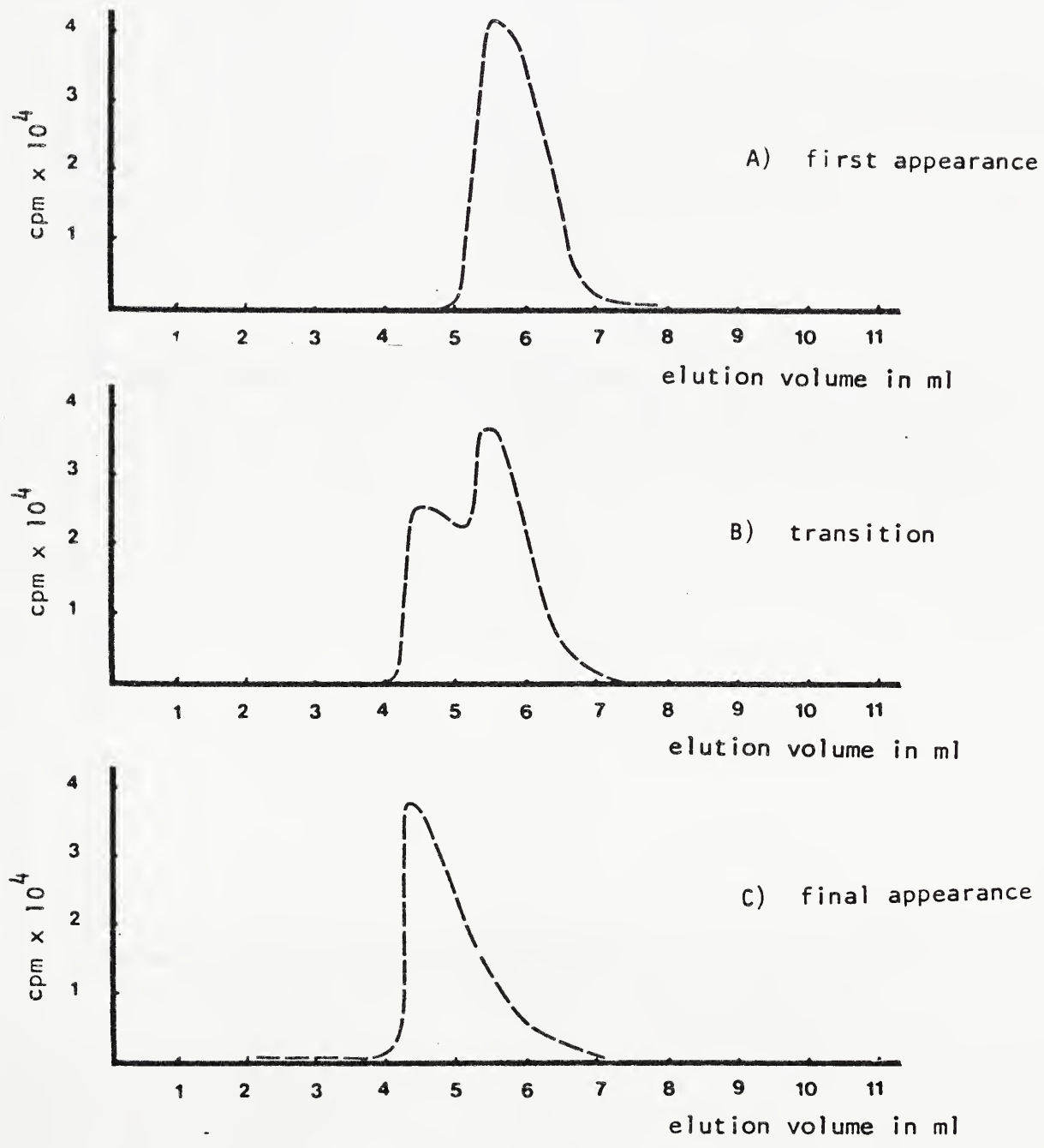

(a) Normal saline as solvent

FIGURE 7

GEL RADIOCHROMATOGRAPHIC PROFILES OF $^{67}GaPPi$ AND $^{67}GaCl_3$ ON SEPHADEX G-25 (a)

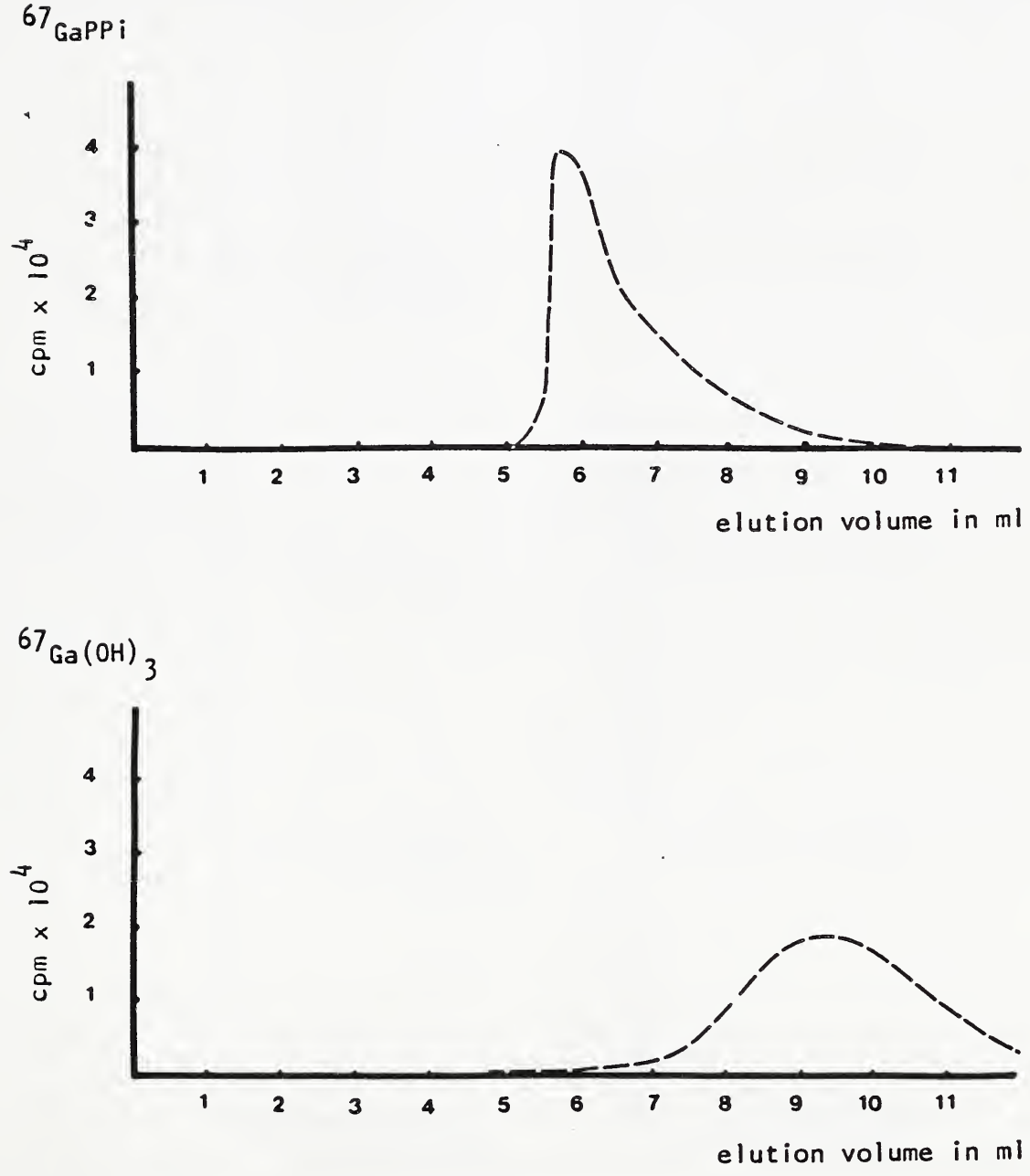

(a) Normal saline as solvent

FIGURE 8

RADIOCHROMATOGRAPHIC PROFILES OF ^{67}GaMDP (a,b)

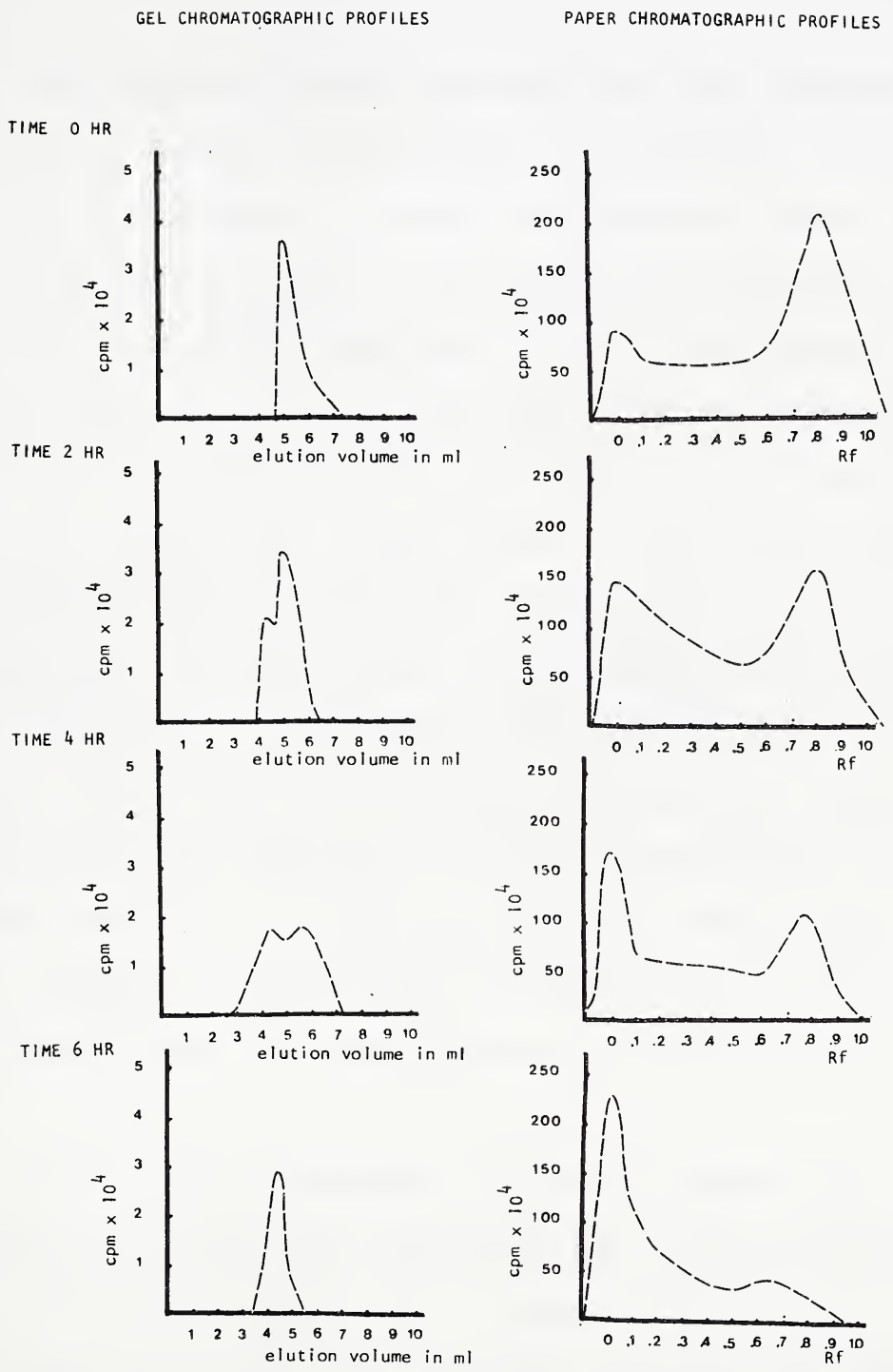
GEL CHROMATOGRAPHIC PROFILES
PAPER CHROMATOGRAPHIC PROFILES
TIME 0 HR
TIME 2 HR
TIME 4 HR
TIME 6 HR
cpm x 10^4
elution volume in ml
Rf
1 2 3 4 5 6 7 8 9 10
0 .1 .2 .3 .4 .5 .6 .7 .8 .9 10

(a) Gel radiochromatographic system consisting of Sephadex G-25 eluted with normal saline

(b) Paper radiochromatographic system consisting of Whatman No. 1 paper developed with a mixture of pyridine:ethanol:water (1:2:4) at pH 7 as solvent.

solution of ^{67}GaMDP at different time intervals at room temperature. It was also noted that the transition occurred at a much slower rate than in the case of ^{67}GaPPi.

The nature of the two observed peaks was intriguing enough to warrant a further chromatographic investigation. In a different series of experiments, a paper chromatographic (Whatman No. 1 and pyridine: ethanol: water, 1:2:4 solvent) examination was conducted on a solution of ^{67}GaMDP immediately prior to loading onto a Sephadex G-25 column, and on the fraction eluted from the latter at the elution volume of 4.5 and 5.5 mL (Fig. 9). It was found that at pH 6, the fraction eluted from the gel column at the 5.5 mL elution volume corresponded to the spot with a Rf value of 0.8 on the paper chromatogram (Fig. 9). At pH 7 no such separation was evident and it was not possible to discriminate chromatographically between the two most likely forms of ^{67}Gallium pyrophosphate because of the manipulation time required to develop the chromatogram and the rapid ^{67}GaPPi transition from one form to another. Almost identical results were observed in the case of ^{67}GaMDP but a small amount of radioactivity was still migrating at an Rf of 0.8 (Fig. 8).

Gallium and pyrophosphate ions were demonstrated to have an attraction to each other (pK equilibrium = 1.10 at pH 3.05 (22) but the resulting complex has a very low solubility in water. Kulprathipanja et al. (4) mentioned the possibility that the low solubility was the result of the instability of the complex and the subsequent formation of $Ga(OH)_3$. On the basis of our own experiments,

FIGURE 9

PAPER RADIOCHROMATOGRAPHIC PROFILES OF ^{67}GaPPi

PRIOR TO AND POST GEL FILTRATION (a,b)

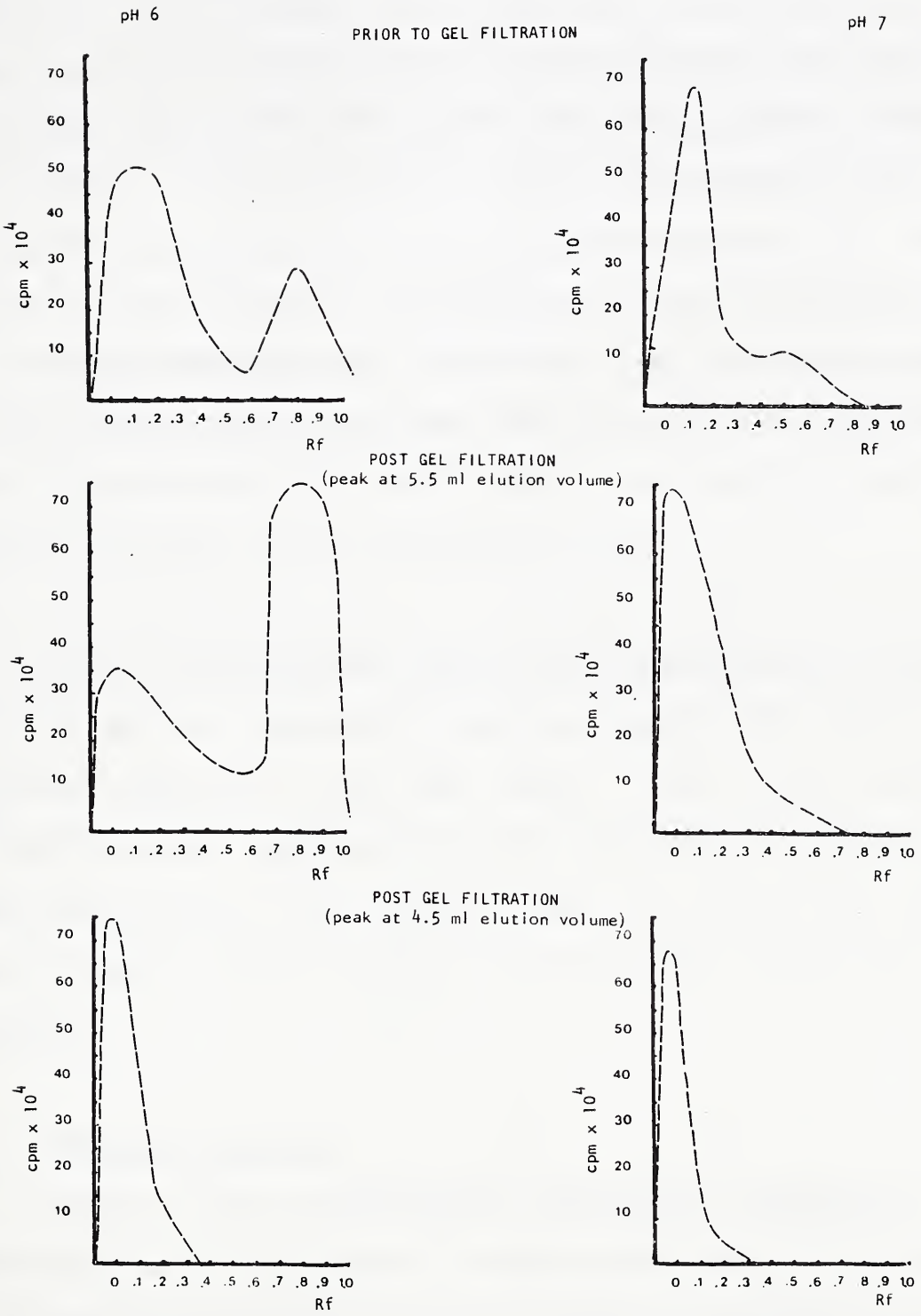

(a) Paper radiochromatographic system consisting of Whatman #1 chromatographic paper developed with a mixture of pyridine:ethanol:water (1:2:4) as solvent.

(b) Gel filtration consisting of Sephadex G-25 (PD-10 column) eluted with normal saline.

this hydroxide form will also behave in many chromatographic systems in a way similar to the pyrophosphate derivative of radiogallium. However, other workers described the low solubility of the pyrophosphate derivative to be due to the transition from the soluble $NaGaP_2O_7$ form to the non soluble $Na_2GaOHP_2O_7$ form. From our experiment, it appears that on paper chromatography (Fig. 6) a transition can be seen at a pH value of approximately 4.5. This pH value fits well with the transition pH described by Chudinova (20). It should be emphasized that in their work, the concentration ratio of PPi/Ga did not have a value higher than ten while in our experiments 1 mg of pyrophosphate and a small amount of gallium N.C.A. were used, leading to higher PPi/Ga concentration ratios.

The gel chromatography results also indicated that a transition in the gallium pyrophosphate species occurred with time with a distinct separation of the two forms. The elution profile of $^{67}Ga(OH)_3$ at the concentration used, was completely different from that observed with ^{67}GaPPi complex. Thus, it is evident that the less soluble complex cannot be simply attributed to the formation of simple $Ga(OH)_3$.

C. Ultracentrifugation

Because of the chromatographic ambiguities encountered in our previous studies, and because it was reported that gallium phosphate was sparingly soluble (6), an effort was made to estimate the relative amount of soluble complex of various ^{67}Ga derivatives. Ultracentrifugation was our method of choice because of its inherent

simplicity. Ultracentrifugation has been reported to be useful for sizing radioparticles (181). Thus, it is possible to estimate the amount of soluble material after appropriate centrifugations. Different aqueous solution of $^{67}GaPPi$, $^{67}GaMDP$ and $^{67}GaCl_3$ were prepared and aliquots of these solutions were ultracentrifuged at 135,000 g (100,000 rpm) for one hour and the activity of the supernatant measured prior to and after centrifugation. The ratio was then used as a solubility index on the assumption that any colloidal form would be precipitated at such centrifugal force. Since the radiogallium used was in a no carrier added form, the absolute amount of the element present could be calculated from the formula:

$$A = \lambda N$$

where A = radioactivity in dpm

λ = decay constant = $0.693/T_{1/2}$ in minutes

N = number of radiogallium atoms present

The amount of radioactivity present in the supernatant after centrifugation is then indicative of the solubility. At the concentration used and at a pH of 7, approximately 63% of the $Ga(OH)_3$ was still in the supernatant after centrifugation and corresponded to a concentration of 12.8×10^{-10} mol/L (Table XIII). For the $^{67}GaPPi$ and $^{67}GaMDP$ the amount in the supernatant was calculated to be 22.4×10^{-10} mol/L and 21.5×10^{-10} mol/L respectively. From these results, it can be deduced that the $^{67}GaPPi$ was almost twice as soluble as the hydroxide form. Moeller (10) has reported a value of $Ga(OH)_3$ solubility of 7×10^{-10} mol/L which is in the same range as the one reported in this experiment.

The significance of these experiments demonstrated that the preparation of non carrier added ^{67}GaPPi did not form any colloidal particles at the concentration used and that it could be used for biological trials.

TABLE XIII

SOLUBILITIES OF VARIOUS GALLIUM COMPLEXES

Product	Exp. No.	% in solution[a]	Concentration mol/l[b,c]
^{67}GaPPi	1	68%	20.1×10^{-10}
	2	77%	23.2×10^{-10}
	3	96%	29.5×10^{-10}
	4	86%	16.0×10^{-10}
	5	100%	25.4×10^{-10}
	6	90%	21.4×10^{-10}
	7	94%	21.6×10^{-10}
			mean: $22.4 \times 10^{-10} \pm 4.24 \times 10^{-10}$
^{67}GaMDP	1	98%	24.2×10^{-10}
	2	100%	24.4×10^{-10}
	3	100%	15.8×10^{-10}
			mean: $21.5 \times 10^{-10} \pm 4.9 \times 10^{-10}$
^{67}Ga(OH)$_3$	1	70%	18.48×10^{-10}
	2	62%	11.63×10^{-10}
	3	62%	9.88×10^{-10}
	4	59%	11.38×10^{-10}
			mean: $12.8 \times 10^{-10} \pm 3.8 \times 10^{-10}$

(a) expressed as

$$\frac{\text{activity in 10 ul of solution after ultracentrifugation}}{\text{activity in 10 ul of solution before ultracentrifugation}} \times 100$$

(b) solutions were at pH value between 6.5 and 7.8.

(c) calculated according to the formula described in the procedure.

II. Biological Behavior of the ^{67}Gallium Phosphate Complexes

Groups of mice were injected intravenously via tail vein with approximate 37 KBq in 0.1 ml solution of prepared ^{67}Ga pyrophosphate*, ^{67}Ga methylenediphosphonate*, ^{67}Ga hydroxide or commercially supplied ^{67}Ga citrate. At time intervals of 5 min, 15 min, 30 min, 1,2,4,6 and 12 hours, mice were sacrificed for tissue distribution studies. Blood samples were collected by cardiac puncture under ether anaesthesia and various organs and tissues were dissected, blotted free of blood and weighed. All samples were analyzed for ^{67}Ga radioactivity in a model 1185 Searle automatic well NaI(Tl) gamma spectrometer or a Beckman 8000 NaI(Tl) gamma spectrometer. The levels of radioactivity were expressed as percent of the injected dose per gram of tissue as well as percent of injected dose accumulated in an entire organ at each time interval. Total blood weight was calculated as 6.5% of the body weight (177) and the skeletal mass was estimated as 10% of the body weight (178).

---

* The sample to be injected was collected from the elution fraction at a volume of 5.5 ml after gel filtration on a Sephadex G-25 PD-10 column, immediately after preparation of the complex.

A. Blood Clearance of ^{67}Ga complexes

The blood levels of the different ^{67}Ga compounds at various times post injection are listed in Table XIV, and blood radioactivity expressed on a per gram basis is illustrated in Figures 10 and 11. It can be noted in Table XIV that the level of radioactivity in the blood following injection of ^{67}GaMDP and ^{67}GaPPi remained relatively stable during the first 15 minutes, followed by a rapid decline. During the first 15 minutes, the blood levels of the ^{67}GaPPi were higher than those seen with ^{67}GaMDP. However, the levels from 30 minutes to 12 hours were almost identical. The drop in the blood level activity was not as prominent with ^{67}Ga citrate, where the blood level remained high for the first hour. The blood level of ^{67}Ga hydroxide showed a lower activity at all time intervals, as expected. Although the mean blood level values of $Ga(OH)_3$ at 15 minutes appeared to increase relative to the levels at 5 minutes post injection,this could be due to the large standard deviation. No statistical difference could be found between the blood level activity at 5 minutes and 15 minutes ($p < 0.3$. t-test).

When the data are expressed in terms of percent of injected dose per gram of blood as illustrated in Figure 10, it is evident that ^{67}GaPPi and ^{67}GaMDP behave similarly with no statistical difference noted between the blood levels of the two products.

Comparison of the blood levels of ^{67}Ga citrate with those of ^{67}GaPPi revealed that the ^{67}Ga citrate followed a different pattern

TABLE XIV

BLOOD LEVEL OF VARIOUS ^{67}Ga-COMPLEXES FOLLOWING IV INJECTION IN MICE [a,b]

	5 min	15 min	30 min	1 hr	2 hr	4 hr	6 hr	12 hr
^{67}GaPPi	30.4 ±6.9	33.7 ±6.3	18.4 ±5.7	13.1 ±4.3	14.2 ±2.6	11.6 ±1.4	9.9 ±1.4	5.6 ±1.0
^{67}GaMDP	23.7 ±3.9	23.0 ±3.6	13.2 ±3.8	15.4 ±1.2	12.3 ±2.5	11.6 ±1.5	10.5 ±1.2	4.3 ±0.8
^{67}Ga-citrate	36.6 ±5.3	35.2 ±7.1	26.2 ±4.2	27.7 ±2.8	15.5 ±1.9	18.9 ±0.6	9.7 ±1.1	3.3 ±2.7
^{67}Ga-$(OH)_3$	20.4 ±3.0	25.3 ±5.6	12.5 ±2.7	10.2 ±3.1	4.7 ±2.5	2.2 ±0.9	3.5 ±0.9	1.7 ±0.9

(a) expressed as % injected dose remaining in the blood at various time intervals after IV injection of37 KBq of ^{67}Ga radioactivity.

(b) each value represents the mean ± standard deviation of 3 to 5 mice.

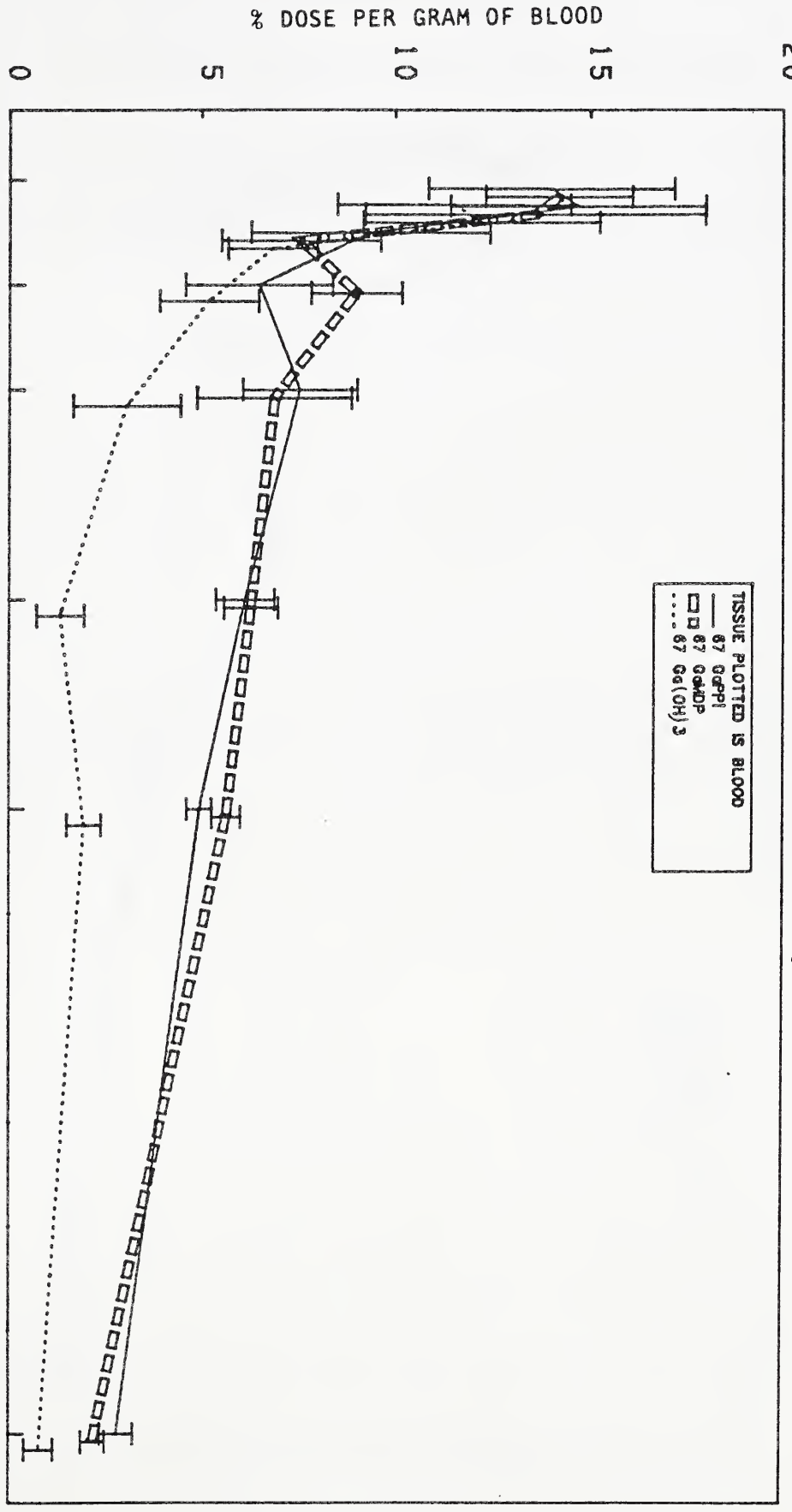

FIGURE 10

BLOOD RADIOACTIVITY LEVELS IN MICE AFTER INJECTION OF $^{67}GaPPi$, $^{67}GaMDP$, $^{67}Ga(OH)_3$

FIGURE 11

BLOOD RADIOACTIVITY LEVELS IN MICE AFTER INJECTION OF ^{67}GaPPi AND ^{67}Ga CITRATE

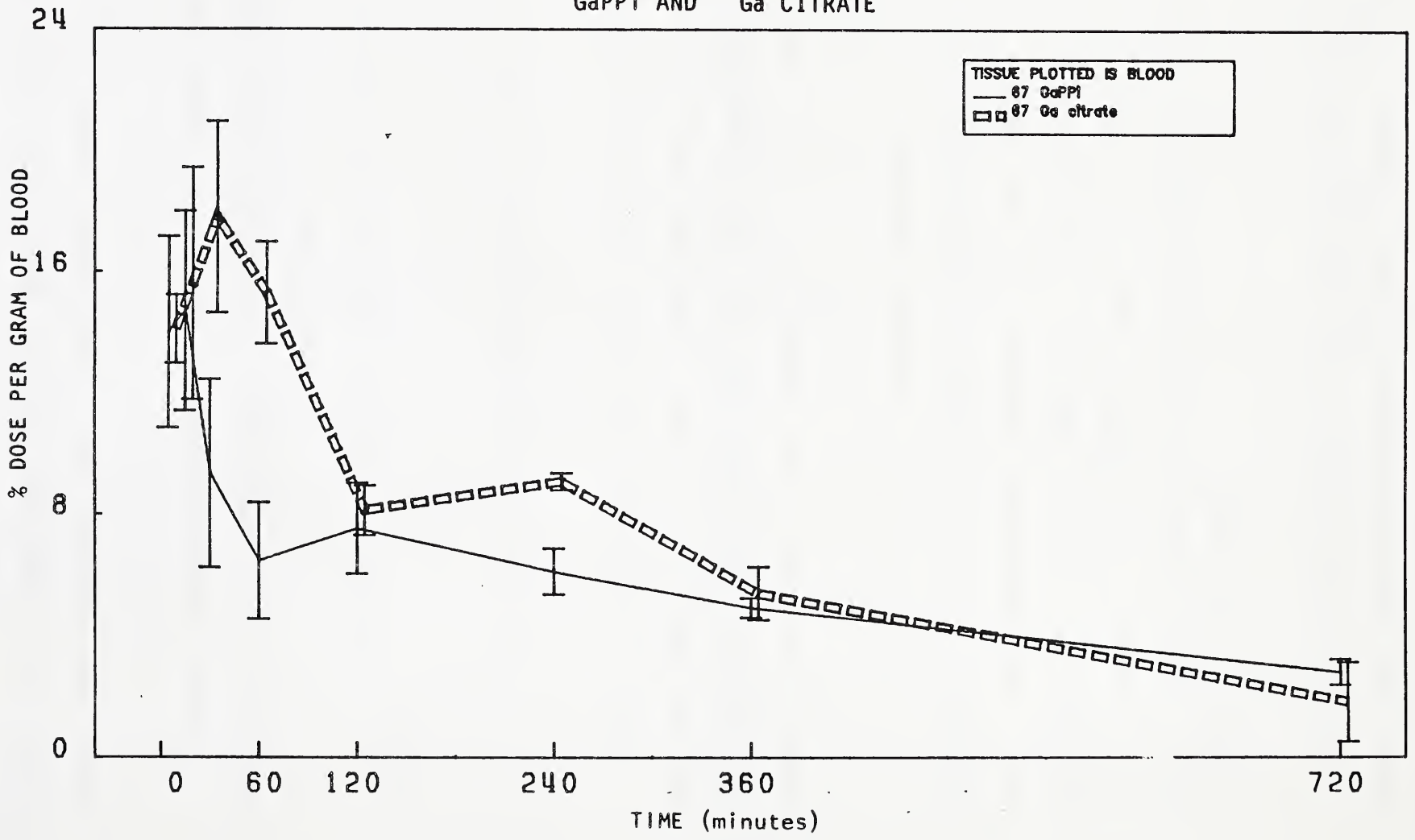

for the first 2 hours post injection; then for the rest of the study, similar blood level were seen in both products (Figure 11).

Standard computerized programs (NONLIN and AUTOAN) were used to determine the best fitting curve of the percent injected dose per gram of blood for each product. The AUTOAN program fits the data into a 1, 2, 3, or 4-exponential equation, then gives the parameters of the equation:

$$C_p = A_1e^{-\lambda 1t} + A_2e^{-\lambda 2t} + A_3e^{-\lambda 3t} + A_4e^{-\lambda 4t}$$

where C_p represents the plasma concentration at time t, A represents the maximum activity in each compartment and λ_1, λ_2, λ_3, λ_4 the individual distribution rate for each compartment, which is related to the slope for each component of the distribution curve.

For each of the four exponential equations, a coefficient of correlation is calculated between the concentration observed and the time. The exponential equation with the highest correlation coefficient will give the best fit. The NONLIN program uses the initial parameters from AUTOAN and improves the fit by minimizing the sum of weighted squares of the deviation and also minimizing the randomness of data points.

From the AUTOAN program, a two compartment model was chosen to describe the blood distribution of ^{67}GaPPi, ^{67}GaMDP, and $^{67}Ga(OH)_3$ up to 12 hours post-injection, and the extrapolated results from the

NONLIN program are plotted in Figure 12. Tables XV, XVI, XVII and XVIII compare the observed percent of injected dose in blood to the values calculated by the NONLIN and AUTOAN programs. The difference between the observed and calculated value is very small resulting in a very high correlation coefficient.

The parameters obtained from the biokinetic studies of ^{67}GaPPi, ^{67}GaMDP and $^{67}Ga(OH)_3$ are listed in Table XIX. The generated curves were divided into 2, one representing a fast distribution component of less than 2 hours, with distribution rate constant λ_1, and a longer distribution phase with an elimination constant λ_2. The coefficient of correlation (r) between the observed values and the time intervals after injection, when a 2 compartment model was chosen, were 0.97, 0.96, and 0.97 for ^{67}GaPPi, ^{67}GaMDP and $^{67}Ga(OH)_3$ respectively.

Again, the ^{67}GaPPi and ^{67}GaMDP data show almost identical pharmacokinetic parameters, as well as very similar initial concentration values in each compartment. Although the λ_1 and λ_2 values of $^{67}Ga(OH)_3$, ^{67}GaPPi and ^{67}GaMDP are not significantly different, as a result of the large standard deviation, the initial concentration of $^{67}Ga(OH)_3$ the second compartment is considerably different from the phosphate complexes (Table XIX).

Little research has been done on the biological behavior of the gallium phosphate complexes. Goulet et al. (72) also observed high blood levels after injection of ^{67}Ga tripolyphosphate; greater than those reported in this study. The high blood level was explained on

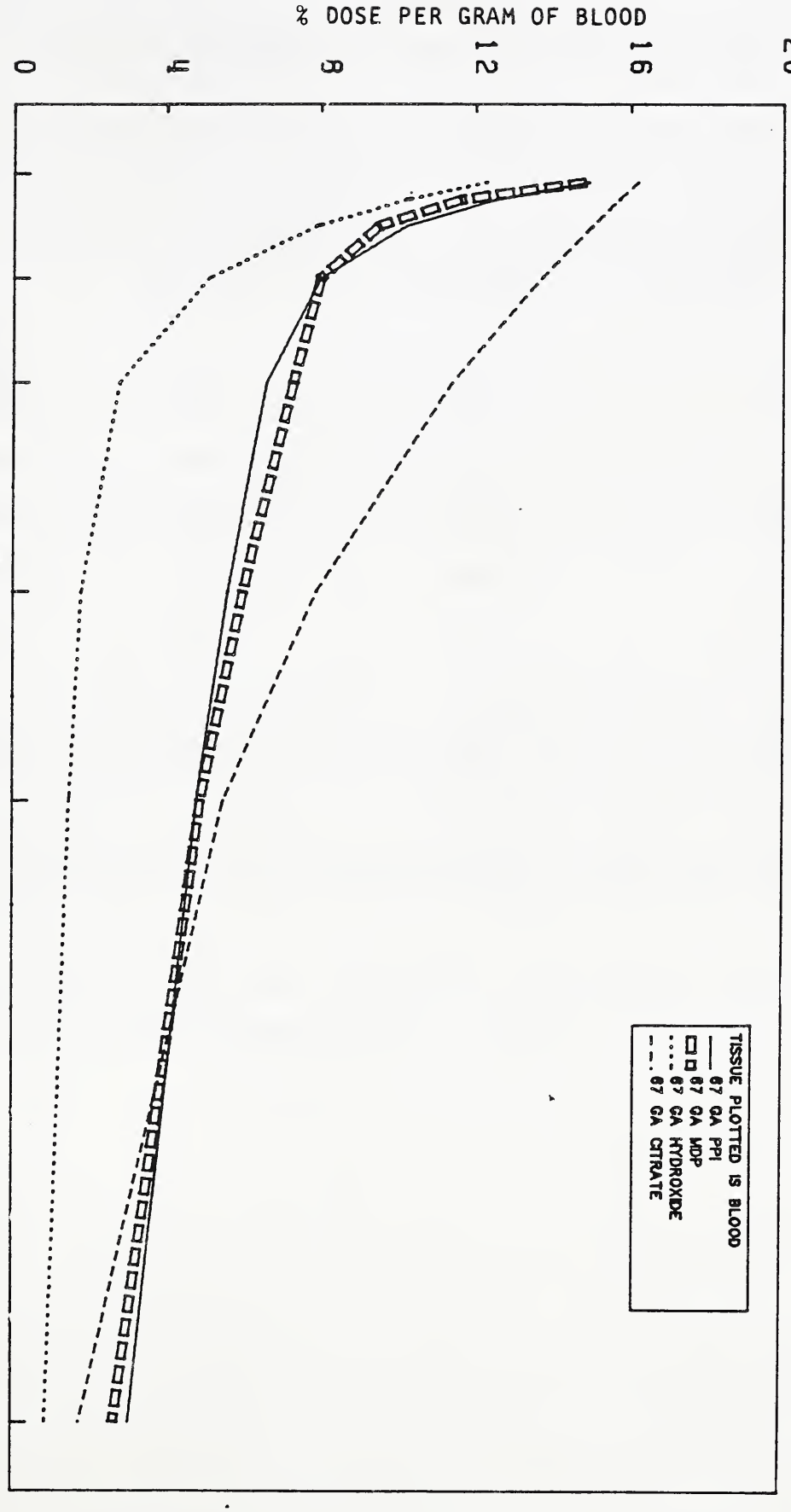

FIGURE 12

COMPUTER FITTED CURVES OF BLOOD CLEARANCE OF $^{67}GaPPi$, ^{67}Ga CITRATE AND $^{67}Ga(OH)_3$

TABLE XV

BLOOD LEVEL FOLLOWING IV INJECTION OF ^{67}GaPPi IN MICE [a,b]

time	observed	calculated	Difference (observed-calculated)
5 min	13.9	14.9	-0.9
15 min	14.7	12.5	2.2
30 min	9.4	10.2	-0.8
1 hr	7.5	7.9	-0.4
2 hr	6.5	6.6	-0.1
4 hr	6.1	5.6	0.5
6 hr	4.9	4.8	0.1
12 hr	2.8	3.1	-0.3

(a) value expressed as % injected dose per gram of blood from 3 to 5 mice.

(b) calculated values were obtained from the computer-fitted curve using the NONLIN/AUTOAN computer program.

TABLE XVI

BLOOD LEVEL FOLLOWING IV INJECTION OF ^{67}GaMDP IN MICE [a,b]

time	observed	calculated	Difference (observed-calculated)
5 min	14.2	14.8	-0.6
15 min	13.6	11.6	0.2
30 min	7.6	9.5	1.9
1 hr	9	8.2	0.8
2 hr	6.9	7.3	-0.4
4 hr	6.3	6.0	0.3
6 hr	5.6	4.9	0.7
12 hr	2.2	2.7	-0.5

(a) values expressed as % injected dose per gram of blood from 3 to 5 mice.

(b) calculated values were obtained from the computer-fitted curve using the NONLIN/AUTOAN computer program.

TABLE XVII

BLOOD LEVEL FOLLOWING IV INJECTION OF $^{67}Ga(OH)_3$ IN MICE [a,b]

time	observed	calculated	Difference (observed-calculated)
5 min	11.5	12.2	-0.5
15 min	12.2	10.2	2.0
30 min	6.8	7.9	-1.1
1 hr	5.2	5.1	0.1
2 hr	3.1	2.8	0.3
4 hr	1.3	1.8	-0.5
6 hr	1.9	1.5	0.4
12 hr	0.8	0.9	-0.1

(a) values expressed as % injected dose per gram of blood from 3 to 5 mice.

(b) calculated values were obtained from the computer-fitted curve using the NONLIN/AUTOAN computer program.

TABLE XVIII

BLOOD LEVEL FOLLOWING IV INJECTION OF ^{67}Ga CITRATE IN MICE [a,b]

time	observed	calculated	Difference (observed-calculated)
5 min	14.1	16.2	-2.1
15 min	15.6	15.7	-0.1
30 min	17.7	15.0	2.7
1 hr	15.3	13.7	1.6
2 hr	8.1	11.4	-3.3
4 hr	9.1	7.9	1.2
6 hr	5.4	5.5	-0.1
12 hr	1.8	1.8	0.0

(a) values expressed as % injected dose per gram from 3 to 5 mice.

(b) calculated values were obtained from the computer-fitted curve using the NONLIN/AUTOAN computer program.

TABLE XIX

COMPARTMENTAL ANALYSIS OF BLOOD CLEARANCE OF $^{67}GaPPi$, $^{67}GaMDP$ AND $^{67}Ga(OH)_3$(a)

Parameter	$^{67}GaPPi$	$^{67}GaMDP$	$^{67}Ga(OH)_3$
A_o	8.9589 ±2.1179	8.5009 ±3.6978	11.0485 ±1.9148
B_o	7.5368 ± 1.5249	8.8847 ± 1.5845	2.3815 ± 1.7168
$\lambda 1$	0.0370 ± 0.0203	0.0707 ± 0.0606	0.0228 ± 0.0088
$\lambda 2$	0.0012 ± 0.0006	0.0017 ± 0.0006	0.0014 ± 0.0018

(a) Parameter

A_o = initial concentration (% dose per gram of blood) in compartment 1

B_o = initial concentration (% dose per gram of blood) in compartment 2

λ_1 = distribution rate of compartment 1 (min^{-1})

λ_2 = elimination rate of compartment 2 (min^{-1})

the basis of the possibility of protein binding of the ^{67}Ga in the blood.

When the best fitting curve for ^{67}Ga citrate was calculated, the resulting curve appeared to fit a single compartment model (Table XX, Figure 12). The extrapolated initial concentration has a value considerably higher than those of the other compounds studied (Table XIX).

When compared to other published data, the level of ^{67}Ga citrate in the blood in the experiments is higher than that observed by Sephton (25) but is the same range as those published by Konikowski (65). The difference may be accounted for on the basis of different mice strains used, and perhaps on a different manufacturing formulation of the ^{67}Ga citrate (183).

The pharmacokinetic analysis obtained from the mouse studies revealed a one compartment model for ^{67}Ga citrate, which differed with the conclusions of other workers who reported a 3 compartment model in humans (30,39). However, in the present experiment, the study model was based on only 8 points for the curve fitting (up to 12 hours post-injection). A different number of compartments may possibly have been obtained if a longer time course of biodistribution had been studied. Since the primary goal of this kinetic study is to compare the biological behavior of different ^{67}Ga products under exactly the same experimental conditions, it is difficult to intercompare the results obtained with those of other workers who conducted their

TABLE XX

COMPARTMENTAL ANALYSIS OF BLOOD CLEARANCE OF ^{67}Ga CITRATE

Parameter	
K_{el}	0.00030 ± 0.0007
C_o	16.4300 ± 1.2500

Parameter

K_{el} = elimination rate constant in the blood (min^{-1})

C_o = initial concentration in the blood (%I.D.per gram of blood)

experiments differently.

The results obtained showed that the amount of radioactivity in the blood for the phosphate complexes of ^{67}Ga and ^{67}Ga citrate were very close after 2 hours post injection. Since ^{67}Ga citrate is known to bind to transferrin in the plasma (27), a similar mechanism was suspected to take place with $^{67}GaPPi$ and $^{67}GaMDP$. An attempt was made to determine the proportion of highly diffusible ^{67}Ga in the plasma one hour after injection of ^{67}Ga phosphate complexes. Blood samples were withdrawn into a heparinized syringe and centrifuged to remove the cellular fraction. Fifty microliters of the plasma were placed on a Millipore type VS desalting filter which was floated on a solution of normal saline, so that any unbound and highly diffusible ^{67}Ga could be removed from the plasma sample. After 15 minutes of diffusion the sample was removed from the floating paper disc with a micropipette and assayed for radioactivity. A fifty microliter standard of the same plasma was counted as a reference. As table XXI indicates, about 95% of the radioactivity in the blood was associated with the plasma fraction and that the ^{67}Ga phosphate complexes were not in a highly diffusible form.

To determine if any gallium pyrophosphate was bound to transferrin after intravenous injection, an *in vitro* study was performed where the $^{67}GaPPi$ was incubated for time periods of one and six hours with ^{125}I transferrin. The mixture was separated by gel filtration on a Sephadex G-200 column, eluted with HEPES buffer at pH 7.45, and the various fractions collected in a fraction collector.

TABLE XXI

BINDING OF ^{67}Ga PHOSPHATE COMPLEXES TO DIFFERENT BLOOD FRACTIONS (a)

	Activity in cellular fraction (b)	Activity in plasma prior to desalting	Activity in plasma post-desalting (c)
^{67}Ga PPi	4.8% ± 2.0	95.2% ± 2.0	90.0% ± 8.7
^{67}Ga MDP	4.3% ± 1.6	95.7% ± 1.6	92.0% ± 8.1

(a) one hour after injection in mice.

(b) the cells were washed 3 times with 2 ml of normal saline

(c) activity measured after 15 minutes of desalting.

Each aliquot was counted in a Beckman 8000 well counter NaI(Tl) set to discriminate between ^{67}Ga and ^{125}I (see appendix I). It was found that the $^{67}GaPPi$ was eluted later than the ^{125}I-TF in accordance with the smaller molecular size as illustrated in Figure 13. At both time intervals of one and six hours of incubation, two peaks of ^{67}Ga radioactivity were observed on the chromatogram; the first one coincided with the peak of ^{125}I-TF and a second with the $^{67}GaPPi$ position. At both times, the amount of ^{67}Ga associated with the ^{125}I-TF peak was approximately 75% of the total ^{67}Ga activity, and only 25% of the total ^{67}Ga activity on the column was eluted in later fractions (Figure 14). This experiment provided in vitro evidence that the $^{67}GaPPi$ complex may have dissociated in the blood, followed by binding of the ^{67}Ga to transferrin molecules.

It has been reported that the presence of phosphate buffer in a ^{67}Ga TF solution results in dissociation of the ^{67}Ga from TF (33). Others, dyalising ^{67}Ga TF with a flow of phosphate buffer, noted that all the gallium was removed from the TF after 24 hours (30). At the concentrations used in this experiment (0.1 mg of PPi and 2 mg of TF/ml), 75% of the ^{67}Ga activity was associated with the transferrin. An excess of phosphate is likely required to remove the gallium from the transferrin, otherwise only a small proportion of the ^{67}Ga activity would have been associated with the protein. In this experiment, it was not possible to determine whether the association of ^{67}Ga with the transferrin was in a free ionic form or in the form of a phosphate complex.

FIGURE 13

GEL RADIOCHROMATOGRAPHIC PROFILES OF ^{67}GaPPi AND ^{125}I-TF ON SEPHADEX G-200 (a,b)

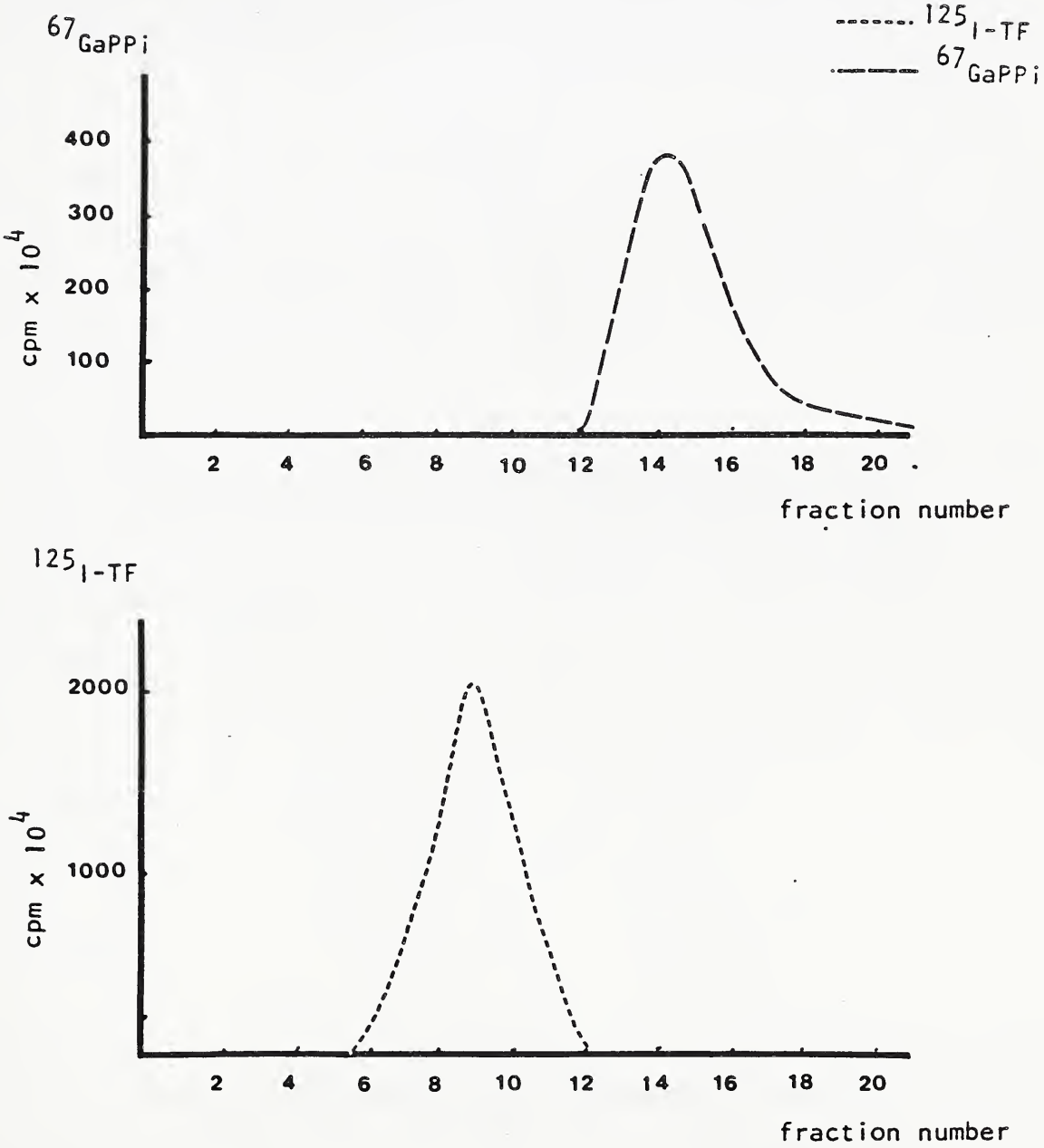

(a) HEPES buffer pH 7.4 as solvent

(b) each fraction represents a volume of 2 ml

FIGURE 14

GEL CHROMATOGRAPHIC PROFILES OF A MIXTURE OF ^{67}GaPPi AND ^{125}I-TF ON SEPHADEX G-200 (a,b)

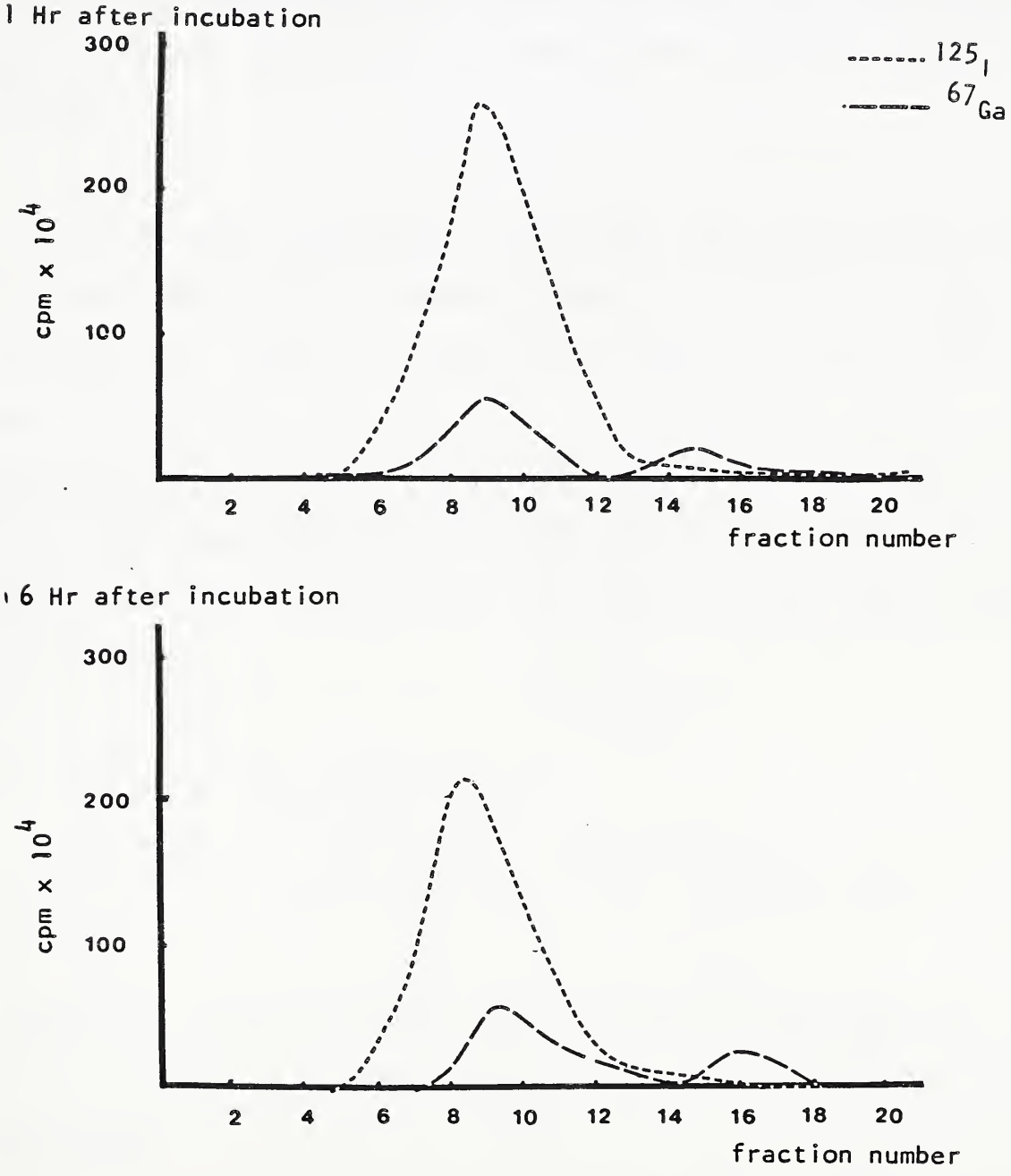

(a) HEPES buffer pH 7.4 as solvent

(b) each fraction represents a volume of 2 ml

These last results of this experiment may explain the blood distribution data of the ^{67}Ga phosphate derivatives and ^{67}Ga citrate, as presented in Table XIV. Differences seen in the early phase of distribution may be due to the presence of non transferrin bound $^{67}GaPPi$ and $^{67}GaMDP$ while the similarity of the curve after 2 hours may represent primarily transferrin bound gallium or gallium complexes.

In the case of $^{67}Ga(OH)_3$, it has been shown that, even in the colloidal form, a certain amount is bound to transferrin *in vitro* and *in vivo* (184). After the removal of colloidal particles, mainly by the liver and the rest of the reticuloendothelial system, some remaining portion of the colloid would still be in circulation in its transferrin bound form, showing a late distribution phase similar to that of other gallium derivatives, but at a much lower level of blood concentration.

B. Uptake of ^{67}Ga Complexes by Liver

The uptake of $^{67}GaPPi$ and $^{67}GaMDP$ by the entire liver did not exceed 8% of the injected dose (Table XXII). Maximum localization of the product was seen after 15 minutes and the level remained essentially constant for the next 12 hours. The uptake of ^{67}Ga citrate was within the same range as that seen with ^{67}Ga phosphate derivatives.

At the concentration used, there was a relatively high uptake of $^{67}Ga(OH)_3$ by the liver and the spleen due to its colloidal form. The

TABLE XXII

LIVER UPTAKE OF VARIOUS ^{67}Ga COMPLEXES FOLLOWING IV INJECTION IN MICE [a,b]

	5 min	15 min	30 min	60 min	120 min	240 min	360 min	720 min
^{67}GaPPi	7.0 ±1.2	7.2 ±0.7	4.3 ±1.2	5.0 ±1.1	5.0 ±0.3	4.9 ±0.2	6.2 ±0.3	6.3 ±0.3
^{67}GaMDP	3.8 ±0.4	7.6 ±1.9	4.2 ±2.7	4.6 ±0.5	4.2 ±1.4	6.5 ±1.1	6.0 ±0.9	4.2 ±0.9
^{67}GaCitrate	5.5 ±0.4	9.2 ±5.0	5.5 ±0.7	6.5 ±0.6	5.7 ±0.5	6.3 ±0.6	4.1 ±0.5	5.1 ±1.8
$^{67}Ga(OH)_3$	39.0 ±6.6	18.4 ±3.5	49.3 ±5.6	54.6 ±7.7	58.8 ±8.9	39.0 ±3.0	44.1 ±4.1	28.5 ±2.5

(a) expressed as % injected dose in the entire organ at different time intervals after injection of 37 KBq of ^{67}Ga radioactivity.

(b) each value represents the mean ± standard deviation of 3-5 mice.

very high liver uptake, reaching almost 60% of the injected dose at 2 hours, was reflected by the low blood levels of the $^{67}Ga(OH)_3$ at this time. It is interesting to note that the highest liver concentration was seen 2 hours after injection, at the time when the initial rapid phase of blood clearance was over. Konikowski et al. (65) reported slightly lower liver uptake values that could probably be attributed to the pH of the injected solution (pH 3), thus yielding a more soluble form of gallium hydroxide.

The observed difference in the liver uptake of the phosphate complexes and the hydroxide reinforces the analytical finding that at the concentration used, the ^{67}Ga pyrophosphate did not act as an insoluble colloid.

Dewanjee et al. (71) reported a higher uptake by the reticuloendothelial system, up to 30% of an injected dose of ^{67}Ga pyrophosphate at one hour in rats. However, the concentration of phosphate was not stated and it is possible that a solution of higher specific activity of $^{67}GaPPi$ was used. Also, from the chemical analysis portion of the present work, it was shown that two forms of gallium pyrophosphate complex existed at neutral pH, a soluble form which was changed with time to a second less soluble one. In this experiment, the product injected was the more soluble one, as separated by gel filtration (i.e. eluted at a volume of 5.5 ml). Dewanjee et al. (71) did not mention which form of the product was used, nor how long after preparation of $^{67}GaPPi$ the injection was made. The presence of the less soluble form could have been

predominant in the preparation, leading to a large uptake by the reticuloendothelial system.

Because the ^{67}Ga phosphate derivatives showed a similar uptake pattern to that of ^{67}Ga citrate, a common mechanism of uptake may be speculated. It has been proposed that the liver uptake is effected by pinocytocis or endocytosis (26,55). It was also reported that after intravenous injection of ^{67}Ga citrate in the rats, the liver accumulated the gallium along with a lysosomal enzyme such as pyrophosphatase and betaglucuronidase (55). During the first 24 hours, the gallium was reported to be associated with the cytoplasm and slowly accumulated into the lysosomes (55). Aulbert et al. (55) subjected an extract of liver lysosomes to electrophoresis, and separated a labelled protein fraction which exhibited the same migration characteristics as transferrin. Using gel filtration techniques on liver and tumor homogenates, Hayes and Carlton (184) found that ^{67}Ga was bound to a glycoprotein of 40,000 to 45,000 daltons, which is half the size of transferrin. They proposed that tissues rich with this protein could have preferential uptake of ^{67}Ga.

C. Uptake of ^{67}Ga Complex by the Kidneys

Fifteen minutes after injection no marked difference was seen between the uptake of $^{67}GaPPi$ and $^{67}GaMDP$ in the kidneys (Table XXIII). The observation that the kidney accumulation of $^{67}Ga(OH)_3$ is considerably lower can be attributed to the initial high liver uptake, thus resulting in a decreased total radioactivity available for distribution to the other parts of the body.

TABLE XXIII

KIDNEY UPTAKE OF VARIOUS ^{67}Ga COMPLEXES FOLLOWING IV INJECTION IN MICE [a,b]

	5 min	15 min	30 min	60 min	120 min	240 min	360 min	720 min
^{67}GaPPi	2.8 ±0.5	2.7 ±0.7	1.8 ±0.3	1.6 ±0.5	1.4 ±0.5	1.6 ±0.2	1.7 ±0.2	1.6 ±0.3
^{67}GaMDP	1.5 ±0.2	2.6 ±0.6	1.6 ±0.9	1.6 ±0.3	1.5 ±0.3	1.9 ±0.1	1.7 ±0.2	1.4 ±0.1
^{67}Ga-citrate	2.6 ±0.3	2.8 ±0.7	2.2 ±0.3	2.7 ±0.1	2.0 ±0.3	2.9 ±0.2	1.7 ±0.2	1.6 ±0.6
$^{67}Ga(OH)_3$	2.6 ±0.1	2.4 ±0.7	1.1 ±0.1	1.1 ±0.2	0.6 ±0.2	0.8 ±0.1	1.2 ±0.1	0.6 ±0.1

(a) expressed as % injected dose in the whole organ at different time intervals after injection of 37 KBq of radioactivity.

(b) each value represents the mean ± standard deviation of 3-5 mice.

The total radioactivity in the kidney for both ^{67}GaPPi and ^{67}GaMDP showed very little fluctuation after 15 minutes, even though the level of blood radioactivity declined with time. This is evidenced by the fact that the kidney to blood ratio of ^{67}GaPPi increased from a value of 0.325 to 1.035 over 12 hours. Similarly, the kidney to blood ratio of ^{67}GaMDP increased from 0.209 to 1.053 during the same period of time.

The values for kidney uptake of ^{67}Ga citrate is in general agreement with those observed by Konikowski (65). In Table XXIII, a significant difference ($p < 0.05$, t-test) was observed between the citrate and phosphate complexes uptake values during the interval of 30 to 240 minutes post injection. This is probably a reflection of differences in the kidney specifity for the different gallium compounds. It has been described that after injection of ^{67}Ga sulfate, the gallium was accumulated by the kidney cells and precipitated as a phosphate crystal, then expelled through the lumina (66). The lower kidney uptake values of ^{67}GaPPi and ^{67}GaMDP could have most likely reflected a preferential elimination of those two compounds over the ^{67}Ga citrate. Knowing that a large proportion of those ^{67}Ga phosphate complexes can bind to transferrin, after the unbound ^{67}Ga complexes are eliminated, the radioactivity would follow an elimination pathway similar to that of ^{67}Ga citrate.

D. Uptake of ^{67}Ga Complexes by the GIT

It is clinically well known that ^{67}Ga citrate accumulates in the GIT to such an extent that bowel cleaning is necessary prior to

scintiscanning of the abdominal region. Table XXIV illustrates that the fraction of the injected dose of ^{67}GaPPi, ^{67}GaMDP and ^{67}Ga citrate present in the GIT increases during the initial 6 hours, reaching a value of 10-15% of the injected dose in the entire GIT and content. The GIT uptake of the hydroxide form of ^{67}Ga remained at relatively low value throughout the 12 hours of observation.

A comparison of the levels of ^{67}GaPPi, ^{67}GaMDP and ^{67}Ga citrate in the entire GIT did not show any statistical differences at any time period tested. Chen et al. (62) reported that the amount of ^{67}Ga citrate radioactivity eliminated in the rat GIT increased to a value of 9% of the injected dose after 24 hours. However, this data applied to GIT contents only, and cannot be compared to the observations of this study, which included the entire GIT tract along with contents. There is no stated mechanism established for the GIT uptake of gallium but a close relation has been described between the serum iron binding capacity and the ^{67}Ga secreted into the GIT. Thus, a transferrin mediated mechanism can be suspected (62).

E. Uptake of ^{67}Ga Complexes by the Bone

The bone uptake of ^{67}GaPPi and ^{67}GaMDP showed a gradual increase with time, with a maximum value of 8.8% and 8.4% respectively of the injected dose per gram of tissue reached by 6 hours, followed by a slight decline by 12 hours (Table XXV). Higher levels of radioactivity in bone were initially seen with the ^{67}GaMDP compound, but after 2 hours the concentration of both gallium phosphate complexes in bone were in the same range. Relatively large variations

TABLE XXIV

GIT UPTAKE OF VARIOUS ^{67}Ga COMPLEXES FOLLOWING IV INJECTION IN MICE [a,b]

	5 min	15 min	30 min	60 min	120 min	240 min	360 min	720 min
^{67}GaPPi	7.8 ±1.4	6.7 ±1.7	9.3 ±1.2	9.5 ±1.9	10.6 ±2.4	12.3 ±1.1	12.5 ±1.6	10.9 ±1.
^{67}GaMDP	7.0 ±0.7	7.2 ±0.4	9.1 ±1.5	9.0 ±1.1	10.8 ±2.2	14.9 ±1.1	14.6 ±0.8	10.5 ±1.4
^{67}Ga-citrate	5.2 ±1.7	6.7 ±1.6	7.4 ±2.9	9.6 ±1.7	10.3 ±1.2	12.1 ±1.6	7.1 ±2.7	10.1 ±5.5
$^{67}Ga(OH)_3$	3.6 ±1.2	4.3 ±1.2	4.5 ±1.2	4.6 ±0.8	5.4 ±1.7	3.9 ±0.5	5.1 ±0.5	3.9 ± 0.6

(a) expressed as % injected dose in the entire GIT and contents at different time intervals after injection of 37 KBq of radioactivity.

(b) each value represents the mean ± standard deviation of 3-5 mice.

TABLE XXV

BONE UPTAKE OF VARIOUS ^{67}Ga COMPLEXES AFTER IV INJECTION IN MICE [a,b]

	5 min	15 min	30 min	1 hr	2 hr	4 hr	6 hr	12 hr
^{67}GaPPi	2.4	2.1	2.7	3.0	5.9	5.0	8.8	7.5
	± 0.6	± 0.1	±0.8	±1.0	±1.9	±1.6	±4.4	±1.3
^{67}GaMDP	4.4	3.7	4.1	4.8	5.1	7.5	8.4	6.9
	±1.8	±1.0	±1.6	±2.1	±0.8	±1.9	±5.2	±0.8
^{67}Ga citrate	4.1	2.1	5.1	5.9	5.0	5.0	11.3	8.0
	±0.5	±0.3	±0.6	±1.0	±1.0	±0.7	±1.5	±0.6
$^{67}Ga(OH)_3$	3.2	1.8	5.2	2.9	6.3	7.5	7.2	4.6
	±0.5	±0.1	±1.3	±0.5	±1.6	±3.0	±1.2	±0.6

(a) expressed as % injection dose per gram at different time intervals after IV injection of 37 KBq of radioactivity.

(b) each value represents the mean ± standard deviation of 3-5 mice.

in bone uptake were observed making statistical analysis difficult.

When compared to the bone uptake of ^{67}Ga tripolyphosphate described by Goulet (72), ^{67}GaPPi and ^{67}GaMDP had a lower uptake. At one hour, 8.5% of the injected dose of ^{67}Ga tripolyphosphate was accumulated per gram of bone, and increased to 19% after 12 hours. However, the author concluded from this experiment that the presence of carrier gallium increased the uptake of the radionuclide by the bone. It is possible to assume that the lower uptake of ^{67}GaPPi and ^{67}GaMDP by the bone may be due to the large distribution of the radiogallium into the whole body, leaving less tracer available to be deposited at the bone sites.

Unlike the ^{99}Tc^{m} phosphate complexes, the nature of the gallium phosphate (MDP or PPi) did not seem to influence the bone uptake of the radiotracer. From these findings, it is obvious that the bone accumulation of the ^{67}Ga products is regulated primarily through a mechanism independent of the phosphate influence.

F. Uptake of ^{67}Ga Complexes by the Myocardium

A major objective of this research was to determine the uptake of ^{67}GaPPi and ^{67}GaMDP by infarcted myocardial tissue, in order to ascertain whether radiogallium complexes would be useful in the delination of diseased heart tissue. The first step of this evaluation was to study the uptake of several radiogallium complexes by normal myocardium. As shown in Table XXVI, the uptake of both

TABLE XXVI

HEART UPTAKE OF VARIOUS ^{67}Ga COMPLEXES FOLLOWING IV INJECTION IN MICE [a,b]

	5 min	15 min	30 min	60 min	120 min	240 min	360 min	720 min
^{67}GaPPi	0.46 ± 0.08	0.48 ±0.07	0.27 ±0.10	0.24 ±0.06	0.27 ±0.06	0.20 ±0.02	0.20 ±0.03	0.13 ±0.02
^{67}GaMDP	0.37 ±0.06	0.41 ±0.11	0.23 ±0.13	0.27 ±0.04	0.20 ±0.01	0.24 ±0.03	0.20 ±0.02	0.11 ±0.03
^{67}Ga-citrate	0.45 ±0.05	0.49 ±0.07	0.39 ±0.08	0.49 ±0.21	0.35 ±0.05	0.33 ±0.02	0.19 ±0.02	0.14 ±0.05
$^{67}Ga(OH)_3$	0.37 ±0.50	0.40 ±0.07	0.27 ±0.08	0.20 ±0.03	0.13 ±0.04	0.11 ±0.04	0.10 ±0.01	0.06 ±0.04

(a) expressed as % injected dose in the whole organ at different time intervals after injection of 37 KBq of radioactivity.

(b) each value represents the mean ± standard deviation of 3-5mice.

TABLE XXVII

HEART TO BLOOD RATIO OF VARIOUS ^{67}Ga PHOSPHATE COMPLEXES AFTER IV INJECTION IN MICE [a,b]

	5 min	15 min	30 min	1 hr	2 hr	4 hr	6 hr	12 hr
^{67}GaPPi	0.259	0.245	0.203	0.281	0.283	0.278	0.341	0.392
	±0.068	±0.020	±0.073	±0.063	±0.032	±0.031	±0.039	±0.017
^{67}GaMDP	0.261	0.275	0.235	0.261	0.245	0.322	0.303	0.382
	±0.105	±0.209	±0.106	±0.045	±0.081	±0.022	±0.010	±0.023

(a) ratio calculated on the basis of % injected activity per gram of heart to % injected dose per gram of blood.

(b) each value represents the mean ± standard deviation of 3-5 mice.

^{67}GaPPi and ^{67}GaMDP in the entire intact heart were similar and revealed a maximum value of just under 0.5% of the total injected dose by 15 minutes post injection. These values decreased gradually over the next 12 hours of the study and were in the same range as those seen with ^{67}Ga citrate at various time intervals (Table XXVI).

The tissue to blood ratio of ^{67}GaPPi and ^{67}GaMDP (Table XXVII) exhibited an interesting finding. The similarity of the ratio throughout the first 2 hours suggested that the radioactivity in the heart muscle was due to a constant equilibrium between myocardial tissue and blood. Then during the 4th to 12th hour of observation, the ratio increased reflecting either an enhanced uptake, or residual radioactivity remaining in heart muscle following a decrease in blood levels.

G. Uptake of ^{67}Ga Phosphate Derivatives in Cardiac Infarct Tissues

Myocardial infarcts were produced in adult male Sprague-Dawley rats by subcutaneous injection of 50 mg of isoproterenol sulfate in 0.5 ml of normal saline. At a time period of 6 hours after the isoproterenol administration, the femoral vein was exposed and 185 KBq of ^{67}GaPPi or ^{67}GaMDP complex, followed by 185 KBq of ^{99}Tc^{m}PPi, were injected i.v.. Control animals were injected following the same procedure, but did not receive isoproterenol sulfate. In this study, the ^{99}Tc^{m}PPi was used as an indicator for the degree of myocardial damage since the uptake of ^{99}Tc^{m} in this kind of infarct model has been established (180). At time intervals of one and six hours following the administration of the radiopharmaceuticals, each rat was

sacrificed by exsanguination, the heart was removed and blotted free of blood, and the level of ^{67}Ga and $^{99}Tc^{m}$ radioactivities were determined in blood and heart, on a Beckman 8000 well counter using a program to correct for ^{67}Ga spillover in the $^{99}Tc^{m}$ channel (see appendix II).

The infarct to normal (ITN) ratio of $^{99}Tc^{m}$ radioactivity was in the range of 4:1 at one hour and 5:1 at six hours except in one experiment where the ITN ratio had a value of 16.5:1 one hour after injection. This was attributed to one animal which responded highly to the isoproterenol injection, showing an infarct uptake value twice as high as the value of the other animals of the same group. Kung et al. (180) reported that, in a myocardial infarct model induced with isoproterenol s.c. in rat, the ITN ratio of $^{99}Tc^{m}PPi$ increased from 7:1 to 16:1 at 1 and 6 hours after injection respectively. This difference in ITN ratio was not observed in the data presented in Tables XXVIII and XXIX. A real uptake was seen in the damaged heart when compared to control for all products ($p < 0.05$ in the first sets of rats, and $p < 0.10$ in the second set, using a standard t-test) but the ITN ratio did not increase with time. The observed variation of $^{99}Tc^{m}PPi$ uptake by the damaged tissue may be due to the difference in animal response to the dose of isoproterenol injected.

The two ^{67}Ga phosphate complexes revealed a significantly increased ($p < 0.05$, t-test) uptake into the damaged heart when compared to the normal animals at one hour after injection. The ratio of ITN were 1.55:1 and 1.78:1 for $^{67}GaPPi$ and $^{67}GaMDP$ respectively.

TABLE XXVIII

ACCUMULATION OF ^{67}Ga AND $^{99}Tc^{m}$ RADIOACTIVITY IN NORMAL AND INFARCTED HEARTS OF RAT AFTER INJECTION OF $^{67}GaPPi$ AND $^{99}Tc^{m}PPi$ (a,b)

Time after Injection	Tissue	$^{67}GaPPi$ uptake		$^{99}Tc^{m}PPi$ uptake	
		Normal	Damaged	Normal	Damaged
1 hr	Blood	1.04	0.96	0.11	0.10
	(n=3)	±0.23	±0.13	±0.03	±0.02
		(n=3)	(n=3)	(n=3)	(n=3)
	Heart	0.38	0.59	0.15	0.77
		±0.12	±0.09	±0.03	±0.86
		(n=3)	(n=3)	(n=3)	(n=3)
6 hr	Blood	0.66	0.46	0.07	0.09
		±0.21	±0.07	±0.01	±0.01
		(n=3)	(n=3)	(n=3)	(n=3)
	Heart	0.35	0.39	0.06	0.25
		±0.03	±0.03	±0.01	±0.13
		(n=3)	(n=3)	(n=3)	(n=3)

(a) values expressed as percent of injected dose per gram.

(b) data expressed as mean ± standard deviation. Number of animals used is given in parentheses.

TABLE XXIX

ACCUMULATION OF ^{67}Ga AND $^{99}Tc^{m}$ RADIOACTIVITIES IN NORMAL AND INFARCTED HEARTS OF RATS AFTER INJECTION OF ^{67}Ga MDP AND $^{99}Tc^{m}$PPi (a,b)

Time after Injection	Tissue	^{67}Ga MDP uptake		$^{99}Tc^{m}$PPi uptake	
		Normal	Damaged	Normal	Damaged
1 hr	Blood	1.06 ±0.07 (n=3)	1.04 ±0.10 (n=3)	0.26 ±0.01 (n=3)	0.31 ±0.09 (n=3)
	Heart	0.41 ±0.08 (n=3)	0.73 ±0.05 (n=3)	0.08 ±0.03 (n=3)	1.34 ±0.73 (n=3)
6 hr	Blood	0.75 ±0.13 (n=4)	0.42 ±0.05 (n=3)	0.08 ±0.01 (n=4)	0.07 ±0.01 (n=3)
	Heart	0.40 ±0.05 (n=4)	0.49 ±0.07 (n=3)	0.07 ±0.04 (n=4)	0.30 ±0.02 (n=3)

(a) values expressed as percent of injected dose per gram.

(b) data expressed as mean ± standard deviation. Number of animals used is given in parentheses.

This cannot be attributed merely to the residual blood in the myocardium since no significant difference existed between the blood level of ^{67}Ga radioactivity in the normal and infarct animals ($p < 0.6$). At 6 hours, no significant difference was noted between the normal and infarct tissue for both products ($p < 0.2$), with an infarct to normal ratio of 1.11:1 and 1.12:1 for $^{67}GaPPi$ and $^{67}GaMDP$ respectively.

The procedure for inducing myocardial damage with isoproterenol in this investigation produces microlesions throughout the entire cardiac muscle, unlike the localized lesion observed after ligation of a coronary artery or burning with a hot iron (160). Consequently, it was ist possible to isolate only hypoxic tissue. If the lesions were more localized the ITN ratio would be more relevant.

A coronary artery ligation infarct model in dogs produced an infarct, which when imaged with ^{67}Ga citrate gave an ITN ratio of 1.9:1 (+ 0.6) at 48 hours after injection (99). It is difficult to compare with the data described above since the animal, as well as the infarct model adopted were different. However, these data in the literature give a relative indication of the ITN ratio of ^{67}Ga citrate and $^{99}Tc^{m}PPi$ in the diseased heart. (See table VI)

When the $^{99}Tc^{m}PPi$ uptake ratio described in table XXVIII-XXIX are compared to the results observed by Kung (180) using the same infarct model in rats, similar values for ITN were observed.

The principal mechanism of $^{99}Tc^{m}PPi$ and $^{99}Tc^{m}MDP$ uptake in myocardial infarct has been proposed to be related to the calcium uptake by the damaged cells followed by a subsequent entry of the technetium derivatives (3). The similarity in biological behavior between gallium and calcium described by Anghileri (40,42,43,44), and the accumulation of $^{99}Tc^{m}$ phosphate into the infarcted tissue, suggested that the gallium phosphate complex might be a useful agent for the delineation of the damaged myocardial area. However, doubt has been cast on this hypothesis by our experiment in view of the ITN ratio observed in the rat infarct model chosen. Of the two $^{99}Tc^{m}$ derivatives $^{99}Tc^{m}PPi$ and $^{99}Tc^{m}MDP$, the latter is known to exhibit a slightly higher ITN ratio (161,162). This was not the case when the ^{67}Ga complexes were used (Table 27,28). The phosphate moiety of the ^{67}Ga complexes does not seem to influence the uptake of radiogallium to a very large extent.

A possible explanation is that the molecular configuration of the gallium phosphate complex may be such that, even if the more soluble form of ^{67}Ga phosphate complex is injected, its uptake through the membrane of the hypoxic cells was impeded much more than the corresponding $^{99}Tc^{m}$ compound.

Also, studies in mice and rabbits showed that addition of relatively high (5-10 mg/kg) levels of carrier gallium would be required to lower blood levels for heart localization of $^{67}GaPPi$ (186). However, these experiments were conducted with

This cannot be attributed merely to the residual blood in the myocardium since no significant difference existed between the blood level of ^{67}Ga radioactivity in the normal and infarct animals ($p < 0.6$). At 6 hours, no significant difference was noted between the normal and infarct tissue for both products ($p < 0.2$), with an infarct to normal ratio of 1.11:1 and 1.12:1 for $^{67}GaPPi$ and $^{67}GaMDP$ respectively.

The procedure for inducing myocardial damage with isoproterenol in this investigation produces microlesions throughout the entire cardiac muscle, unlike the localized lesion observed after ligation of a coronary artery or burning with a hot iron (160). Consequently, it was not possible to isolate only hypoxic tissue. If the lesions were more localized the ITN ratio would be more relevant.

A coronary artery ligation infarct model in dogs produced an infarct, which when imaged with ^{67}Ga citrate gave an ITN ratio of 1.9:1 (+ 0.6) at 48 hours after injection (99). It is difficult to compare with the data described above since the animal, as well as the infarct model adopted were different. However, these data in the literature give a relative indication of the ITN ratio of ^{67}Ga citrate and $^{99}Tc^{m}PPi$ in the diseased heart. (See table VI)

When the $^{99}Tc^{m}PPi$ uptake ratio described in table XXVIII-XXIX are compared to the results observed by Kung (180) using the same infarct model in rats, similar values for ITN were observed.

The principal mechanism of $^{99}Tc^{m}$PPi and $^{99}Tc^{m}$MDP uptake in myocardial infarct has been proposed to be related to the calcium uptake by the damaged cells followed by a subsequent entry of the technetium derivatives (3). The similarity in biological behavior between gallium and calcium described by Anghileri (40,42,43,44), and the accumulation of $^{99}Tc^{m}$ phosphate into the infarcted tissue, suggested that the gallium phosphate complex might be a useful agent for the delineation of the damaged myocardial area. However, doubt has been cast on this hypothesis by our experiment in view of the ITN ratio observed in the rat infarct model chosen. Of the two $^{99}Tc^{m}$ derivatives $^{99}Tc^{m}$PPi and $^{99}Tc^{m}$MDP, the latter is known to exhibit a slightly higher ITN ratio (161,162). This was not the case when the ^{67}Ga complexes were used (Table 27,28). The phosphate moiety of the ^{67}Ga complexes does not seem to influence the uptake of radiogallium to a very large extent.

A possible explanation is that the molecular configuration of the gallium phosphate complex may be such that, even if the more soluble form of ^{67}Ga phosphate complex is injected, its uptake through the membrane of the hypoxic cells was impeded much more than the corresponding $^{99}Tc^{m}$ compound.

Also, studies in mice and rabbits showed that addition of relatively high (5-10 mg/kg) levels of carrier gallium would be required to lower blood levels for heart localization of ^{67}GaPPi (186). However, these experiments were conducted with

no-carrier-added ^{67}GaPPi, and even when the blood was washed out of the heart, the uptake of ^{67}GaPPi and ^{67}GaMDP was not be sufficient to produce a high delineation of the necrotic heart.

The conclusions from the present series of experiments are that the radiogallium phosphate complexes do not offer any specific advantage over the corresponding ^{99}Tc^{m} phosphates. The partial dissociation of the radiogallium from the phosphate complex and its association with transferrin as observed chromatographically, is possibly a strong indication as to the discrepancy in the behavior of both the ^{67}Ga and ^{99}Tc^{m} phosphate derivatives.

Summary and Conclusions

SUMMARY AND CONCLUSIONS

1. ^{67}GaPPi and ^{67}GaMDP were prepared by simple incubation of $^{67}GaCl_3$ (no-carrier-added) with sodium pyrophosphate and methylenediphosphonic acid respectively.

2. The ^{67}Ga-phosphate complexes obtained have a very low solubility but differ from the hydroxide form of gallium.

3. A transformation of the ^{67}Ga-phosphate complexes leading to a less soluble form occurs with time and when the pH is beyond 4.5. These two forms can be separated paper chromatography using a pyridine:ethanol:water 1:2:4 solvent system at various pH and quantitatively by gel filtration on Sephadex G-25 medium eluted with normal saline.

4. Tissue biodistribution studies performed on mice following i.v. injections of ^{67}GaPPi, ^{67}GaMDP, ^{67}Ga citrate and $^{67}Ga(OH)_3$ indicated that the uptake of ^{67}GaPPi and MDP were very similar with localization mainly in the GIT, skeleton, liver, kidney. The liver uptake of ^{67}GaPPi and MDP complexes were not as high as that observed with $^{67}Ga(OH)_3$ indicating that the phosphate complexes were not in a colloidal form at the concentration used. ^{67}GaPPi and ^{67}GaMDP compared to citrate showed that after 2 hours

post injection, the 3 products acted similarly in mice.

5. After i.v. injection, the plasma disappearance pattern of ^{67}GaPPi and ^{67}GaMDP is more rapid than that of ^{67}Ga citrate during the initial 3 hours, but similar from 3 to 12 hours post injection. The blood levels of the phosphate derivatives were always higher than those of $^{67}Ga(OH)_3$.

6. Following a 1 hour <u>in vitro</u> incubation of ^{67}GaPPi with transferrin, 75% of the ^{67}Ga radioactivity eluted from the Sephadex 6-25 column was associated with the transferrin fraction. Such transferrin binding could explain the similarity between tissue biodistribution of ^{67}GaPPi and MDP and ^{67}Ga citrate at time intervals of 3 hours or more following i.v. injection.

7. A rat cardiac infarct animal model was produced by s.c. injection of isoproterenol sulfate (250mg/kg). Simultaneous injection of ^{67}GaPPi or ^{67}GaMDP along with $^{99}Tc^{m}$PPi, followed by analysis of the entire heart 1 hour later indicated an infarct:normal ratio of 1.55:1 for ^{67}GaPPi, 1.78:1 for ^{67}GaMDP and 4:1 for $^{99}Tc^{m}$PPi.

8. In the model used in this study, radiogallium pyrophosphate and methylenediphosphonate complexes prepared with a no-carrier-added specific activity were found to be inferior to $^{99}Tc^{m}$PPi for localization in myocardial infarcts.

REFERENCES

1. POE, W.D., Rationale and radiopharmaceuticals for myocardial imaging. Semin. Nucl. Med. 71: 7-13, 1977.

2. PARKEY, R.W., BONTE, F.J., BUJA, L.M., et al. Myocardial infarct imaging with technetium 99m phosphates. Semin. Nucl. Med. 7: 15-28, 1977.

3. GROSSMAN, Z.D., FOSTER, A.B., RICHARDSON, R. Myocardial uptake of Tc 99m skeletal agent in the rats after experimental induction of microscopic foci of injury. J. Nucl. Med. 18: 1003-1007, 1977.

4. KULPRATHIPANJA, S., HNATOWICH, D.J. Method for determinating the pH stability range of gallium radiopharmaceuticals. Int. J. Appl. Rad. Isot. 28: 229-233, 1977.

5. DYMOV, A.M., SAVOSTIN, A.P. "Analytical chemistry of Gallium". Ann Harbor Science Publisher, A.P. Vinogradov editor, Ann Harbor London, 1970, pp. 1-30.

6. SEKA, I.A., CHAUSS, I.S., MITYUREVA, T.T. "The chemistry of gallium". Elsevier Publishing Company, Amsterdam London, New York, 1966, pp. 1-100.

7. RAFAELOFF, R. Separation of gallium from group III elements, germanium, copper, arsenic and iron. Anal. Chem. 43: 272-274, 1971.

8. PRABHUE, B.M., KHOPKAN, S.M. Solvent extraction of gallium III as the monothiodibenzoylmethane complex. Talanta 25: 109-110, 1978.

9. CLOUTIER, R.J., WATSON, E.E., HAYES, R.L. et al. MIRD Dose estimate report No. 2 Summary of current radiation dose estimates to humans from ^{66}Ga, ^{67}Ga, ^{68}Ga and ^{72}Ga-citrate. J. Nucl. Med. 14: 755-756, 1973.

10. MOELLER, T., KING, G.L. Some physical studies on gallium salt solution. J. Phy. Colloid. Chem. 54: 999-1011, 1950.

11. KUFF, K.F., TYREE, S.Y. Light scattering studies on aqueous gallium perchlorate solutions. J. Am. Chem. Soc. 80: 5654-5657, 1958.

12. PASCAL, P. Traite de chimie mineral tome VI, Masson et Cie, Paris, pp 476, 1961.

13. HNATOWICH, D.A. Method of separation and quality control of ^{68}Ga radiopharmaceuticals. J. Nucl. Med. 16: 764-768, 1975.

14. THAKUR, M.L. Gallium-67 and Indium-111 radiopharmaceuticals. Int. J. Appl. Rad. Isot. 28: 183-201, 1977.

15. GLICKSON, J.D., PITNER, T.P., WEBB, J. et al. Hydrogen-1 and gallium-71 nuclear magnetic resonance study of gallium citrate in aqueous solution. J. Am. Chem. Soc. 97: 1679-1683, 1975.

16. KUL'BA, F.Y., BABKINA, N.A., ZHARKOV, A.P. Potentiometric investigation of complex formation by gallium III with citric acid. Zh. Neorg. Khim. 20: 2640-2644, 1975.

17. CHANG, C.H.F., PITNER, T.P., LENKINSKI, P.E. Carbon-13 fourrier transform nuclear magnetic resonance study of gallium citrate in aqueous solution. J. Am. Chem. Soc. 99: 5858-5963, 1977.

18. CHUDINOVA, N.N., TANANAEV, I.V. An investigation of gallium chloride with sodium and potassium pyrophosphate. Neorg. Mater. 2: 1235-1239, 1966.

19. CHUDINOVA, N.N., TANANAEV, I.V. An investigation of the reaction of gallium chloride with lithium, rubidium, cesium and ammonium phosphate. Neorg. Mater 3: 1608-1611, 1967.

20. CHUDINOVA, N.N., TANANAEV, I.V., LAVROV, A.V. Effect of pH on the reaction of gallium with pyrophosphate. Inorg. Mater. 5: 1810-1811, 1968.

21. SHEKA, I.A., BARCHUK, L.P., SENEMOVA, G.S.S. Infrared absorption spectra of complex of Indium and gallium with polyphosphate. Russian Journal of Inorg. Chem. 16: 1701-1704, 1971.

22. BARCHUK, L.P., SHEKA, I.A. Complex formation by gallium with sodium pyrophosphate in aqueous solution. Russian J. Inorg. Chem. 16: 1268-1270, 1971.

23. DUDLEY, H.C., MADDOX, G.E. Deposition of radiogallium (^{72}Ga) in skeletal tissues. J. Pharmacol. Exp. Ther. 96: 224-227, 1949.

24. DUDLEY, H.C., MADDOX, G.E.., LA RUE, H.C. Studies of the metabolism of gallium. J. Pharmacol. Exp. Ther. 96: 135-138, 1949.

25. SEPHTON, R.G., HODGSON, G.S., De ABREW, S., et al. Ga-67 and Fe-59 distributions in mice. J. Nucl. Med. 19: 930-935, 1978.

26. HAYES, R.L., BROWN, D.H. Biokinetics of radiogallium in "Nuklearmedizin, Fortshcritte der Nuklearmedizin in Klinischer und Technologischer Sicht", H.W. Pabst, G. Hor, H.A.E. Schmidt, eds., Schattauer Verlag, New York, 1975, pp. 837-848.

27. GUNASEKERA, S.W., KING, L.J., LAVENDER, P.J. The behavior of tracer gallium-67 towards serum proteins. Clin. Chim. Acta.. 39: 401-406, 1972.

28. TSAN, M.F., CHEN, W.Y., SCHEFFEL, U., et al. Studies on gallium accumulation in inflammatory lesions: I. Gallium uptake by human polymorphonuclear leukocytes. J. Nucl. Med. 19: 36-43, 1978.

29. HIRSCH, J.I., FRATKIN, M.J., SHARPE, A.R. Gallium-67 citrate. Drug Intel. and Clin. Pharmaco. 7: 519-523, 1973.

30. CLAUSEN, J., EDELING, C.J., FOGH, J. ^{67}Ga binding to human serum proteins and tumor components. Cancer Res. 34: 1931-1937, 1974.

31. VALLABHAJOSULA, S.R., HARWIG, J.F., SIEMSEN, J.K., et al. Radiogallium localization in tumor:blood binding and transport and the role of transferrin. J. Nucl. Med. 21: 650-656, 1980.

32. HARRIS, D.C., GRAY, G.A., AISEN, P. ^{13}C nuclear magnetic study of the spatial relation of the metal and anion-binding sites of human transferrin. J. Biol. Chem. 249: 5261-5264, 1974.

33. LARSON, S.M., RASEY, J.S., ALLEN, D.R., et al. Common pathway for tumor cell uptake of gallium-67 and iron-59 via transferrin receptor. J.N.C.I. 64: 41-53, 1980.

34. HAMMERSLEY, P.A.G., TAYLOR, D.M. The effect of the administration of iron on gallium 67 citrate uptake in tumors. Brit. J. Radiol. 53: 563-571, 1980.

35. HALPERN, S.E., HAGAN, P.L., CHAUNCEY, D.P. The effect of certain variables on the tumor and tissue distribution of tracers. Part I: Carrier. Invest. Rad. 14: 482-492, 1979.

36. HAYES, R.L., RAFTER, J.J., CARLTON, J.E., et al. Studies of the in vivo uptake of ^{67}Ga by an experimental abcess: concise communication. J. Nucl. Med. 23: 8-14, 1982.

37. HOFFER, P.B., SAMUEL, A., BUSHBERG, J.T., et al. Desferoxamine Mesylate (Desferal): A contrast-enhancing agent for gallium-67 imaging. Radiology 131: 775-779, 1979.

38. BRADLEY, W.P., ALDERSON, P.O., WEISS, J.F. Effect of iron deficiency on the biodistribution and tumor uptake of Ga-67 citrate in animals: concise communication. J. Nucl. Med. 20: 243-247, 1979.

39. BRADLEY, W.P., ALDERSON, P.O., ECKELMAN, W.C., et al. Decreased tumor uptake of gallium-67 in animals after whole-body irradiation. J. Nucl. Med. 19: 204-209, 1978.

40. ANGHILERI, L.J. Studies on the relationship between ^{67}Ga-citrate accumulation and calcium metabolism in tumor cells. Nuklearmedizin 12: 257-265, 1974.

41. ANGHILERI, L.J., HEIDBREDER, M. On the mechanism of accumulation of ^{67}Ga by tumors. Oncology 34: 74-77, 1977.

42. PATERSON, A.H.G., YOXALL, A., SMITH, et al. The concentration of ^{67}Ga and ^{45}Ca in the lactating mammary gland and its relevance to the tumor uptake of ^{67}Ga citrate. Cancer Res. 36: 452-457, 1976.

43. ANGHILERI, L.J. The effects of gallium (Ga^{3+} on radiocalcium metabolism in tumors. Int. J. Nucl. Biol. Med. 17: 1-4, 1972.

44. ANGHILERI, L.J. Studies on the accumulation mechanisms of ^{67}Ga in tumors: role of calcium metabolism. Strahlentherapie 144: 29-34, 1972.

45. LARSON, S.M., RASEY, J.S., ALLEN, D.R., et al. A transferrin-mediated uptake of gallium-67 by EMT-6 sarcoma. I. Studies in tissue culture. J. Nucl. Med. 20: 837-842, 1979.

46. SEPHTON, R.G., HARRIS, A.W. Gallium-67 citrate uptake by cultured tumor cells stimulated by serum transferrin. J.N.C.I. 54: 1263-1266, 1974.

47. NOUJAIM, A.A., LENTLE, B.C., HILL, J.R., et al. On the role of transferrin in the uptake of gallium by tumor cells. Int. J. Nucl. Med. Biol. 6: 193-199, 1979.

48. HARRIS, N.W., SEPHTON, R.G. Transferrin promotion of ^{67}Ga and ^{59}Fe uptake by cultured mouse myeloma cells. Cancer Res. 37: 3634-3637, 1977.

49. AULBERT, E., GEBHARDT, A., SCHULZ, E., et al. Mechanism of ^{67}Ga accumulation in normal rat liver lysosomes. Nuklearmedizin 15: 185-194, 1976.

50. WONG, H., TERNER, U.K., ENGLISH, D., et al. The role of transferrin in the in vivo uptake of gallium-67 in a canine tumor. Int. J. Nucl. Med. Biol. 7: 9-16, 1980.

51. ROGERS, J.A., NOUJAIM, A.A. Gallium-67 transport across artificial biological membranes. Int. J. Nucl. Med. Biol. 9: 315-322, 1981.

52. SWARTZENDRUBER, D.C., NELSON, B., HAYES, R.L. Gallium-67 localization in lysosomial-like granules of leukemic and nonleukemic murine tissues. J.N.C.I. 46: 941-952, 1971.

53. ORII, H. Tumor scanning with gallium (^{67}Ga) and its mechanisms studied in rats. Strahlentherapie 144: 192-199, 1972.

54. BROWN, D.H., SWARTZENDRUBER, D.C., CARLTON, J.E., et al. The isolation and characterization of gallium binding granules from soft tissue tumors. Cancer Res. 33: 2063-2067, 1973.

55. AULBERT, E., HAUBOLD, V. Isolation of the ^{67}gallium accumulating fraction in normal rat liver. Nuklearmedizin 13: 72-84, 1974-1975.

56. BROWN, D.H., BYRD, B.L., CARLTON, J.E., et al. A quantitative study of the subcellular localization of ^{67}Ga. Cancer Res. 36: 956-963, 1979.

57. SAMAZINA, K., ORII, H. In vivo localization of Ga-citrate in rat liver as determined by cell fractionation with isopycnic rate-zonal ultracentrifugation. Eur. J. Nucl. Med. 5: 281-288, 1980.

58. PIERREZ, J., BERTRAND, A. Fixation of gallium. J. Nucl. Med. 20: 456-457, 1979.

59. LOGAN, K..J., NG, P.K., TURNER, C.J., et al. Comparative pharmacokinetics of ^{67}Ga and ^{59}Fe in humans. Int. J. Nucl. Med. Biol. 8: 271-276, 1981.

60. EDWARDS, C.L., HAYES, R.L. Localization of tumors with radioisotopes. "Clinical Uses of Radionuclides: Critical Comparison with Other Techniques", F.A. Goswitz, G.A. Andrews, M. Viamonte, eds., U.S. Atomic Energy Commission Office of Information Services, Springfield, 1972, pp 618-639.

61. NEWSTEAD, G., TAYLOR, D.M., McREADY, V.R., et al. Gallium-67 deposition in the human gastrointestinal tract. Int. J. Nucl. Med. Biol. 4: 109-112, 1977.

62. CHEN, D.C, SCHEFFEL, V., CAMARGO, E.E., et al. The source of gallium-67 in gastrointestinal contents. J. Nucl. Med. 21: 1146-1150, 1980.

63. ZIVANOVIC, M.A., TAYLOR, D.M., McREADY, V.R. The chemical form of gallium-67 in urine. Int. J. Nucl. Med. Biol. 5: 97-100, 1978.

64. SYKES, T.R., NOUJAIM, A.A., et al. Unpublished data.

65. KONIKOWSKI, T., GLENN, N.J., HAYNIE, T.P. Kinetics of ^{67}Ga compounds in brain sarcomas and kidneys of mice. J. Nucl. Med. 14: 164-171, 1973.

66. GALLE, P. Mechanism of renal concentration and elimination of indium and gallium: a study by nuclear tomography at the microscopic level. Eur. J. Nucl. Med. 6: A14, 1981.

67. NEWMAN, R.A., BRODY, A.R., KRAKOFF, I.H. Gallium nitrate (NSC-15200) induced toxicity in the rat. Cancer 44: 1728-1740, 1979.

68. BRUNER, H.D., COOPER, B.M., REHBOCK, D.J. Toxicity of gallium citrate in dogs and rats. Radiology 61: 550-555, 1953.

69. GOULD, A.A., ROOT, S.W., KERMAN, H.D. Clinical studies with gallium^{72}. Radiology 61: 570-577, 1953.

70. DEWANJEE, M., HNATOWICH, D.J., BEH, R. New ^{68}Ga labelled skeletal imaging agents for positron tomography. J. Nucl. Med. 17: 1003-1007, 1979.

71. DEWANJEE, M.K. Localization of ^{113m}In and ^{68}Ga labelled polymethylene-phosphonates in myocardial infarct. Nuklearmedizin 16: 151-156, 1977.

72. GOULET, R.T., SHYSH, A., NOUJAIM, A.A. Investigation of ^{68}Ga-tripolyphosphate as a potential bone scanning agent. Int. J. Appl. Radiat. Isot. 26: 195-199, 1975.

73. GAMS, R.A., WEBB, J., GLICKSON, J.D. Serum inhibition of in vitro ^{67}Ga binding by L1210 leukemic cells. Cancer Res. 35: 1422-1426, 1975.

74. TERNER, U.K., WONG, H., NOUJAIM,A.A., et al. ^{67}Ga and ^{59}Fe uptake in human melanoma cells. Int. J. Nucl. Med. Biol. 6: 23-28, 1979.

75. GLICKSON, J.D., WEBB, J., GAMS, R.A. Effects of buffers and pH on in vitro binding of ^{67}Ga by L1210 leukemic cells. Cancer Res. 34: 2957-2960, 1974.

76. STAAB, E.V., McCARTNEY, W.H. Role of gallium-67 in inflammatory disease. Semin. Nucl. Med. 8: 216-234, 1977.

77. LEE, V.W., TIU, S., SHAPIRO, J.H. Early detection of pneumonia by gallium-67 scintigraphy in patient with normal chest radiography. Clin. Nucl. Med. 5: 258-259, 1980.

78. McKUSIK, K.A., SOIN, J.S., GHILADI, A., et al. Gallium-67 accumulation in pulmonary sarcoidosis. J.A.M.A. 223: 688-690, 1973.

79. SIEMSEN, J.K., GREBE, S.F., WAXMAN, A.D. The use of gallium-67 in pulmonary disorders. Semin. Nucl. Med. 8: 235-249, 1978.

80. BURLESON, R.L., HOLMAN, B.L., TOW, D.F. Scintigraphic demonstration of abcesses with radioactive gallium labelled leucocytes. Surg. Gyneco. Obst. 141: 379-382, 1975.

81. WISEMAN, J., ROULEAU, J., RIGO, P., et al. Gallium-67 myocardial imaging for the detection of bacterial endocarditis. Radiology 120: 135-138, 1976.

82. SPIES, S.M., MEYERS, S.N., BARRESI, V., et al. A case of myocardial abcess evaluated by radionuclide techniques: case report. J. Nucl. Med. 18: 1089-1090, 1977.

83. KAPLAN, L.R., GRIEP, R.J., SCHUFFLER, M.D., et al. ^{67}Gallium scanning at 6 hours in active inflammatory bowel disease: case report. J. Nucl. Med. 18: 448-449, 1977.

84. WAXMAN, A.D., SIEMSEN, J.K. Gallium gallbladder scanning in cholescystitis. J. Nucl. Med. 16: 148-150, 1975.

85. GELRUD, L.G., ARSENEAU, J.C., MILDER, M.S., et al. The kinetics of ^{67}Gallium incorporation into inflammatory lesions: experimental and clinical studies. J. Lab. Clin. Med. 83: 489-495, 1974.

86. LISBONNA, R., CASSOFFF, J., ANGTIAGO, E. Comparative accuracy and complementary use of ^{67}Ga citrate imaging and ultrasound in the diagnostic of abdominal abcess. Clin. Nucl. Med. 4: 108-110, 1979.

87. KUMAR, B., COLEMAN, R.E. Significance of delayed gallium localization in the kidney. J. Nucl. Med. 17: 872-876, 1976.

88. HOFFER, P. Gallium and infection. J. Nucl. Med. 21: 484-488, 1980.

89. CAMARGO, E.E., WAGNER, H.N., TSAN, M.F. Studies of gallium in inflammatory lesions: IV Kinetics of accumulation and role of polymorphonuclear leukocytes in the distribution of gallium in experimental inflammatory exudates. Nucl. Med. 18: 147-150, 1979.

90. OSTROY, F., JOHNSTON, R.B., GAMS, R.A. Effects of hypoxia on ^{67}Ga incorporation into human granulocytes. Cancer Res. 39: 4971-4974, 1979.

91. HOFFER, P.B., HUBERTY, J., KHAYAM-BASHI, H. The association of Ga-67 and lactoferrin. J. Nucl. Med. 18: 713-717, 1977.

92. WEINER, R., HOFFER, P.B., THAKUR, M.L. Lactoferrin: Its role as a Ga-67 binding protein in polymorphonuclear leukocytes. J. Nucl. Med. 22: 32-37, 1981.

93. WEINER, R., SCHREIBER, G., HOFFER, P.B., et al. The relative stabilities of the ^{67}Ga complex of lactoferrin and transferrin at various pH's. Int. J. Nucl. Med. Biol. 8: 371-378, 1981.

94. TZEN, K.Y., OSTER, Z.H., WAGNER, H.N., et al. Role of iron binding proteins and enhanced capillary permeability on the accumulation of gallium-67. J. Nucl. Med. 21: 31-35, 1980.

95. DHAWAN, V.M., SZIKLAS, J.J., SPENCER, R.P. Localization of Ga-67 in inflammations in the absence of circulating polymorphonuclear leukocytes. J. Nucl. Med. 19: 292-294, 1978.

96. TSAN, M.F. Studies on gallium accumulation in inflammatory lesions III. Roles of polymorphonuclear leucocytes and bacteria. J. Nucl. Med. 19: 492-495, 1978.

97. TERNER, U.K., NOUJAIM, A.A., LENTLE, B.C., et al. Uptake of gallium complexes in canine sterile abcess. In press. Int. J. Nucl. Med. Biol. 1982.

98. KRAMER, R.J., GOLDSTEIN, R.E., HIRSCHFELD, J.W., et al. Accumulation of gallium 67 in regions of acute myocardial infarct. Amer. J. Cardiol. 33: 861-866, 1974.

99. ZWEIMAN, F.G., HOLMAN, B.L., O'KEEFE, A., et al. Selective uptake of $^{99}Tc^{m}$ complexes and ^{67}Ga in acutely infarcted myocardium. J. Nucl. Med. 16: 975-979, 1975.

100. SCHOR, R.A., MASSIE, B.M., BOTVINICK, E., et al. Gallium-67 uptake in silent myocardial infarction: a case report. Radiology 129: 117, 1978.

101. GREENFIELD, S., CLIFT, M. Analytical chemistry of the condensed phosphates. Robert Maxwell publisher, Pergamon Press, Oxford, New York-Toronto, 1975, pp 1-34.

102. FREEDMAN, L.D., DOAK, G.O. The preparation and properties of phosphonic acid. Chem. Rev. 57: 479-523, 1957.

103. MOEDRIETZEN, K., IRAMI, R.R. Synthesis and properties of mono, poly, methylene deiphosphonate acid and ester. J. Inorg. Nucl. Chem. 22: 297-304, 1961.

104. TOFE, A.J., BENEDICT, J.J., BEVAN, J.A. Imaging the skeletal system. Radiopharmaceuticals II: Proceedings 2nd international symposium on radiopharmaceuticals March 19-22, 1979, Seattle, Washington, Society of Nuclear Medicine publisher, 603-614, 1979.

105. TERMINE, J.D., POSNER, A.S. Amorphous crystalline interrelationship in bone mineral. Calc. Tiss. Res. 1: 8-23, 1967.

106. JONES, A.G., FRANCIS, M.D., DAVIS, M.A. Bone scanning radionuclides reaction mechanism. Semi. Nucl. Med. 6: 3-15, 1976.

107. HANSEN, N.M., FELIX, R., BIZAZ, S., et al. Aggregation of hydroxyapatite crystals. Biochim. Biophy. Acta. 451: 549-559, 1975.

108. BARNETT, B.L., STRICKLAND, L.C. Structure of disodium dihydrogen 1-hydroxy ethylidenidiphosphonate tetrahydrate: a bone growth regulator. Acta. Cryst. B35: 1212-1214, 1979.

109. JUNG, A., BISAZ, S., FLEISCH, H. The binding of pyrophosphate and two disphosphonates by hydroxyapatite crystals. Calc. Tiss. Res. 11: 269-280, 1973.

110. EVANS, J.R., ROBERTSON, W.G., MORGAN, D.B., et al. Effects of pyrophosphate and diphosphonates on the dissolution of hydroxyapatites using a flow system. Calcif. Tiss. Int. 31: 153-159, 1980.

111. MEYERS, J.L., NANCOLLAS, G.H. The influence of multidentate organic phosphonates on the crystal growth of hydroxyapatite. Calc. Tiss. Res. 13: 295-303, 1973.

112. LIBSON, K., DEUTSCH, E., BARNETT, B.L. Structural characterization of a ^{99}Tc diphosphonate complex. Implications for the chemistry of ^{99m}Tc skeletal imaging agents. J. Am. Chem. Soc. 102: 2476-2478, 1980.

113. KRISHNAMURTHY, G.T., HUEBOTTER, R.J., WALSH, C.F., et al. Kinetics of ^{99m}Tc-labelled pyrophosphate and polyphosphate in man. J. Nucl. Med. 16: 109-115, 1975.

114. SUBRAMANIAN, G., McAFEE, J.G., BLAIR, R.J., et al. Technetium-99m-methylene diphosphonate a superior agent for skeletal imaging: comparison with other technetium complexes. J. Nucl. Med. 16: 744-755, 1975.

115. MAKLER, P.T., CHARKES, N.D. Studies of skeletal tracers kinetics IV. Optimum time delay for Tc-99m-(Sn) methylene diphosphonate bone imaging. J. Nucl. Med. 21: 641-645, 1980.

116. RUDD, T.G., ALLEN, D.R., HARNETT, D.E. Biological and clinical comparison. Tc 99m MDP versus Tc 99m pyrophosphate. J. Nucl. Med. 18: 872-976, 1977.

117. SAHA, G.B., BOYD, C.M. A study of protein binding of Tc-methylene diphosphonate in plasma. Int. J. Nucl. Med. and Biol. 6: 201-106, 1979.

118. SCHUMICHEN, C., KOCH, K., KRAUS, A., et al. Binding of technetium-99m to plasma proteins: influence on the distribution of Tc-99m-phosphate agents. J. Nucl. Med. 21: 1080-1085, 1980.

119. SCHUMICHEN, C., KORFGEN, T., HOFFMAN, G. Relationship between complex stability and biokinetics of ^{99m}Tc phosphate compounds. Nucl. Med. 19: 7-10, 1980.

120. SCHUMICHEN, C., SEIFRITZ, R., HOFFMAN, G. Bone uptake of ^{99m}Tc pyrophosphate via labelled plasma protein. Nucl. Med. 19: 174-177, 1980.

121. OWUNWANNE, A., O'MARA, R.F., O'BRIEN, C. The interaction of tc-99m phosphorous radiopharmaceuticals and serum proteins. J. Nucl. Med. 20: 653,. 1979.

122. RUDD, T.G., ALLEN, D.R., SMITH, F.D. Technetium-99m labelled methylene diphosphonate and hydroxyethilidine diphosphonate-biologic and clinical comparison: concise communication. J. Nucl. Med. 20: 821-826, 1979.

123. HECK, L.L. Extra-osseous localization of phosphate bone agents. Semin. Nucl. Med. 10: 311-313, 1980.

124. FONT, D., HARDOFF, R., MASHOUR, N. Stomach artifact in bone scintigraphy. J. Nucl. Med. 19: 974, 1979.

125. SUBRAMANIAN, G., McAFEE, J.G., BLAIR, R.J., et al. An evaluation of ^{99}Tc-labelled phosphate compounds as low imaging agents, "Radiopharmaceutical" Society of Nuclear Medicine publisher, G. Subramaniam editor, New York, 1975.

126. DHAWAN, V., YEH, S.D. Labelling efficiency and stomach concentration in methylene disphosphonate bone imaging. J. Nucl. Med. 20: 791-793, 1979.

127. SILBERSTEIN, E.B., FRANCIS, M.D., TOFE, A.J., et al. Distribution of ^{99m}Tc-Sn phosphonate and free ^{99m}Tc-pertechnate in selected soft and hard tissues. J. Nucl. Med. 16: 58-61, 1975.

128. SILVER, A.S., WANG, S.T., FAWWAZ, R.A., et al. Protein binding of ^{99}Tc diphosphonate in malignant ascites. Nucl. Med. 19: 44-46, 1980.

129. DUDCZACK, R., ANGELBERGER, P., KETTLER, K., et al. Transient accumulation of Tc 99m MDP in the liver. Euro. J. Nucl. Med. 5: 189-191, 1980.

130. SUBRAMANIAN, G., McAFEE, J.G., BLAIR, R.J., et al. Technetium-99m-labelled stannous imidodiphosphate, a new radiodiagnostic agent for bone scanning: comparison with other ^{99m}Tc-complexes. J. Nucl. Med. 16: 1137-1143, 1975.

131. WANG, T.S., FAWWAZ, R.A., JOHNSON, L.J., et al. Bone-seeking properties of Tc-99m-carbonyl diphosphonic acid, dihydroxymethylene diphosphonic acid and monohydroxymethylene phosphoric acid: concise communication. J. Nucl. Med. 21: 767-770, 1980.

132. JONES, A.G., FRANCIS, M.D., DAVIS, M. Bone scanning agents: radionuclidic reaction mechanisms. Semin. Nucl. Med. 6: 3-18, 1976.

133. SAGAR, V.V., PICCONE, J.M., CHARKES, N.D. Studies of skeletal tracer kinetics III. Tc-99m (Sn) methylene diphosphonate in the canine tibia as a function of blood flow. J. Nucl. Med. 20: 1257-1261, 1979.

134. TILDEN, R.L., JACKSON, ENNEKING, W.F., et al. ^{99m}Tc polyphosphate: histological localization in human femurs by autoradiography. J. Nucl. Med. 14: 576-578, 1973.

135. SUBRAMANIAN, G., McAFEE, J.G., BLAIR, R.J., et al. ^{99m}Tc EHDP: a potential radiopharmaceutical for skeletal imaging. J. Nucl. Med. 13: 947-950, 1972.

136. Le PAPE, A., GUILLEMART, A. Autoradiographic comparison of ^{96}Tc-pyrophosphate and ^{45}Calcium bone uptake. Eur. J. Nucl. Med. 7: 127-129, 1982.

137. KAYE, M., SILVERTON, S., ROSENTHALL, L. Technetium 99m pyrophosphate: studies in vivo and in vitro. J. Nucl. Med. 16: 40-45, 1975.

138. MARTY, R., DENNEY, J.D., McKARNEY, M.R., et al. Bone trauma and related benign disease: assessment by bone imaging. Semin. Nucl. Med. 6: 107-120, 1976.

139. BONTE, F.J., PARKEW, R.W., GRAHAM, K.D., et al. A new method for radionuclide imaging of myocardial infarcts. Radiology 110: 473-474, 1974.

140. LESSEM, J., POLIMENT, P.I., PAGE, F., et al. Accumulation of Tc-99m-pyrophosphate in experimental infarction on the rat. Cardiovasc. Res. 14: 352-359, 1980.

141. DEWANJEE, M.K., KHAN, P.C. Mechanism of localization of ^{99m}Tc-labelled pyrophosphate and tetracycline in infarcted myocardium. J. Nucl. Med. 17: 639-646, 1976.

142. BUJA, M.L., PARKEY, R.W., DEES, J.H. Morphologic correlates of technetium 99m stannous pyrophosphate imaging of acute myocardial infarcts in dogs. Circulation 52: 596-607, 1975.

143. RUDE, R.E., PARKEY, R.W., BONTE, F.J. Clinical implications of the technetium 99m stannous pyrophosphate myocardial scintigraphies "doughnut" pattern in patients with acute myocardial infarct. Circulation 59: 721-730, 1979.

144. HOILUND-CARLSEN, P.F., BADSKJAER, H., BOITIUS, J., HERTZ, J., et al. The predictive value of myocardial scintigraphy with ^{99m}Tc pyrophosphate in diagnosing acute myocardial infarction. Acta. Med. Scand. Supp. 623: 55-60, 1979.

145. PARKEY, R.W., BONTE, F.J. BUJA, M.L., et al. Myocardial infarct imaging with Tc 99m phosphates. Semin. Nucl. Med. 7: 15-28, 1977.

146. LYONS, K.P., OLSON, H.G., ARONOW, W.S. Pyrophosphate myocardial imaging. Semin. Nucl. Med. 10: 168-177, 1980.

147. MALIN, E.R., ROLLO, F.D., GERTZ, E.W. Sequential myocardial scintigraphy with technetium 99m stannous pyrophosphate following myocardial infarction. J. Nucl. Med. 19: 1111-1115, 1979.

148. PEREZ, L.A. Clinical experience: Technetium 99m labelled phosphates in myocardial imaging. Clin. Nucl. Med. 1: 2-9, 1976.

149. SHAMES, D.M., BOTVINICK, E., LAPPIN, H., et al. Quantitation of myocardial infarct size with Tc 99 pyrophosphate and correlation between CPK depletion and radionuclide uptake. J. Nucl. Med. 16: 569, 1975.

150. WILLERSON, J.T., BUJA, L.M., STOKELY, E.M., et al. Infarct sizing in awake, unsedated dogs with acute anterior myocardial infarcts. J. Nucl. Med. 17: 534, 1976.

151. LESSEM, J. Radionuclides in acute myocardial infarction. Acta. Medic. Scandi. Supp. 623: 27-37, 1979.

152. CURY, R.C., JACKMAN, W.M. Persistently positive ^{99m}Tc pyrophosphate myocardial scintigram in a patient with left ventricular aneurysm. Clin. Nucl. Med. 1: 91-92, 1976.

153. McDANIEL, M.M., MORTON, M.E. ^{99m}Tc pyrophosphate imaging demonstrating skeletal muscle and myocardial activity following cardioversion. Clin. Nucl. Med. 2: 57-59, 1977.

154. SLUTSKY, L., PASSALAQUA, A., OSTER, Z.H. Uptake of ^{99m}Tc pyrophosphate in chest wall tissues due to defibrillation. Clin. Nucl. Med. 2: 6-7, 1977.

155. KIM, E. Calcified costal cartilage as a cause of false interpretation in myocardial imaging. Clin. Nucl. Med. 1: 159-161, 1976.

156. BUJA, L.P., POLINER, L.R., PARKEY, R.W. Clinicopathologic study of persistently positive technetium 99m stannous pyrophosphate myocardial scintigram. Circulation 56: 1016-1023, 1977.

157. OLSON, H.G., LYONS, K.P., ARONOV, W.S. Prognostic value of persistently positive technetium 99m stannous pyrophospate myocardial scintigram after myocardial infarction. Am. J. Cardio. 43: 889-898, 1979.

158. COWLEY, M.J., MANTLE, J.A., ROGERS, W.J. Technetium 99m stannous pyrophosphate myocardial scintigraphy; reliability and limitations in assessment of acute myocardial infarction. Circulation 56: 193-198, 1977.

159. DATZ, F.L., BUJA, L.M., LEWIS, S.E., et al. Pathophysiology of persistently positive myocardial scintigrams. J. Nucl. Med. 20: 895, 1979.

160. DAVIS, A.D., HOLMAN, B.L., CARMEL, A.N. Evaluation of radiopharmaceuticals sequestered by acutely damaged myocardium. J.. Nucl. Med. 17: 911-917, 1976.

161. MILLER, D.G., GILMOUR, R.F., GROSSMAN, Z.D., et al. Myocardial uptake of Tc 99m skeletal agents in the rat after experimental induction of microscopic foci of injury. J. Nucl. Med. 18: 1003-1007, 1977.

162. JONES, A.G., DAVIS, M.A. The affinity of radiolabelled bone seeking compounds for injured myocardium in the rat. Int. J. Appl. Rad. and Isotop. 28: 203-206, 1977.

163. SINGH, A., UGHER, M. Comparison of Tc-99m methylene diphosphonate with Tc-99m pyrophosphate in the detection of acute myocardial infarction. J. Nucl. Med. 18: 790-792, 1977.

164. LYONS, K.P., MORTON, M.E. Phosphate myocardial imaging. Are the bone seeking agents better? Clin. Nucl. Med. 4: 132-133, 1979.

165. MAKLER, P.T., LEDERMAN, S., CHARKES, D. Myocardial infarct imaging with ^{99}Tc pyrophosphate and ^{99m}Tc diphosphonate: lack of correlation. Clin. Nucl. Med. 4: 89-91, 1979.

166. KELLY, R.J., CHILTON, H., HACKSHAW, B.T., et al. Comparison of Tc 99m pyrophosphate and Tc 99m methylene diphosphonate in acute myocardial infarction: concise communication. J. Nucl. Med. 20: 402-406, 1979.

167. D'AGOSTINO, A.N. An electron microscopic study of cardiac necrosis produced by 9-a fluorocortisol and sodium phosphate. Am. J. Patho. 45: 633-644, 1964.

168. D'AGOSTINO, A.N., CHIGA, M. Mitochondrial mineralization in human myocardium. Am. J. Clin. Path. 53: 820-924, 1970.

169. SHEN, A.C., JENNING, R.B. Myocardial calcium and magnesium in acute ischemic injury. Am. J. Patho. 67: 417-433, 1972.

170. TOFE, A.J., BONTE, F.J., PARKEY, R.W., et al. Scintigraphy of canine myocardial infarcts: role of calcium and Tc 99m diphosphonate/pyrophosphate bone agents. J. Nucl. Med. 17: 534- , 1976.

171. MUKLERJEE, A. Correlation between alteration in mitochondrial function of Tc pyrophosphate. Circulation 64: supp. 4 576.

172. DEWJANEE, M.K., KAHN, P.C. Mechanism of localization of $^{99}Tc^{m}$ labelled pyrophosphate and tetracycline in infarcted myocardium. J. Nucl. Med. 17: 639-646, 1976.

173. BUJA, M.L., TOFE, A.J., BONTE, F.J., et al. Sites and mechanisms of localization of Technetium-99m phosphorous radiopharmaceuticals in acute myocardial infarcts and other tissues. J. Clin. Invest. 60: 724-740, 1977.

174. COLEMAN, R.E., KLEIN, M.S., ASHMED, S.A., et al. Mechanisms contributing to myocardial accumulation of the Tc 99m stannous pyrophosphate after coronary artery occlusion. Am. J. Cardiol. 39: 55-59, 1977.

175. SHELBERT, INGWALL, J.S., SYBERS, H.D., et al. Uptake of infarct imaging agents in reversibly and irreversibly injured myocardium in cultured mouse heart. Circ. Res. 39: 860-868, 1976.

176. RANDERATH, K., RANDERATH, E. Ion exchange chromatography of nucleotide on poly-(ethyleneimine) cellulose thin layer. J. Chromato. 16: 111-125, 1964.

177. Health Protection Branch, Analytical techniques for the determination of radiochemical purity of radiopharmaceutical prepared from kit. Part I. 77-EHD-16, 1977.

178. MARUSYK, R., SERGEANT, A. A simple method for dialysis of small volume samples. Ana. Biochem. 105: 403-404, 1980.

179. KUNG, H.F., BLAU, M. Subcutaneous isoproterenol: A convenient rat model for early detection of myocardial necrosis. J. Nucl. Med. 19: 948-951, 1978.

180. KUNG, H.F., BLAU, M., ACKERHALT, R. Uptake of radiopharmaceuticals in developing myocardial lesions. Radiopharmaceuticals II, proceedings 2nd International Symposium on Radiopharmaceuticals, March 19-22, 1979, Seattle, Washington, 475-485, 1979.

181. WARBICK, A., EGE, G.N., HENKELMAN, R.M. An evaluation of radiocolloid sizing techniques. J. Nucl. Med. 18: 827-834, 1977.

182. WAXMAN, A.D., KAWADA, T., WOLF, W., et al. Are all gallium citrate preparations the same? Radiology 117: 647-648, 1975.

183. HNATOWICH, D.J., KULPRATHIPANJA, S., BEH, R. The importance of pH and citrate concentration on the in vitro and in vivo behavior of radiogallium. Int. J. App. Rad. Isot. 28: 925-931, 1977.

184. HAYES, R.L., CARLTON, J.E. "A study of the macromolecular binding granules from soft tissue tumors". Cancer Res. 33: 2053-2058, 1973.

185. WILLIAM, C.C., NIGHIGAMA, H.R., ADOLPH, R.J., et al. A comparison of technetium etidronate and pyrophosphate for myocardial infarct imaging. J. Nucl. Med. 18: 905-909, 1977.

186. KLOPPER, J.F., SRIVASTAVA, S., MEINKEN, G., et al. Preliminary investigation of gallium-68 pyrophosphate as a potential scanning agent. ERDA Energy Res. Abstract 14(2): 36267, 1977.

APPENDICES

APPENDIX I

DUAL LABEL SPILLOVER OF ^{125}I AND ^{67}Ga FOR THE BECKMAN 8000 GAMMA COUNTER*

Energy range: 0.5

Channel 1

2 sigma %:	0.20
Lower level:	30
Upper level:	160

Channel 2

2 sigma %:	0.20
Lower Level:	160
Upper level:	900

Channel 3

2 sigma %:	0.20
Lower level:	10
Upper level:	1000

---

* - Channel 1 was set for the lower energy nuclide.
  - Channel 2 was set for the highest energy nuclide insuring that the lowest level is set to exclude all counts from the low energy nuclide.
  - With a standard of the high energy nuclide a ratio of the number of counts in channel 1 to the number of counts in channel 2 was determined to evaluate the spillover.
  - The counts in channel 2 multiplied by the channel ratio value was then subtracted from the counts in channel 1. The residual value was attributed to the low energy nuclide and used as the corrected count of the low energy nuclide.

APPENDIX II

DUAL LABEL SPILLOVER CORRECTION OF $^{99}Tc^{m}$ AND ^{67}Ga FOR THE BECKMAN 8000 GAMMA COUNTER*

Energy range: 0.5

Channel 1

2 sigma %:	0.20
Lower level:	240
Upper lvel:	370

Channel 2

2 sigma %:	0.20
Lower level:	370
Upper Level:	900

Channel 3

2 sigma %:	0.20
Lower level:	10
Upper level:	1000

---

* - Channel 1 was set for the lower energy nuclide.
  - Channel 2 was set for the highest energy nuclide, insuring that the lowest level is set to exclude all counts from the low energy nuclide.
  - With a standard of the high energy nuclide, a ratio of the number of counts in channel 1 to the number of counts in channel 2 was determined to evaluate the spillover.
  - The counts in channel 2 multiplied by the channel ratio value was then subtracted from the counts in channel 1. The residual value was attributed to the low energy nuclide and used as the corrected counts of the low energy nuclide.